THE ANALYTICAL COMPUTATION OF RESIDUAL THERMAL STRESSES

Thesis by

Herbert Arthur Lassen

In Partial Fulfillment of the Requirements

For the Degree of

Doctor of Philosophy

California Institute of Technology

Pasadena, California

1951

ACKNOWLEDGEMENTS

The author gratefully acknowledges the inspiration, advice and valuable criticism given by his advisor, Dr. George W. Housner.

The author wishes to express his appreciation to Dr. Donald S. Clark for free use of his personal library and for the interest shown by him in the progress of the thesis.

The author wishes to thank Dr. Donald E. Hudson, Dr. Pol Duwez, Dr. Peter R. Kyropoulos and Dr. David S. Wood for valuable aid in connection with this thesis and in connection with the experimental work which led to a consideration of the subject matter of this thesis.

The author finally wishes to express his indebtedness to his wife for tracing the curves, typing the manuscript and for her invaluable aid in carrying out the numerical calculations.

ABSTRACT

An analytical method is developed in detail whereby it is possible to calculate, with arbitrary accuracy, the temperature, the stresses, and the residual strains as a function of the radial position and time induced in an infinitely long solid isotropic cylinder by a quench in a large body of fluid, assuming that all of the pertinent parameters are known (graphical) functions of the temperature.

In the course of this development, a general theory is presented whereby it is theoretically possible to predict the stresses and the residual strains in an isotropic body at any time during a thermal and mechanical history if the following very general assumptions are satisfied.

1) The temperature and the boundary conditions are known functions of the position and time and the free thermal expansion is a known function of the temperature.

2) There are values of E, G and ν which are known functions of the temperature and which relate, through Hooke's Law, the changes in the stresses with the changes in the strains which occur if the stresses are removed from an infinitesmal element of the body.

3) There is a theory of strength available which either predicts the maximum stresses which the material can sustain, as a function of the temperature and the past history, or which predicts the plastic strain rates as a function of the stresses, the temperature and the past history.

Selecting the values of the pertinent parameters from the literature, a numerical calculation of the residual stresses is made for a specific case of a quenched solid cylinder. The results are compared with experimental values for the same case determined by other investigators.

The developments for a solid cylinder are extended to a hollow cylinder and a flat plate. Various suitable theories of strength are considered. The modifications to the general theory and the additional information required if a phase change is involved are briefly indicated.

TABLE OF CONTENTS

TABLE OF CONTENTS

INTRODUCTION

The problem of residual stresses is receiving increased interest due to the important influence residual stresses sometimes exert upon fatigue strength and dimensional stability. The gradual industrial acceptance of the techniques of shot peening, surface rolling, coining operations near oil holes and carburizing to achieve surface residual compressive stresses is evidence of the value of favorable residual stresses upon fatigue properties. The techniques of auto-frettage for gun barrels and over-speed for turbine rotors increase the dimensional stability and effectively increase the strength of the parts through the formation of favorable residual stresses. The utilization of the most common source of residual stresses - quenching - is, however, conspicuously absent from the foregoing list. This may be attributed largely to a lack of appreciation of the fact that surface residual compressive stresses of yield point magnitude may be induced in steel, under favorable conditions, by a quench from tempering temperatures.

Existing knowledge of the disposition and magnitude of residual stresses resulting from quenching is based largely upon experimental determinations resulting from appropriately cutting up the specimen and noting the distortion which occurs, or, more recently, by X-ray methods. Reliable experimental determinations of three dimensional residual stresses have been made only for the case of a long cylinder where the residual stresses are symmetrical and independent of axial position. In this case the boring out technique of Sachs (1) is mathematically accurate. Using

Sachs' technique, several experimenters, notably Buhler and his associates (2), (3), (4); Wishart and Potter (5); and Horger and Neifert (6), have determined the residual stresses in long steel cylinders of various compositions resulting from quenching from above and below the austenite range. A summary of other methods of experimentally estimating the values of residual stresses is given by Barrett (7) and Sachs and Espey (8). The type of residual stress determined in the foregoing references must be distinguished from the "tessellated" stresses, estimated by Laszlo (9), which are set up within the individual structural elements, e.g. pearlite, graphite-in-ferrite, and etc. when they are heated or cooled. The former may be considered to be the average, or "macro", stresses which are superimposed upon the "tessellated" stresses. In this thesis, the assumptions of isotropy and of the dependence of the physical properties upon temperature immediately remove all considerations of "tessellated" stresses.

Although the foregoing discussion indicates the desirability of the development of an analytical technique for computing the residual stresses resulting from a quench, even if limited to simple bodies, there has been no full scale attempt, prior to this thesis, to develop the necessary techniques. Russell (10) calculated the temperature versus time in a cylinder subject to an infinite quench, assuming that the conductivity and the thermal diffusivity were constant. His calculation is of particular interest because an approach to the problem of including the effects of a phase change is introduced. He then attempted to calculate the stresses due to this temperature distribution, assuming that no yielding occurs, and using a constant value of the coefficient of thermal expansion

and variable values of E and ν. His equations for the stress are, however, incorrect in that several terms required by the variation of E and ν are neglected. Treppschuh (11) obtained experimental values of the temperature distribution versus time for a cylinder quenched from the austenite range. He then assumed that the stress level in the cylinder at the completion of the phase change was zero, and calculated the residual stresses on the assumption that they were caused by the difference in thermal expansion between the completion of phase change and room temperature.

The specific purpose of this thesis is the development, in a form suitable for numerical solution, of an analytical method for the determination of the temperature, the residual (or plastic) strains and the true stresses as a function of the position and time and for the determination of the final residual stresses induced in an infinitely long solid isotropic cylinder by symmetrically quenching it in a large body of fluid. Within the limitations of the accuracy with which the conditions tabulated below are satisfied, a semi-graphical finite difference method is developed which, as the steps in position and time are decreased in size, approaches the exact solution to the problem.

1) There are values of the thermal conductivity and of the thermal diffusivity which are known (graphical) functions of the temperature and there is a boundary layer conductivity which can be represented as a known (graphical) function of the surface temperature of the cylinder.

2) The free thermal expansion is a known function of the temperature. There are values of the elastic coesfficients, E, G, and ν which are known functions of the temperature and which related, through Hooke's Law, the changes in the stresses with the changes in the strains which occur if the stresses are removed from an infinitesmal element of the body.

3) There is a theory of strength available which either predicts the maximum stresses which the material can sustain, as a function of the temperature and the past history, or which predicts the plastic strain rates as a function of the stresses, the temperature and the past history.

For purposes of illustration, the method is applied to a specific case of a quenched cylinder. The values of the pertinent parameters are selected from the literature and the character of the numerical calculations is illustrated.

The general purpose of the thesis is the extension of the foregoing developments to other cases and, as indicated in the abstract, the development of a general theory whereby it is theoretically possible, under very general assumptions, to predict the stresses and the residual (or plastic) strains in an isotropic body at any time during a thermal and mechanical history.

PART I

The development of an analytical method for the prediction of the residual stresses induced in an infinitely long solid isotropic cylinder by a symmetrical quench in a large body of fluid, assuming that all of the pertinent parameters are known (graphical) functions of temperature.

CHAPTER I

This chapter will be devoted to the development of a semigraphical method for the prediction of the temperature as a function of the radial position and time in an infinitely long solid isotropic cylinder, resulting from a symmetrical quench in a large body of fluid. It will be assumed that the boundary layer conductivity is a known (graphical) function of the surface temperature of the cylinder. This is not a restrictive assumption in the sense that, in any specific case, any other parameters which influence the boundary layer conductivity may be introduced as functions of the surface temperature of the cylinder. The thermal conductivity and the thermal diffusivity will be assumed to be known (graphical) functions of temperature.

The following notation will be used in this chapter:

Let:	r	be the radius to any point.	cm.
	r_1	be the outer radius of the cylinder.	cm.
	x	be the radial position parameter = r/r_1	cm./cm.
	T	be the temperature at any point r.	$^{o}C.$
	T_o	be the bulk temperature of the fluid.	$^{o}C.$
	t	be the time.	sec.
	k	be the thermal conductivity.	cal./cm. sec. $^{o}C.$
	ρ	be the specific weight.	gm./cm.^{3}
	c_p	be the specific heat.	cal./gm. $^{o}C.$
	a	be the thermal diffusivity = $k/\rho c_p$.	cm.^{2}/sec.
	h	be the boundary layer conductivity.	cal./cm.^{2} sec. $^{o}C.$

The differential equation of heat flow in cylindrical coordinates, assuming that the temperature is a function of the radial position and time only, will now be derived.

Consider a ring of unit length, inner radius r and outer radius $r + dr$. The rate of heat entering the ring from the inner radius r equals the rate of heat storage in the ring plus the rate of heat leaving across the outer radius $r + dr$.

The rate of heat entering $= -2\pi r k \frac{\partial T}{\partial r}$ cal./cm. sec.

The rate of heat leaving $= -2\pi \left[rk \frac{\partial T}{\partial r} + \frac{\partial}{\partial r}\left(rk \frac{\partial T}{\partial r}\right) dr \right]$ cal./cm. sec.

The rate of heat storage $= 2\pi r dr \rho c_p \frac{\partial T}{\partial t}$ cal./cm. sec.

Equating these heat rates, as stated above, and simplifying the result, gives the following equation for heat flow in cylindrical coordinates:

$$(1) \qquad \frac{\partial T}{\partial t} = q \left[\frac{1}{r} \frac{\partial}{\partial r}\left(r \frac{\partial T}{\partial r}\right) + \frac{1}{K} \frac{\partial K}{\partial r} \frac{\partial T}{\partial r} \right] \quad {}^{\circ}C./sec.$$

(Eq. 1) applies to the interior material of the cylinder. The boundary condition which the solution to (Eq. 1) must match at the surface of the cylinder, will now be developed.

An instantaneous boundary layer conductivity h is defined such that the rate with which heat passes from the surface of the cylinder into the quenching fluid per unit length of the cylinder is given by:

$$-2\pi r_1 h(T - T_0)\Big|_{r=r_1} \qquad \text{cal./cm. sec.}$$

This rate of heat flow through the boundary layer must equal the rate of heat flow through the material of the cylinder at the surface of the cylinder. This latter heat flow rate is given by:

$$-2\pi r_1 \left(k \frac{\partial T}{\partial r}\right)\Big|_{r=r_1}$$

Equating these heat flow rates, as stated above, results in the fundamental boundary condition equation:

$$(2) \qquad \frac{\partial T}{\partial r}\Big|_{r=r_1} = -\frac{h}{k}(T - T_0)\Big|_{r=r_1}$$

(Eq. 1), (Eq. 2) and the initial conditions (temperature versus radial position at the start of the quench) define the temperature problem. However, since k, a and h are assumed to be known (graphical) functions of the temperature, these equations are nonlinear and it will be necessary to solve them by a semigraphical finite difference technique. The remainder of this chapter will be devoted to the development of this technique. V. E. Schmidt (12) demonstrated a graphical technique for solving this set of equations when a and k are assumed constant and the development which follows will be an original extension of his technique to cover the case of variable a and k .

The finite difference form of (Eq. 1) will now be derived. The steps which follow are required for this derivation.

The time t is divided into intervals Δt_j (not necessarily equal), the end of each interval being distinguished by the subscripts: 0, 1, 2, ... j-1, j, j+1, ... The value of t at the end of the k'th interval will then be: $t_k = \sum_{j=1}^{k} \Delta t_j$

The radius is divided into n equal intervals Δr (where $n\Delta r = r_1$), the center of each interval being distinguished by the subscripts: $\frac{1}{2}$, $1\frac{1}{2}$, $2\frac{1}{2}$, ... m-1, m, m+1, ... $n-\frac{1}{2}$.

In terms of this notation, the following approximations may be made:

$$\frac{\partial T}{\partial t} \cong \frac{T_{m,j+1} - T_{m,j}}{\Delta T_{j+1}}$$

$$r\frac{\partial T}{\partial r}\Big|_{r=(m+1/2)\Delta r} \cong (m+1/2)(T_{m+1,j} - T_{m,j})$$

$$r\frac{\partial T}{\partial r}\Big|_{r=(m-1/2)\Delta r} \cong (m-1/2)(T_{m,j} - T_{m-1,j})$$

$$\therefore \frac{1}{r}\frac{\partial}{\partial r}\left(r\frac{\partial T}{\partial r}\right)\Big|_{r=m\Delta r} \cong \frac{1}{m(\Delta r)^2}\left[(m-1/2)T_{m+1,j} - 2T_{m,j} + (m-1/2)T_{m-1,j}\right]$$

$$\cong \frac{1}{(\Delta r)^2}\left[(T_{m+1,j} - 2T_{m,j} + T_{m-1,j}) + \frac{1}{2m}(T_{m+1,j} - T_{m-1,j})\right]$$

$$\frac{\partial T}{\partial r}\Big|_{r=m\Delta r} \cong \frac{1}{2(\Delta r)}(T_{m+1,j} - T_{m-1,j})$$

$$\frac{\partial T}{\partial r}\Big|_{r=m\Delta r} \cong \frac{1}{2(\Delta r)}(K_{m+1,j} - K_{m-1,j})$$

$$\therefore \frac{1}{K}\frac{\partial K}{\partial r}\frac{\partial T}{\partial r}\Big|_{r=m\Delta r} \cong \frac{1}{(\Delta r)^2}\frac{1}{4K_{m,j}}(K_{m+1,j} - K_{m-1,j})(T_{m+1,j} - T_{m-1,j})$$

In terms of these approximations (when the radial position is measured in terms of the parameter $x = r/r_1$) (Eq. 1), for heat flow in cylindrical coordinates, may be written in the following finite difference form:

$$(3) \qquad T_{m,j+1} - T_{m,j} \cong \left(\frac{2q_{m,j}}{r_1^2}\,\frac{\Delta t_{j+1}}{(\Delta x)^2}\right)\left\{\frac{1}{2}\left[\left(T_{m+1,j} - 2T_{m,j} + T_{m-1,j}\right) + \frac{1}{2m}\left(T_{m+1,j} - T_{m-1,j}\right)\right] + \frac{1}{8K_{m,j}}\left(K_{m+1,j} - K_{m-1,j}\right)\left(T_{m+1,j} - T_{m-1,j}\right)\right\}$$

With the equation for heat flow in cylindrical coordinates written in the finite difference form of (Eq. 3), the development of a semi-graphical technique for the solution of the temperature problem proceeds from the demonstration that there is a graphical construction, first developed by V. E. Schmidt (12), which gives the value of the following term of (Eq. 3):

$$\frac{1}{2}\left[\left(T_{m+1,j} - 2T_{m,j} + T_{m-1,j}\right) + \frac{1}{2m}\left(T_{m+1,j} - T_{m-1,j}\right)\right]$$

To carry out this demonstration, consider the following graphical construction and development:

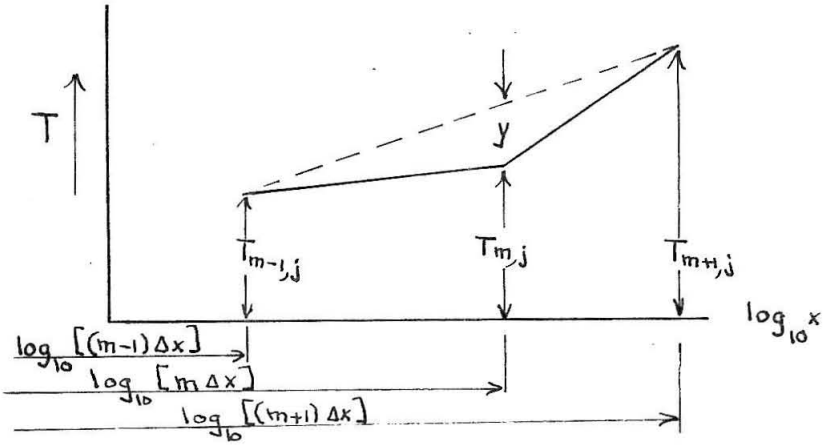

It will now be shown that the distance y in this construction is approximately equal to the desired term. By the principles of geometry, the distance y becomes:

$$y = \left(T_{m+1,j} - T_{m-1,j}\right)\left[\frac{\log_{10}[m\Delta x] - \log_{10}[(m-1)\Delta x]}{\log_{10}[(m+1)\Delta x] - \log_{10}[(m-1)\Delta x]}\right] - \left(T_{m,j} - T_{m-1,j}\right)$$

$$= \frac{\log_{10}\frac{m}{m-1}}{\log_{10}\frac{m+1}{m-1}}\left(T_{m+1,j} - T_{m-1,j}\right) - \left(T_{m,j} - T_{m-1,j}\right)$$

The series expansion for the logarithmic term is:

$$\frac{\log_{10}\frac{m}{m-1}}{\log_{10}\frac{m+1}{m-1}} = \frac{\left(\frac{1}{m} + \frac{1}{m^2} + \frac{1}{m^3} + \text{-----}\right)}{\frac{1}{2}\left(\frac{1}{m} + \frac{1}{3m^3} + \frac{1}{5m^5} + \text{----}\right)} = \frac{1}{2} + \frac{1}{4m} + \frac{1}{12m^3} + \frac{7}{180m^5} + \text{-----}$$

On neglecting the third and higher order terms this becomes:

$$\frac{\log_{10}\frac{m}{m-1}}{\log_{10}\frac{m+1}{m-1}} \simeq \frac{1}{2}\left(1 - \frac{1}{2m}\right)$$

Using this value for the logarithmic function, the distance y becomes:

$$y \simeq \frac{1}{2}\left[\left(T_{m+1,j} - 2T_{m,j} + T_{m-1,j}\right) + \frac{1}{2m}\left(T_{m+1,j} - T_{m-1,j}\right)\right]$$

This is the value of the required term of (Eq. 3).

Since the graphical construction just developed uses $\log_{10}x$ for the radial position parameter, the further development of a semigraphical method for the solution of the temperature problem requires that the boundary condition, (Eq. 2), be expressed in terms of this variable.

This may be done by noting that:

$$\left.\frac{\partial T}{\partial x}\right|_{x=1} = \frac{\partial T}{\partial(\log_{10} x)} \left.\frac{d(\log_{10} x)}{dx}\right|_{x=1} = \left.\frac{1}{x}\log_{10} e \frac{\partial T}{\partial(\log_{10} x)}\right|_{x=1} = \left.\log_{10} e \frac{\partial T}{\partial(\log_{10} x)}\right|_{x=1}$$

(Eq. 2), therefore, becomes:

$$(4) \qquad \left.\frac{\partial T}{\partial(\log_{10} x)}\right|_{x=1} = -\left.\frac{r_1 h}{k \log_{10} e}(T - T_0)\right|_{x=1}$$

The complete development of a semigraphical technique for the solution of the temperature problem may now be made most easily by referring to (Fig. 1). While this represents a specific example, made with $n = 5$ or $\Delta x = 0.2$, the technique is general. The first step is to select a value of Δt such that the function $2a_{m,j}\Delta t/r_1^2(\Delta x)^2$ has approximately the value 1.0 for the range of temperatures which will be encountered. Values of this function which are less than 0.5 make the solution unnecessarily tedious, while values in excess of 1.5 may result in poor convergence due to excessive magnification of any graphical or difference equation approximation errors. This function is then plotted on the right, as shown in (Fig. 1), to the same scale of temperature as is used for the temperature distribution. The thermal conductivity, k and 8k are plotted on the right in a similar manner.

The value of the function:

$$\frac{1}{2}\left[\left(T_{m+1,j} - 2T_{m,j} + T_{m-1,j}\right) + \frac{1}{2m}\left(T_{m+1,j} - T_{m-1,j}\right)\right]$$

is then obtained for every value of m by applying the graphical const-

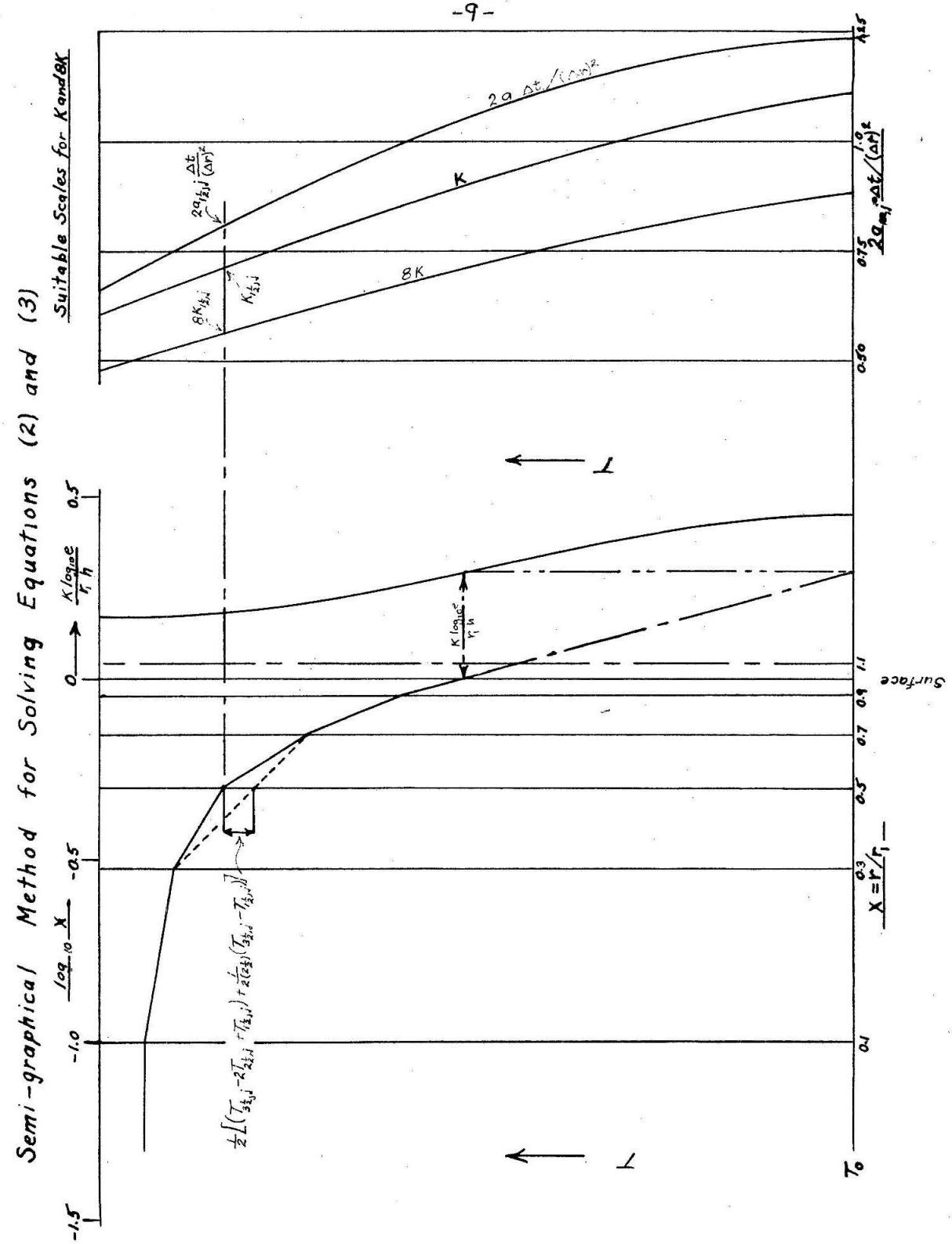
Semi-graphical Method for Solving Equations (2) and (3)
Suitable Scales for K and δK
2q Δt/(Δr)²
K
δK
Surface
T
T₀
X = r/r₁

(Fig. 1)

ruction developed on page 6, and indicated for one value of m by the dotted line in (Fig. 1). Note that for $m = \frac{1}{2}$, the value of this function is obtained by drawing a horizontal line from the temperature at $m = 1\frac{1}{2}$, and that for $m = n-\frac{1}{2}$, the value of this function is obtained from the neighboring points, one of which is in a fictitious layer at a distance $\Delta x/2$ beyond the surface of the cylinder.

The value of the function:

$$\frac{1}{8K_{m,j}}\left(K_{m+1,j} - K_{m-1,j}\right)\left(T_{m+1,j} - T_{m-1,j}\right)$$

is then obtained by carrying out the indicated operations upon the values of $T_{m+1,j}$, $T_{m-1,j}$, the corresponding values of $k_{m+1,j}$, $k_{m-1,j}$, and the value of $8k_{m,j}$ (corresponding to $T_{m,j}$) which are read directly from (Fig. 1).

The sum of these two functions is then multiplied by the corresponding value of $2a_{m,j}\Delta t_{j+1}/r_1^2(\Delta x)^2$, which is also read directly from (Fig. 1). This results in the increment of temperature during the interval Δt_{j+1}:

$$(3)\qquad T_{m,j+1} - T_{m,j} = \left(\frac{2a_{m,j}}{r_1^2}\,\frac{\Delta t_{j+1}}{(\Delta x)^2}\right)\left\{\frac{1}{2}\left[\left(T_{m+1,j} - 2T_{m,j} + T_{m-1,j}\right) + \frac{1}{2m}\left(T_{m+1,j} - T_{m-1,j}\right)\right] + \frac{1}{8K_{m,j}}\left(K_{m+1,j} - K_{m-1,j}\right)\left(T_{m+1,j} - T_{m-1,j}\right)\right\}$$

This increment of temperature $T_{m,j+1} - T_{m,j}$, is then added to the existing temperature $T_{m,j}$, for every value of m from $m = \frac{1}{2}$ to $m = n-\frac{1}{2}$,

giving the temperature $T_{n,j+1}$ at the end of the succeeding time interval for the interior points of the cylinder.

The temperature at the surface of the cylinder is then determined by drawing a straight line from the point $T_{n-\frac{1}{2},j+1}$ in such a manner that it intersects the surface of the cylinder with a slope which satisfies the boundary condition:

$$(4) \qquad \left.\frac{\partial T}{\partial(\log_{10} x)}\right|_{x=1} = -\frac{\eta h}{k(\log_{10} e)}\left(T - T_o\right)\Big|_{x=1}$$

When h is assumed to be a known function of the surface temperature of the cylinder, (Eq. 4) may be satisfied by the application of the steps which follow. These steps are illustrated in (Fig. 1) for the temperature distribution at the time t_j.

The function $k \log_{10} e/r_1 h$ is plotted as a distance from the surface of the cylinder versus temperature, where the unit of length is the length of one cycle of the $\log_{10} x$ scale.

A straight line is then drawn from the point $T_{n-\frac{1}{2},j}$, in such a manner that it intersects the datum temperature line T_o at a distance $k \log_{10} e/r_1 h$ from the surface of the cylinder. By the principles of geometry, the slope of this line at the surface of the cylinder is given by (Eq. 4). Referring to (Fig. 1), it is evident that, in spite of the interrelationship between the intercept distance and the surface temperature, this line is readily drawn with the aid of a little graphical trial and error.

The intersection of this line with the fictitious surface, $\Delta x/2$ from the true surface of the cylinder, is considered to be the temperature $T_{n+\frac{1}{2},j}$, which is required in the succeeding calculation for the determination of $T_{n-\frac{1}{2},j+1}$.

The technique required to determine the temperature distribution at the time $t_j+\Delta t_{j+1}$, from the temperature at the time t_j, has now been indicated. For the determination of the temperature distribution at a later time, the calculation is merely repeated until that time is reached.

The development of a semigraphical method for the prediction of the temperature as a function of the radial position and time, in an infinitely long solid isotropic cylinder resulting from a symmetrical quench in a large body of fluid, may now be considered complete, except for a discussion of some minor points in the utilization of the method.

The labor involved in carrying out a numerical solution will be a minimum if the number of intervals n into which the radius is divided is kept as small as is consistent with the required accuracy: the number of points at which the temperature is determined, a rough measure of the labor involved, is proportional to the cube of n. This means, in general, that it is desirable to decrease the value of n as the solution progresses and the temperature distribution becomes less irregular. To change the value of n to n', draw a smooth curve through the last values of the temperatures $T_{m,j}$ and consider that the intersections of this curve with the new intervals define the values of $T_{m',j}$, which will be used in the continued calculation.

The technique developed for the determination of the temperature distribution in the interior of the cylinder is quite general and may be adapted for use with completely different boundary conditions. As long as the heat flow through the surface of the cylinder is a known function of the surface temperature and, or, time, the problem may be solved. For example, if the cylinder were heated by radiation, the boundary conditions might be of the form:

$$\left.\frac{\partial T}{\partial r}\right|_{r=r_i} = -\frac{\alpha}{K}\left(T^4 - T_o^4\right)\Big|_{r=r_i}$$

where α is a function of the emissivities and T_o is the temperature of the radiating body. Another example, which could be handled, would be a quench into a small body of fluid, where the bulk temperature of the fluid T_o is a function of the time integral of the heat flow across the surface of the cylinder, and where the boundary layer conductivity is a function of this bulk temperature as well as the surface temperature of the cylinder. To recapitulate, any boundary condition which in a calculable manner determines the rate of heat flow through the surface of the cylinder may be used with the techniques developed in this chapter to determine the temperature as a function of the radial position and time.

A completely different type of boundary condition, which could be handled, is that of requiring the temperature at some point in the body, preferably near the surface, to be a known function of time. This type of boundary condition is the most satisfactory for an actual physical case where such a temperature can be experimentally determined, since it

eliminates all of the errors inherent in the assumption of the value of the boundary layer conductivity.

CHAPTER II

This chapter will be devoted to the extension of the homogeneous-isotropic theory of elasticity to include the effects of thermal dilation, residual strain and the variation of physical properties with position due to temperature (or other) effects. The basic assumption used is that there are values of Young's Modulus E and Poisson's Ratio ν which are unique functions of the temperature (or of position and time) only, and which relate, through Hooke's Law, the changes in strain with the changes in stress which occur in an element of the body if the stresses are removed from that element of the body but no other changes take place.

The development will start from the unchanged equations of equilibrium and compatability and will proceed, through the use of the concepts of "strains caused by stresses" (in the unloading sense of the basic assumption), "strains of thermal dilation" and "residual strains", to a modified form of Hooke's Law which relates the stresses to the total strains. The equations of equilibrium, compatability and this modified Hooke's Law, together with the boundary conditions, define a unique stress solution in terms of the thermal dilation and the residual strains. It will then be shown that this solution may be divided up into stresses due to the thermal dilation, stresses due to the boundary forces and stresses due to the residual strains. In Chapter IV it will be shown how stresses due to the first two factors, with additional information in the form of a theory of strength, may be used to determine the values of the residual strains as a function of position and time.

The following notation will be used in this chapter:

Let: E	be Young's Modulus for unloading.
ν	be Poisson's Ratio for unloading.
G	$= E / 2(1 + \nu)$.
$x,\ y,\ z$	be rectangular coordinates.
$\sigma_x,\ \sigma_y,\ \sigma_z$	be the normal stresses.
$\tau_{xy},\ \tau_{yz},\ \tau_{zx}$	be the shear stresses.
$u_x,\ u_y,\ u_z$	be the components of displacement of a point.
$\epsilon_x,\ \epsilon_y,\ \epsilon_z$	be the normal strains.
$\gamma_{xy},\ \gamma_{yz},\ \gamma_{zx}$	be the shear strains.
$\epsilon_x^\sigma,\ \epsilon_y^\sigma,\ \epsilon_z^\sigma$	be the normal strains caused by stresses.
$\gamma_{xy}^\sigma,\ \gamma_{yz}^\sigma,\ \gamma_{zx}^\sigma$	be the shear strains caused by stresses.
$\epsilon_x^\circ,\ \epsilon_y^\circ,\ \epsilon_z^\circ$	be the residual normal strains.
$\gamma_{xy}^\circ,\ \gamma_{yz}^\circ,\ \gamma_{zx}^\circ$	be the residual shear strains.
ϵ^T	be the linear component of the thermal dilation.
$s_x,\ s_y,\ s_z$	be the components of the surface forces per unit surface area.
$\ell_x,\ \ell_y,\ \ell_z,$	be the direction cosines of the external normal to the surface of the body at the point under consideration.

The subscript 1 refers to stresses, displacements and strains due to thermal dilation.

The subscript 2 refers to stresses, displacements and strains due to boundary forces.

The subscript 3 refers to stresses, displacements and strains due to residual strains.

The equations of equilibrium are well known* and, assuming that there are no body forces, may be written in the following form:

$$\frac{\partial \sigma_x}{\partial x} + \frac{\partial \tau_{xy}}{\partial y} + \frac{\partial \tau_{zx}}{\partial z} = 0$$

$$\frac{\partial \sigma_y}{\partial y} + \frac{\partial \tau_{yz}}{\partial z} + \frac{\partial \tau_{xy}}{\partial x} = 0$$

$$\frac{\partial \sigma_z}{\partial z} + \frac{\partial \tau_{zx}}{\partial x} + \frac{\partial \tau_{yz}}{\partial y} = 0$$

If the boundary conditions are introduced as known forces on the surface of the body, they may be written in the following form:

$$\sigma_x l_x + \tau_{xy} l_y + \tau_{zx} l_z = S_x$$

$$\sigma_y l_y + \tau_{yz} l_z + \tau_{xy} l_x = S_y$$

$$\sigma_z l_z + \tau_{zx} l_x + \tau_{yz} l_y = S_z$$

Within the limitations of small displacements, as used by Timoshenko, the equations of compatability may be written in the following form:

---

* The development of the equations of equilibrium, compatibility, and the ordinary form of Hooke's Law, the techniques for eliminating the displacements and the strains from the equations, the proof of the uniqueness of the stress solution and etc. are given in Timoshenko, "Theory of Elasticity". The reader is referred to this text as a background for this chapter.

$$\epsilon_x = \frac{\partial u_x}{\partial x} \qquad \gamma_{xy} = \frac{\partial u_x}{\partial y} + \frac{\partial u_y}{\partial x}$$

$$\epsilon_y = \frac{\partial u_y}{\partial y} \qquad \gamma_{yz} = \frac{\partial u_y}{\partial z} + \frac{\partial u_z}{\partial y}$$

$$\epsilon_z = \frac{\partial u_z}{\partial z} \qquad \gamma_{zx} = \frac{\partial u_z}{\partial x} + \frac{\partial u_x}{\partial z}$$

In these equations it is assumed that the displacements are small quantities varying continuously over the volume of the body.

If it is possible to relate the stresses to the strains, there will be a unique stress solution which satisfies the equations of equilibrium and compatibility and which matches the boundary conditions. Hooke's Law, as it is ordinarily presented, relates the stresses to the strains when E and ν are assumed to be constant and there are no thermal dilation or residual strain terms. In the following section, a modified form of Hooke's Law will be developed which will include these factors. This development will proceed from the definition of the following concepts: "strains caused by stresses", "strains of thermal dilation", and "residual strains".

In defining the concept "strains caused by stresses", it will be necessary to generalize Hooke's Law by the understanding that E and ν are variables of position and time but are not functions of the stress level, and it will be necessary to restrict Hooke's Law by defining "strains caused by stresses" in such a manner that yielding or creep do not affect it's validity.

The strains caused by the stresses are defined to be the negative of the changes of the strains which would appear if the stresses were removed from an infinitesmal element of the body, but all other conditions were kept constant. It will further be assumed that there are known values of E and ν, which are unique functions of the temperature only (more generally, which are unique functions of position and time, but which are independent of the stress level), which when put into the following equations will properly relate the strains and stresses described above.

$$\epsilon_x^\sigma = \frac{1}{E}\left[\sigma_x - \nu(\sigma_y + \sigma_z)\right] \qquad \gamma_{xy} = \frac{1}{G}\tau_{xy}$$

$$\epsilon_y^\sigma = \frac{1}{E}\left[\sigma_y - \nu(\sigma_z + \sigma_x)\right] \qquad \gamma_{yz} = \frac{1}{G}\tau_{yz}$$

$$\epsilon_z^\sigma = \frac{1}{E}\left[\sigma_z - \nu(\sigma_x + \sigma_y)\right] \qquad \gamma_{zx} = \frac{1}{G}\tau_{zx}$$

In these equations ϵ_x^σ, ϵ_y^σ, ϵ_z^σ and γ_{xy}^σ, γ_{yz}^σ, γ_{zx}^σ are the negative of the changes of the strains which would appear if the stresses, σ_x, σ_y, σ_z and τ_{xy}, τ_{yz}, τ_{zx} were removed from an infinitesimal element of the body, but all other conditions were kept constant. G is defined to be: $G = E/2(1+\nu)$.

The concept of "strains of thermal dilation" may be illustrated in the following way. Consider an infinitesmal element of the body, from which the stresses have been removed; in general it will not have the same volume as it had in the original state. The strains which result in this volume change are defined to be the "strains of thermal dilation",

and will be denoted by:

$$\epsilon_x^T = \epsilon_y^T = \epsilon_z^T = \epsilon^T \qquad \gamma_{xy}^T = \gamma_{yz}^T = \gamma_{zx}^T = 0$$

Only one symbol, ϵ^T, is necessary to describe these strains, since they are the linear components of a volume change and are, by the assumption of isotropy, presumed to be equal in all directions. It will further be assumed that the value of ϵ^T is a known function of the temperature only (or more generally, of position and time only). In the literature, this term is commonly approximated by $\epsilon^T = \alpha T$, where α is the coefficient of linear thermal expansion.

The concept of "residual strains" may be illustrated in the following way. Consider an infinitesimal element of the body, from which the stresses have been removed; in general the element will not have the same shape as it had in the original state. The strains which are responsible for this change of shape will be defined to be the "residual strains". These strains correspond to the amount the element has yielded during it's past history, and are sometimes called plastic strains or permanent strains. Strains of this type will be denoted as follows:

$$\epsilon_x^0, \ \epsilon_y^0, \ \epsilon_z^0, \quad \text{and} \quad \gamma_{xy}^0, \ \gamma_{yz}^0, \ \gamma_{zx}^0$$

It will be assumed that these strains do not change the volume of the element, i.e.:

$$\epsilon_x^0 + \epsilon_y^0 + \epsilon_z^0 = 0$$

These concepts will now be synthesized into a modified form of Hooke's Law which will relate the stresses to the strains, when residual strains and thermal dilation are present. The strains actually present in the body corresponds to the sum of the three types of strains defined in the previous paragraphs. It is possible, therefore, to write the following equations to replace the usual form of Hooke's Law:

$$\epsilon_x = \epsilon_x^{\sigma} + \epsilon^{T} + \epsilon_x^{o} = \frac{1}{E}\left[\sigma_x - \nu(\sigma_y + \sigma_z)\right] + \epsilon^{T} + \epsilon_x^{o}$$

$$\epsilon_y = \epsilon_y^{\sigma} + \epsilon^{T} + \epsilon_y^{o} = \frac{1}{E}\left[\sigma_y - \nu(\sigma_z + \sigma_x)\right] + \epsilon^{T} + \epsilon_y^{o}$$

$$\epsilon_z = \epsilon_z^{\sigma} + \epsilon^{T} + \epsilon_z^{o} = \frac{1}{E}\left[\sigma_z - \nu(\sigma_x + \sigma_y)\right] + \epsilon^{T} + \epsilon_z^{o}$$

$$\gamma_{xy} = \gamma_{xy}^{\sigma} + \gamma_{xy}^{o} = \frac{1}{G}\tau_{xy} + \gamma_{xy}^{o}$$

$$\gamma_{yz} = \gamma_{yz}^{\sigma} + \gamma_{yz}^{o} = \frac{1}{G}\tau_{yz} + \gamma_{yz}^{o}$$

$$\gamma_{zx} = \gamma_{zx}^{\sigma} + \gamma_{zx}^{o} = \frac{1}{G}\tau_{zx} + \gamma_{zx}^{o}$$

If it is assumed that the value of the thermal dilation and the values of the residual strains are known functions of position at any time, then at that time these equations relate the stresses to the strains. Under these circumstances, the above equations, together with the boundary conditions and the equations of equilibrium and compatibility, form a set of equations which uniquely determine the stress distribution in the body.

The next step in the development will be to show that the solution for the stresses, determined from this set of equations may be divided into three parts: the stresses due to the thermal dilation, the stresses due to the boundary forces, and the stresses due to the residual strains. The necessity for this division, and also for the division of the stresses due to residual strains into two parts, will appear in Chapter IV, where the techniques for determining the values of the residual strains as a function of position and time are developed. These techniques depend upon the introduction of additional information in the form of a theory of strength, and further discussion of them will be deferred until Chapter IV.

The separability of the solution into stresses due to thermal dilation, stresses due to boundary forces, and stresses due to residual strains may be indicated by showing that the sum of the solutions, due to each of these factors, satisfies the original set of equations. When this is shown, the separability follows from the uniqueness of the separate and complete solutions.

The set of equations which define the complete solution are repeated below. For purposes of simplicity, only the first of the equations of each type are written, the other two of each type being obtained by a cyclic permutation of the subscripts.

Equilibrium: Inside the body: $$\frac{\partial \sigma_x}{\partial x} + \frac{\partial \tau_{xy}}{\partial y} + \frac{\partial \tau_{zx}}{\partial z} = 0$$

At the surface : $$\sigma_x \ell_x + \tau_{xy} \ell_y + \tau_{zx} \ell_z = S_x$$

Compatibility:

$$\epsilon_x = \frac{\partial u_x}{\partial x}$$

$$\gamma_{xy} = \frac{\partial u_y}{\partial z} + \frac{\partial u_z}{\partial y}$$

Modified Hooke's Law:

$$\epsilon_x = \frac{1}{E}\left[\sigma_x - \nu(\sigma_y + \sigma_z)\right] + \epsilon^T + \epsilon_x^\circ$$

$$\gamma_{xy} = \frac{1}{G}\tau_{xy} + \gamma_{xy}^\circ$$

In these equations, at any given time, the elastic constants, the thermal dilation, the residual strains, and the components of the surface forces are presumed to be known functions of position, and the stresses, strains, and displacements are presumed to be unknowns. The uniqueness of the solution will not be proved here, but it is indicated since there are 15 unknowns and 15 equations which apply to the interior of the body.

The set of equations which define the stresses due to the residual strains are presented below. This set of equations is identical to the original set except that the boundary forces and the residual strains are set equal to zero. The solution to these equations for the stresses, strains, and displacements are denoted by the subscript 1. (Again, only one third of the equations are written, the remainder being obtained by cyclic permutation of the subscripts.)

Equilibrium: Inside the body:

$$\frac{\partial \sigma_{x_1}}{\partial x} + \frac{\partial \tau_{xy_1}}{\partial y} + \frac{\partial \tau_{zx_1}}{\partial z} = 0$$

At the surface:

$$\sigma_{x_1} \ell_x + \tau_{xy_1} \ell_y + \tau_{zx_1} \ell_z = 0$$

Compatibility:

$$\epsilon_{x_1} = \frac{\partial u_{x_1}}{\partial x}$$

$$\gamma_{xy_1} = \frac{\partial u_{y_1}}{\partial z} + \frac{\partial u_{z_1}}{\partial y}$$

Modified Hooke's Law:

$$\epsilon_{x_1} = \frac{1}{E}\left[\sigma_{x_1} - \nu(\sigma_{y_1} + \sigma_{z_1})\right] + \epsilon^T$$

$$\gamma_{xy_1} = \frac{1}{G}\tau_{xy_1}$$

The set of equations which define the stresses due to the boundary forces are presented below. This set of equations is identical to the original set except that the thermal dilation and the residual strains are set equal to zero. The solution to these equations for the stresses, strains, and displacements are denoted by the subscript 2 . (Only one third of the equations are written.)

Equilibrium: Inside the body:

$$\frac{\partial \sigma_{x_2}}{\partial x} + \frac{\partial \tau_{xy_2}}{\partial y} + \frac{\partial \tau_{zx_2}}{\partial z} = 0$$

At the surface :

$$\sigma_{x_2} \ell_x + \tau_{xy_2} \ell_y + \tau_{zx_2} \ell_z = S_x$$

Compatibility:

$$\epsilon_{x_2} = \frac{\partial u_{x_2}}{\partial x}$$

$$\gamma_{xy_2} = \frac{\partial u_{y_2}}{\partial z} + \frac{\partial u_{z_2}}{\partial y}$$

Modified Hooke's Law:

$$\epsilon_{x_2} = \frac{1}{E}\left[\sigma_{x_2} - \nu(\sigma_{y_2} + \sigma_{z_2})\right]$$

$$\gamma_{xy_2} = \frac{1}{G}\tau_{xy_2}$$

The set of equations which define the stresses due to the residual strains are presented below. This set of equations is identical to the original set except that the thermal dilation and the boundary forces are set equal to zero. The solution to these equations for the stresses, strains, and displacements are denoted by the subscript 3 . (Only one third of the equations are written.)

Equilibrium: Inside the body: $$\frac{\partial \sigma_{x_3}}{\partial x} + \frac{\partial \tau_{xy_3}}{\partial y} + \frac{\partial \tau_{zx_3}}{\partial z} = 0$$

At the surface : $$\sigma_{x_3} \ell_x + \tau_{xy_3} \ell_y + \tau_{zx_3} \ell_z = 0$$

Compatability: $$\epsilon_{x_3} = \frac{\partial u_{x_3}}{\partial x}$$

$$\gamma_{xy_3} = \frac{\partial u_{y_3}}{\partial z} + \frac{\partial u_{z_3}}{\partial y}$$

Modified Hooke's Law: $$\epsilon_{x_3} = \frac{1}{E}\left[\sigma_{x_3} - \nu(\sigma_{y_3} + \sigma_{z_3})\right] + \epsilon^{o}_{x_3}$$

$$\gamma_{xy_3} = \frac{1}{G}\tau_{xy_3} + \gamma^{o}_{xy}$$

The equations of equilibrium, compatability, and Modified Hooke's Law which the sum of the separate solutions satisfy may be obtained by addition. The equations are: (Only one third of the equations are written.)

Equilibrium: Inside the body:

$$\frac{\partial}{\partial x}(\sigma_{x_1} + \sigma_{x_2} + \sigma_{x_3}) + \frac{\partial}{\partial y}(\tau_{xy_1} + \tau_{xy_2} + \tau_{xy_3}) + \frac{\partial}{\partial z}(\tau_{zx_1} + \tau_{zx_2} + \tau_{zx_3}) = 0$$

Equilibrium: At the surface:

$$(\sigma_{x_1}+\sigma_{x_2}+\sigma_{x_3})\,l_x + (\tau_{xy_1}+\tau_{xy_2}+\tau_{xy_3})\,l_y + (\tau_{zx_1}+\tau_{zx_2}+\tau_{zx_3}) = S_x$$

Compatability: $$(\epsilon_{x_1}+\epsilon_{x_2}+\epsilon_{x_3}) = \frac{\partial}{\partial x}(u_{x_1}+u_{x_2}+u_{x_3})$$

$$(\gamma_{xy_1}+\gamma_{xy_2}+\gamma_{xy_3}) = \frac{\partial}{\partial z}(u_{y_1}+u_{y_2}+u_{y_3}) + \frac{\partial}{\partial y}(u_{z_1}+u_{z_2}+u_{z_3})$$

Modified Hooke's Law:

$$(\epsilon_{x_1}+\epsilon_{x_2}+\epsilon_{x_3}) = \frac{1}{E}\left[(\sigma_{x_1}+\sigma_{x_2}+\sigma_{x_3}) - \nu\left\{(\sigma_{y_1}+\sigma_{y_2}+\sigma_{y_3})+(\sigma_{z_1}+\sigma_{z_2}+\sigma_{z_3})\right\}\right] + \alpha\epsilon^T + \epsilon_x^o$$

$$(\gamma_{xy_1}+\gamma_{xy_2}+\gamma_{xy_3}) = \frac{1}{G}(\tau_{xy_1}+\tau_{xy_2}+\tau_{xy_3}) + \gamma_{xy}^o$$

However, this set of equations is identical with the set of equations which defines the complete solution. Hence, if the sum of the separate solutions satisfies the set of equations which defines the complete solution, the sum of the separate solutions must be identical with the complete solution.

In a similar manner it could be shown that, within the solution for the stresses due to the residual strains, two solutions for the stresses due to different values of the residual strains are additive.

In this chapter a theory, which is an extension of the ordinary theory of elasticity, has been developed which includes the effects of thermal dilation and residual strain upon the stresses in a body. The

basic assumption required in this theory is that there are known values of Young's Modulus and Poisson's Ratio which are unique functions of the temperature (or more generally, functions of position and time which are independent of the stress level), and which relate, through Hooke's Law, the changes in the strains with the changes in the stresses in an element of the body when the stresses are removed from that element. The conceptions of "strains caused by stresses", "strains of thermal dilation", and "residual strains" have been defined. The set of equations which determines the stresses in terms of the boundary conditions, the thermal dilation, and the residual strains has been presented. The separability of the solution to this set of equations into the stresses due to thermal dilation, the stresses due to boundary forces, and the stresses due to residual strains has been indicated.

The theory has a wide range of applicability in the sense that almost all metals, within engineering temperature limits, reasonably satisfy the required assumptions. The present utility of the theory is , however, limited by the lack of adequate data on physical properties, particularly at higher temperatures, and by the mathematical difficulties involved in the determination of the values of the residual strains as a function of the stress-temperature history. Methods for determining the residual strains as a function of position and time, through the introduction of additional information in the form of a theory of strength will be developed in Chapter IV. A numerical example using a specific theory of strength is computed in Chapter VII.

CHAPTER III

This chapter will be devoted to the application of the theory of Chapter II to the case of an infinitely long solid isotropic cylinder, when all of the variables are functions of the radial position only. The set of equations whose solution gives the stresses will be derived. This set of equations will be divided into three sets, whose solutions give the stresses due to thermal dilation, the stresses due to the boundary forces, and the stresses due to the residual strains. Semigraphical techniques for the solution of these sets of equations will then be indicated. The sum of these solutions will correspond to the stresses existing at any particular time, and as such, all variations of the variables with time will be neglected.

The mathematical development proceeds from the assumptions that all factors are radially symmetrical, and that plane cross sections of the cylinder remain plane. With these assumptions, the principal stresses and strains coincide in direction with the directions of the cylindrical coordinates.

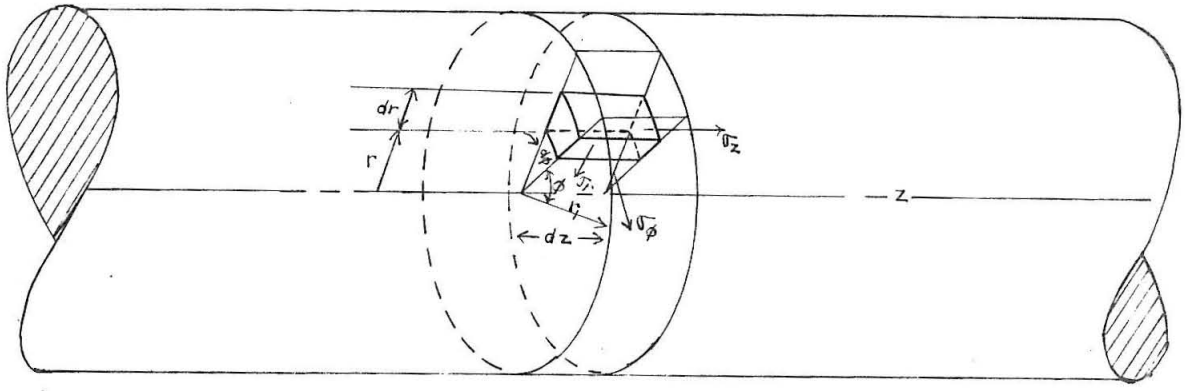

The following notation will be used in this chapter:

Let: E be Young's Modulus. (for unloading)

ν be Poisson's Ratio. (for unloading)

G $= E / 2(1 + \nu)$.

r, ϕ, z be the cylindrical coordinates.

r_1 be the outer radius of the cylinder.

A $= r^2/r_1^2$ (dimensionless radial position parameter).

σ_r, σ_ϕ, σ_z be the principal stresses.

$\bar{\sigma}_r$ be the 1'st approximation to the radial stress.

$\sigma_{z\ avg.}$ be the total axial force in the cylinder $/\pi r_1^2$

p be the external pressure.

ϵ_r, ϵ_ϕ, ϵ_z be the principal strains.

$\bar{\epsilon}_z$ be the 1'st approximation to the constant axial strain.

ϵ^T be the linear component of the thermal dilation. (normally considered zero at the center of the cyl.)

C be a constant of integration.

$\bar{C}$ be the 1'st approximation to this constant.

C' be an alternate form of the constant of integration.

$f_1(\sigma_r)$ $= \frac{2G}{1-\nu}\int_0^A \sigma_r \frac{d}{dA}\left(\frac{1}{2G}\right) dA$

$f_2(\sigma_r)$ $= \frac{2\nu G}{1-\nu}\int_0^A \sigma_r \frac{d}{dA}\left(\frac{1}{2G}\right) dA$

The subscripts 1, 2, and 3 refer to the separated solutions: the stresses due to thermal dilation, the stresses due to boundary forces, and the stresses due to residual strains, respectively. (Exceptions are the terms $f_1(\sigma_r)$, $f_2(\sigma_r)$, and r_1)

The pertinent equations for this specific problem appear below. The equations of equilibrium and compatibility are well known, and are presented without their derivation. The Modified Hooke's Law was developed in Chapter II, and the boundary conditions are self-explanatory.

Equilibrium:

$$\sigma_\phi = \frac{d}{dr}(r\sigma_r) \tag{5}$$

Compatibility:

$$\epsilon_r = \frac{d}{dr}(r\epsilon_\phi) \tag{6}$$

$$\epsilon_z = \text{constant} \tag{7}$$

Modified Hooke's Law:

$$\epsilon_r = \frac{1}{E}\left[\sigma_r - \nu(\sigma_\phi + \sigma_z)\right] + \epsilon_r^o + \epsilon^T \tag{8}$$

$$\epsilon_\phi = \frac{1}{E}\left[\sigma_\phi - \nu(\sigma_z + \sigma_r)\right] + \epsilon_\phi^o + \epsilon^T \tag{9}$$

$$\epsilon_z = \frac{1}{E}\left[\sigma_z - \nu(\sigma_r - \sigma_\phi)\right] + \epsilon_z^\bullet - \epsilon^T \tag{10}$$

Boundary Conditions:

$$\sigma_r\Big|_{r=0} < \infty \tag{11}$$

$$\sigma_r\Big|_{r=r_i} = -p \tag{12}$$

$$\int_0^{r_i} \sigma_z \, 2\pi r \, dr = \pi r_i^2 \, \sigma_{z\,avg.} \tag{13}$$

The manipulation of these equations required to eliminate the unknown variable strains ϵ_r and ϵ_ϕ, and to form a set of equations from which the stresses may be readily determined, will now be made. In particular, the equations will be expressed in terms of the radial position parameter, $A = r^2/r_1^2$, since the final equations have their simplest form in terms of this variable.

By suitable manipulation, (Eq. 5) may be written in terms of the variable A in either of the following equivalent forms:

$$(5a) \qquad \frac{\sigma_\phi - \sigma_r}{2A} = \frac{d\sigma_r}{dA}$$

$$(5b) \qquad \sigma_\phi + \sigma_r = 2\frac{d}{dA}(A\sigma_r)$$

In a similar fashion, (Eq. 6) may be written in terms of the variable A in the following form:

$$(6a) \qquad \frac{\epsilon_r - \epsilon_\phi}{2A} = \frac{d\epsilon_\phi}{dA}$$

The solution of (Eq. 10) for σ_z gives the following alternate form for that equation:

$$(10a) \qquad \sigma_z = \nu(\sigma_\phi + \sigma_r) + E(\epsilon_z - \epsilon_z^\circ - \epsilon^T)$$

The substitution of (Eq. 10a) in (Eq. 9) results in the following alternate form for (Eq. 9), in which σ_z is eliminated.

$$(9a) \qquad \epsilon_\phi = \frac{1+\nu}{E}\left[(1-\nu)\sigma_\phi - \nu\sigma_r\right] + (1+\nu)\epsilon^T + \epsilon_\phi^\circ + \nu(\epsilon_z^\circ - \epsilon_z)$$

The subtraction of (Eq. 9) from (Eq. 8), followed by the division of the difference by 2A, results in (Eq. 14) below. The substitution of (Eq. 5a) in (Eq. 14) results in (Eq. 14a). (Eq. 14b) is an alternate form of (Eq. 14a).

$$(14) \qquad \frac{\epsilon_r - \epsilon_\phi}{2A} = -\frac{1+\nu}{E}\,\frac{\sigma_\phi - \sigma_r}{2A} - \frac{\epsilon_\phi^\circ - \epsilon_r^\circ}{2A}$$

$$(14a) \qquad = -\frac{1+\nu}{E}\,\frac{d\sigma_r}{dA} - \frac{\epsilon_\phi^\circ - \epsilon_r^\circ}{2A}$$

$$(14b) \qquad = -\frac{d}{dA}\left(\frac{1+\nu}{E}\sigma_r\right) + \sigma_r\frac{d}{dA}\left(\frac{1+\nu}{E}\right) - \frac{\epsilon_\phi^\circ - \epsilon_r^\circ}{2A}$$

The substitution of (Eq. 9a) in the right hand side of (Eq. 6a) results in another equation containing the term $(\epsilon_r - \epsilon_\phi)/2A$.

$$(15) \qquad \frac{\epsilon_r - \epsilon_\phi}{2A} = \frac{d}{dA}\left\{\frac{1+\nu}{E}\left[(1-\nu)\sigma_\phi - \nu\sigma_r\right] + (1-\nu)\epsilon^T + (\epsilon_\phi^\circ + \nu\epsilon_z^\circ) - \nu\epsilon_z\right\}$$

The elimination of $(\epsilon_r - \epsilon_\phi)/2A$ between (Eq. 14b) and (Eq. 15), followed by a single integration, results in :

$$(16) \qquad \frac{1-\nu^2}{E}(\sigma_\phi + \sigma_r) = \int_0^A \sigma_r \frac{d}{dA}\left(\frac{1+\nu}{E}\right)dA - \int_0^A \frac{\epsilon_\phi^\circ - \epsilon_r^\circ}{2A}\,dA$$
$$-(\epsilon_\phi^\circ + \nu\epsilon_z^\circ) - (1+\nu)\epsilon^T + \nu\epsilon_z + C$$

In (Eq. 16), C is the constant of integration, and the limits of integration, 0 to A , are selected for later convenience. In this

equation, ϵ_z is a constant which has the status of a constant of integration. If ϵ_z had been eliminated earlier, one more integration would have been required, and this integration would have introduced a constant of integration equivalent to ϵ_z.

(Eq. 17) is an alternate form of (Eq. 16), in which the relationship, $2G = E/(1-\nu)$, has been used. The substitution of (Eq. 5b) in (Eq. 16) results in (Eq. 18), which contains σ_r as its only unknown variable of position.

$$(17)\qquad \sigma_\phi + \sigma_r = \; = \left[\frac{2G}{1-\nu} \int_0^A \sigma_r \frac{d}{dA}\left(\frac{1}{2\theta}\right) dA - \frac{2G}{1-\nu} \int_0^A \frac{\epsilon_\phi^\circ - \epsilon_r^\circ}{2A} dA \right.$$

$$(18)\qquad 2\frac{d}{dA}(A\sigma_r) = \qquad \left. - \frac{2G}{1-\nu}\left(\epsilon_\phi^\circ + \nu\epsilon_z^\circ\right) - \frac{E}{1-\nu}\epsilon^T + \frac{2\nu G}{1-\nu}\epsilon_z + \frac{2G}{1-\nu} C \right]$$

The boundary conditions which apply to (Eq. 18), in terms of the variable A, are:

$$(19)\qquad 2A\sigma_r\Big|_{A=0} = 0$$

$$(20)\qquad 2A\sigma_r\Big|_{A=1} = -2p$$

The result of the substitution of (Eq. 17) in (Eq. 10a) is:

$$(21)\qquad \sigma_z = \frac{2\nu G}{1-\nu}\int_0^A \sigma_r \frac{d}{dA}\left(\frac{1}{2G}\right) dA - \frac{2\nu G}{1-\nu}\int_0^A \frac{\epsilon_\phi^\circ - \epsilon_r^\circ}{2A} dA$$

$$- \frac{2G}{1-\nu}\left(\nu\epsilon_\phi^\circ + \epsilon_z^\circ\right) - \frac{E}{1-\nu}\epsilon^T + \frac{2G}{1-\nu}\epsilon_z + \frac{2\nu G}{1-\nu} C$$

The boundary condition which applies to (Eq. 21), in terms of the variable A, is:

$$(22) \qquad \int_0^1 \sigma_z \, dA = \sigma_{z\,avg.}$$

The set of equations, (Eq. 17) through (Eq. 22), constitutes the basic relationships from which the stresses may be determined. The stresses σ_r and σ_z and the constants ϵ_z and C may be determined from the set of equations, (Eq. 18) through (Eq. 22). With these known, σ_ϕ may be determined from (Eq. 17). Using the notation,

$$f_1(\sigma_r) = \frac{2G}{1-\nu}\int_0^A \sigma_r \frac{d}{dA}\left(\frac{1}{2G}\right) dA \quad \text{and} \quad f_2(\sigma_r) = \frac{2\nu G}{1-\nu}\int_0^A \sigma_r \frac{d}{dA}\left(\frac{1}{2G}\right) dA \,,$$

the solution of the set of equations, (Eq. 18) through (Eq. 22), is complicated by the fact that the terms, $f_1(\sigma_r)$ and $f_2(\sigma_r)$, appear on the right hand side of (Eq. 18) and (Eq. 22) respectively. This difficulty can be circumvented by the use of Piccard's Method*. The following discussion indicates how the method will be applied to this case. The set of equations, (Eq. 18) through (Eq. 22) will be solved on the basis of the assumption that $f_1(\sigma_r) = f_2(\sigma_r) = 0$. This will result in a first approximation to the radial stress, which

---

* A discussion of Piccard's Method for solving equations in which an unknown appears in functional form as well as explicitly is given in many applied mathematics texts; for example, "Applied Mathematics for Engineers", Reddick and Miller, p 174.

will be denoted by $\bar{\sigma}_r$. A second approximation to σ_r may then be obtained by assuming that $f_1(\sigma_r) = f_1(\bar{\sigma}_r)$ and that $f_2(\sigma_r) = f_2(\bar{\sigma}_r)$ and solving (Eq. 18) through (Eq. 22) on the basis of this assumption. This process is continued until satisfactory values of σ_r versus A are obtained. When this is accomplished, σ_ϕ and σ_z may be determined from (Eq. 17) and (Eq. 21) respectively.

Before discussing in detail the technique of solving these equations, it will be convenient to divide this set of equations into three sets. These sets will determine the stresses due to the thermal dilation, the stresses due to the boundary forces, and the stresses due to the residual strains. The proof of this separability was indicated in Chapter II. The three sets of equations appear below. The sets will be distinguished by the subscripts 1, 2, and 3.

The stresses due to the thermal dilation:

$$\left.\begin{array}{ll} (17)_1 & \bar{\sigma}_{\phi_1} + \bar{\sigma}_{r_1} \\ (18)_1 & 2\frac{d}{dA}(A\bar{\sigma}_{r_1}) \end{array}\right\} = f_1(\bar{\sigma}_{r_1}) - \frac{E}{1-\nu}\epsilon^T + \frac{2\nu G}{1-\nu}\epsilon_{z_1} + \frac{2G}{1-\nu}C_1$$

$$(19)_1 \quad 2A\bar{\sigma}_{r_1}\Big|_{A=0} = 0 \qquad\qquad (20)_1 \quad 2A\bar{\sigma}_{r_1}\Big|_{A=1} = 0$$

$$(21)_1 \quad \bar{\sigma}_{z_1} = f_2(\bar{\sigma}_{r_1}) - \frac{E}{1-\nu}\epsilon^T + \frac{2G}{1-\nu}\epsilon_{z_1} + \frac{2\nu G}{1-\nu}C_1$$

$$(22)_1 \quad \int_0^1 \bar{\sigma}_{z_1}\, dA = 0$$

The stresses due to the boundary forces:

$$\left.\begin{array}{ll}(17)_2 & \sigma_{\phi_2}+\sigma_{r_2}\\ (18)_2 & 2\frac{d}{dA}(A\sigma_{r_2})\end{array}\right\} = f_1(\sigma_{r_2}) + \frac{2\nu G}{1-\nu}\epsilon_{z_2} + \frac{2G}{1-\nu}C_2$$

$$(19)_2 \quad 2A\sigma_{r_2}\Big|_{A=0} = 0 \qquad (20)_2 \quad 2A\sigma_{r_2}\Big|_{A=1} = -2p$$

$$(21)_2 \quad \sigma_{z_2} = f_2(\sigma_{r_2}) + \frac{2G}{1-\nu}\epsilon_{z_2} + \frac{2\nu G}{1-\nu}C_2$$

$$(22)_2 \quad \int_0^1 \sigma_{z_2}\,dA = \sigma_z \text{ avg.}$$

The stresses due to the residual strains:

$$\left.\begin{array}{ll}(17)_3 & \sigma_{\phi_3}+\sigma_{r_3}\\ (18)_3 & 2\frac{d}{dA}(A\sigma_{r_3})\end{array}\right\} = f_1(\sigma_{r_3}) - \frac{2G}{1-\nu}\int_0^A \frac{\epsilon^\circ_\phi-\epsilon^\circ_r}{2A}dA - \frac{2G}{1-\nu}(\epsilon^\circ_\phi+\nu\epsilon^\circ_z) + \frac{2\nu G}{1-\nu}\epsilon_{z_3} + \frac{2G}{1-\nu}C_3$$

$$(19)_3 \quad 2A\sigma_{r_3}\Big|_{A=0} = 0 \qquad (20)_3 \quad 2A\sigma_{r_3}\Big|_{A=1} = 0$$

$$(21)_3 \quad \sigma_{z_3} = f_2(\sigma_{r_3}) - \frac{2\nu G}{1-\nu}\int_0^A \frac{\epsilon^\circ_\phi-\epsilon^\circ_r}{2A}dA - \frac{2G}{1-\nu}(\nu\epsilon^\circ_\phi+\epsilon^\circ_z) + \frac{2G}{1-\nu}\epsilon_{z_3} + \frac{2\nu G}{1-\nu}C_3$$

$$(22)_3 \quad \int_0^1 \sigma_{z_3}\,dA = 0$$

As was indicated in Chapter II, the foregoing separation is possible if E, ν, and $2G = E/(1-\nu)$ are the same in each of the separated sets of equations. Since, in the complete calculation, the stresses of the first two kinds will be used, through some theory of strength, to predict the residual strains, the restrictions on E and ν take the following practical form. At any given time, E and ν must be known functions of position, independent of the stress level. The most useful form of this functional dependence will be that E and ν are known functions of the temperature. With this assumption, the particular separation indicated may be shown to be valid, since it is apparent that the sum of the separate solutions: $(\sigma_{r_1}+\sigma_{r_2}+\sigma_{r_3})$, $(\sigma_{\phi_1}+\sigma_{\phi_2}+\sigma_{\phi_3})$, $(\sigma_{z_1}+\sigma_{z_2}+\sigma_{z_3})$, $(\epsilon_{z_1}+\epsilon_{z_2}+\epsilon_{z_3})$, and $(C_1+C_2+C_3)$, must satisfy the original set of equations.

The remainder of this chapter will be devoted to the development of specific techniques for solving each of the separated sets of equations.

A semigraphical method for solving the set of equations which gives the stresses due to the thermal dilation will now be developed. At any given time, ϵ^T will be assumed to be a known (graphical) function of position, in the sense that it is a known (graphical) function of the temperature, and the temperature is a known (graphical) function of position. It is desirable to mention at this point that the solution to this set of equations for a constant value of ϵ^T is zero, or that the solution is independent of a constant part of ϵ^T. For example, if the data for ϵ^T is measured from a 20 °C base, and this data is called ϵ^T_{20}, then for later convenience in graphical integration, ϵ^T may be defined as follows:

$$\epsilon^T = \epsilon^T_{20} - \epsilon^T_{20}\Big|_{A=0}$$

When ϵ^T is defined in this manner, the axial strain ϵ_{z_1} becomes the difference between the existing axial strain and the axial strain which would be present if the cylinder were uniformly at the temperature of the center of the cylinder. i.e.:

$$\epsilon_{z_1} = (\epsilon_{z_1})_{20} - \epsilon^T\Big|_{A=0}$$

The first step in the development will be the introduction of a modified constant of integration:

$$C_1' = C_1 - \epsilon_{z_1}$$

The resulting modifications in $(\text{Eq. } 18)_1$ and $(\text{Eq. } 21)_1$ are made by noting that:

$$\frac{2\nu G}{1-\nu}\epsilon_{z_i} + \frac{2G}{1-\nu} C_1 = \frac{E}{1-\nu}\epsilon_{z_i} + \frac{2G}{1-\nu} C_1'$$

$$\frac{2G}{1-\nu}\epsilon_{z_i} + \frac{2\nu G}{1-\nu} C_1 = \frac{E}{1-\nu}\epsilon_{z_i} + \frac{2\nu G}{1-\nu} C_1'$$

This modification is made in order that in the first step of the iterative solution (Piccard's Method), the constant C_1' will be zero.

In terms of this alternate constant of integration, the set of

equations which give the stresses due to the thermal dilation are:

$$\left.\begin{array}{ll} (17a)_1 & \sigma_{\phi_1}+\sigma_{r_1} \\ (18a)_1 & 2\frac{d}{dA}(A\sigma_{r_1}) \end{array}\right\} = f_1(\sigma_{r_1}) - \frac{E}{1-\nu}\epsilon^T + \frac{E}{1-\nu}\epsilon_{z_1} + \frac{2G}{1-\nu}C_1'$$

$$(19)_1 \quad 2A\sigma_{r_1}\Big|_{A=0} = 0 \qquad (20)_1 \quad 2A\sigma_{r_1}\Big|_{A=1} = 0$$

$$(21a)_1 \quad \sigma_{z_1} = f_2(\sigma_{r_1}) - \frac{E}{1-\nu}\epsilon^T + \frac{E}{1-\nu}\epsilon_{z_1} + \frac{2\nu G}{1-\nu}C_1'$$

$$(22)_1 \quad \int_0^1 \sigma_{z_1}\, dA = 0$$

The results of the integration of $(\text{Eq. } 18a)_1$ and $(\text{Eq. } 21a)_1$ are indicated below.

$$(23)_1 \quad 2A\sigma_{r_1} = \int_0^A f_1(\sigma_{r_1})dA - \int_0^A \frac{E}{1-\nu}\epsilon^T dA + \epsilon_{z_1}\int_0^A \frac{E}{1-\nu}dA + C_1'\int_0^A \frac{2G}{1-\nu}dA$$

$$(24)_1 \quad \int_0^A \sigma_{z_1}dA = \int_0^A f_2(\sigma_{r_1})dA - \int_0^A \frac{E}{1-\nu}\epsilon^T dA + \epsilon_{z_1}\int_0^A \frac{E}{1-\nu}dA + C_1'\int_0^A \frac{2\nu G}{1-\nu}dA$$

Note that $(\text{Eq. } 23)_1$ automatically satisfies the boundary condition, $2A\sigma_{r_1}\Big|_{A=0} = 0$, due to the limits of integration which were selected. It is presumed that $\frac{E}{1-\nu}\epsilon^T$, $\frac{E}{1-\nu}$, $\frac{2G}{1-\nu}$, and $\frac{2\nu G}{1-\nu}$ are known functions of the radial parameter A, in the sense that graphical plots of their values versus A are known. Hence the indicated integrations of these terms may be carried out graphically, and it may be presumed that the values of the integrals of these terms are also known (graphical) functions of A.

A first approximation to the value of the radial stress, denoted by

$\bar{\sigma}_{r_1}$, may now be made. This approximation will be obtained by setting the terms, $f_1(\sigma_{r_1})$ and $f_2(\sigma_{r_1})$, equal to zero, and applying the remaining boundary conditions to the remaining terms of $(\text{Eq. } 23)_1$ and $(\text{Eq. } 24)_1$. This will result in a first approximation to the values of the constants, which will be denoted by $\bar{\epsilon}_{z_1}$ and $\bar{C}_1'$. These constants may then be used to obtain the value of $\bar{\sigma}_{r_1}$.

The application of the boundary conditions, $2A\sigma_{r_1}\big|_{A=1} = 0$ and $\int_0^1 \sigma_{z_1} dA = 0$, to $(\text{Eq. } 23)_1$ and $(\text{Eq. } 24)_1$, in which $f_1(\sigma_{r_1})$ and $f_2(\sigma_{r_1})$ have been set equal to zero, results in the following equations for the determination of $\bar{\epsilon}_{z_1}$ and $\bar{C}_1'$.

$$0 = -\int_0^1 \frac{E}{1-\nu} \epsilon^T dA + \bar{\epsilon}_{z_1} \int_0^1 \frac{E}{1-\nu} dA + \bar{C}_1' \int_0^1 \frac{2G}{1-\nu} dA$$

$$0 = -\int_0^1 \frac{E}{1-\nu} \epsilon^T dA + \bar{\epsilon}_{z_1} \int_0^1 \frac{E}{1-\nu} dA + \bar{C}_1' \int_0^1 \frac{2\nu G}{1-\nu} dA$$

The solution to this pair of equations for $\bar{\epsilon}_{z_1}$ and $\bar{C}_1'$ is given below.

$$(25)_1 \qquad \bar{\epsilon}_{z_1} = \frac{\int_0^1 \frac{E}{1-\nu} \epsilon^T dA}{\int_0^1 \frac{E}{1-\nu} dA}$$

$$(26)_1 \qquad C_1' = 0$$

Using these values for the constants, the value of $2A\bar{\sigma}_{r_1}$ may be obtained from the following equation.

$$(23a)_1 \qquad 2A\bar{\sigma}_{r_1} = -\int_0^A \frac{E}{1-\nu}\epsilon^T dA + \bar{\epsilon}_{z_1}\int_0^A \frac{E}{1-\nu}dA$$

The results, divided by 2A, give the value of $\bar{\sigma}_{r_1}$ everywhere except at $A = 0$. The following equation, obtained from $(\text{Eq. } 18a)_1$, gives its value at the center.

$$2\frac{d}{dA}(A\bar{\sigma}_{r_1})\Big|_{A=0} = 2\bar{\sigma}_{r_1}\Big|_{A=0} = -\frac{E}{1-\nu}\epsilon^T\Big|_{A=0} + \bar{\epsilon}_{z_1}\frac{E}{1-\nu}\Big|_{A=0}$$

This value for $\bar{\sigma}_{r_1}$ is now put into the neglected terms, $f_1(\bar{\sigma}_{r_1})$ and $f_2(\bar{\sigma}_{r_1})$, of $(\text{Eq. } 23)_1$ and $(\text{Eq. } 24)_1$, giving:

$$(23b)_1 \qquad 2A\bar{\sigma}_{r_1} \cong \int_0^A f_1(\bar{\sigma}_{r_1})dA - \int_0^A \frac{E}{1-\nu}\epsilon^T dA + \epsilon_{z_1}\int_0^A \frac{E}{1-\nu}dA + C_1'\int_0^A \frac{2G}{1-\nu}dA$$

$$(24b)_1 \qquad \int_0^A \bar{\sigma}_{z_1}dA \cong \int_0^A f_2(\bar{\sigma}_{r_1})dA - \int_0^A \frac{E}{1-\nu}\epsilon^T dA + \epsilon_{z_1}\int_0^A \frac{E}{1-\nu}dA + C_1'\int_0^A \frac{2\nu G}{1-\nu}dA$$

in which the values of all of the terms on the right are known except ϵ_{z_1} and C_1'.

A second approximation to the values of the constants ϵ_{z_1} and C_1' may now be obtained by applying the boundary conditions to $(\text{Eq. } 23b)_1$ and $(\text{Eq. } 24b)_1$. These constants may then be used to obtain a second approximation to $\bar{\sigma}_{r_1}$.

The application of the boundary conditions, $2A\bar{\sigma}_{r_1}\Big|_{A=1} = 0$ and

$\int_0^1 \sigma_{z_1} dA = 0$, to $(\text{Eq. 23b})_1$ and $(\text{Eq. 24b})_1$ results in the following equations for the determination of the second approximation to the values of ϵ_{z_1} and C_1'

$$\int_0^1 f_1(\bar{\sigma}_{r_1})dA - \int_0^1 \frac{E}{1-\nu}\epsilon^T dA + \epsilon_{z_1}\int_0^1 \frac{E}{1-\nu}dA + C_1'\int_0^1 \frac{2G}{1-\nu}dA = 0$$

$$\int_0^1 f_2(\bar{\sigma}_{r_1})dA - \int_0^1 \frac{E}{1-\nu}\epsilon^T dA + \epsilon_{z_1}\int_0^1 \frac{E}{1-\nu}dA + C_1'\int_0^1 \frac{2\nu G}{1-\nu}dA = 0$$

The solution of this pair of equations for ϵ_{z_1} and C_1' is given below.

$$(25a)\qquad C_1' \cong \frac{-\int_0^1 f_1(\bar{\sigma}_{r_1})dA + \int_0^1 f_2(\bar{\sigma}_{r_1})dA}{\int_0^1 \frac{2G}{1-\nu}dA - \int_0^1 \frac{2\nu G}{1-\nu}dA}$$

$$(26a)\qquad \epsilon_{z_1} \cong \bar{\epsilon}_{z_1} + \frac{\int_0^1 \frac{2\nu G}{1-\nu}dA\int_0^1 f_1(\bar{\sigma}_{r_1})dA - \int_0^1 \frac{2G}{1-\nu}dA\int_0^1 f_2(\bar{\sigma}_{r_1})dA}{\int_0^1 \frac{E}{1-\nu}dA\left[\int_0^1 \frac{2G}{1-\nu}dA - \int_0^1 \frac{2\nu G}{1-\nu}dA\right]}$$

Using these values for the constants, a second approximation for σ_{r_1} may now be obtained from $(\text{Eq. 23b})_1$. Notice that the value of σ_{r_1} at the center is now obtained from:

$$2\sigma_{r_1}\Big|_{A=0} \cong -\frac{E}{1-\nu}\epsilon^T\Big|_{A=0} + \epsilon_{z_1}\frac{E}{1-\nu}\Big|_{A=0} + C_1'\frac{2G}{1-\nu}\Big|_{A=0}$$

The resulting values of σ_{r_1} may now be used to replace the values of $\bar{\sigma}_{r_1}$ in the foregoing argument, and the process may be repeated, or, as in the numerical case to be considered in Chapter VI, this second approximation will be close enough without subsequent iterations.

With the value of σ_{r_1} known, the remaining stresses are determined from the following equations, in which all of the terms on the right are known.

$$(17a)_1 \qquad \sigma_{\phi_1} = -\sigma_{r_1} + f_1(\sigma_{r_1}) - \frac{E}{1-\nu}\epsilon^T + \epsilon_{z_1}\frac{E}{1-\nu} + C_1'\frac{2G}{1-\nu}$$

$$(21a)_1 \qquad \sigma_{z_1} = f_2(\sigma_{r_1}) - \frac{E}{1-\nu}\epsilon^T + \epsilon_{z_1}\frac{E}{1-\nu} + C_1'\frac{2\nu G}{1-\nu}$$

A numerical example of this calculation, determining the stresses due to the thermal dilation, is given in Chapter VI. As will be seen in that calculation, the method readily lends itself to tabular-graphical form. In that calculation, it will be seen that satisfactory accuracy may be obtained if the values of the terms are calculated at only a few radial positions, and the required intermediate points are graphically interpolated.

A semigraphical method for solving the set of equations which gives the stresses due to the boundary forces will now be developed. The boundary forces in this case are the external pressure p and the average axial stress $\sigma_{z\ avg.}$. Since the general approach has been developed in the previous case, the accompanying remarks will be more terse.

The equations which apply to this case are repeated below.

$$\left.\begin{aligned} (17)_2 \qquad & \sigma_{\phi_2} + \sigma_{r_2} \\ (18)_2 \qquad & 2\frac{d}{dA}(A\sigma_{r_2}) \end{aligned}\right\} = f_1(\sigma_{r_2}) + \frac{2\nu G}{1-\nu}\epsilon_{z_2} + \frac{2G}{1-\nu}C_2$$

$$(19)_2 \quad 2A\sigma_{r_2}\Big|_{A=0} = 0 \qquad (20)_2 \quad 2A\sigma_{r_2}\Big|_{A=1} = -2p$$

$$(21)_2 \quad \sigma_{z_2} = f_2(\sigma_{r_2}) + \frac{2G}{1-\nu}\epsilon_{z_2} + \frac{2\nu G}{1-\nu}C_2$$

$$(22)_2 \quad \int_0^1 \sigma_{z_2}\,dA = \sigma_{z\,avg.}$$

The results of the integration of $(Eq.\ 18)_2$ and $(Eq.\ 21)_2$ are:

$$(23)_2 \quad 2A\sigma_{r_2} = \int_0^A f_1(\sigma_{r_2})dA + \epsilon_{z_2}\int_0^A \frac{2\nu G}{1-\nu}dA + C_2\int_0^A \frac{2G}{1-\nu}dA$$

$$(24)_2 \quad \int_0^A \sigma_{z_2}dA = \int_0^A f_2(\sigma_{r_2})dA + \epsilon_{z_2}\int_0^A \frac{2G}{1-\nu}dA + C_2\int_0^A \frac{2\nu G}{1-\nu}dA$$

Note that $(Eq.\ 23)_2$ automatically satisfies the boundary condition: $2A\sigma_{r_2}\Big|_{A=0} = 0$, due to the limits of integration which were selected.

The application of the boundary conditions: $2A\sigma_{r_2}\Big|_{A=1} = -2p$ and $\int_0^1 \sigma_{z_2}dA = \sigma_{z\ avg.}$, to $(Eq.\ 23)_2$ and $(Eq.\ 24)_2$, in which $f_1(\sigma_{r_2})$ and $f_2(\sigma_{r_2})$ have been set equal to zero, results in the first approximation to the constants, denoted by $\bar{\epsilon}_{z_2}$ and $\bar{C}_2$.

$$(25)_1 \quad \bar{\epsilon}_{z_2} = \frac{\sigma_{z\,avg.}\int_0^1 \frac{2G}{1-\nu}dA - (-2p)\int_0^1 \frac{2\nu G}{1-\nu}dA}{\left[\int_0^1 \frac{2G}{1-\nu}dA\right]^2 - \left[\int_0^1 \frac{2\nu G}{1-\nu}dA\right]^2}$$

$$(26)_1 \quad \bar{C}_2 = \frac{(-2p)\int_0^1 \frac{2G}{1-\nu}dA - \sigma_{z\,avg.}\int_0^1 \frac{2\nu G}{1-\nu}dA}{\left[\int_0^1 \frac{2G}{1-\nu}dA\right]^2 - \left[\int_0^1 \frac{2\nu G}{1-\nu}dA\right]^2}$$

Using these values for the constants, a first approximation to the value of the radial stress, denoted by $\bar{\sigma}_{r_2}$, may be obtained from the following equations.

$$(23a)_2 \qquad 2A\bar{\sigma}_{r_2} = \bar{\epsilon}_{z_2}\int_0^A \frac{2\nu G}{1-\nu}\,dA + \bar{C}_2\int_0^A \frac{2G}{1-\nu}\,dA$$

$$2\bar{\sigma}_{r_2}\Big|_{A=0} = \bar{\epsilon}_{z_2}\,\frac{2\nu G}{1-\nu}\Big|_{A=0} + \bar{C}_2\,\frac{2G}{1-\nu}\Big|_{A=0}$$

The resulting values of $\bar{\sigma}_{r_2}$ are now put into the neglected terms: $f_1(\sigma_{r_2})$ and $f_2(\sigma_{r_2})$ of $(\text{Eq. } 23)_2$ and $(\text{Eq. } 24)_2$, giving:

$$(23b)_2 \qquad 2A\sigma_{r_2} \cong \int_0^A f_1(\bar{\sigma}_{r_2})\,dA + \epsilon_{z_2}\int_0^A \frac{2\nu G}{1-\nu}\,dA + C_2\int_0^A \frac{2G}{1-\nu}\,dA$$

$$(24b)_2 \qquad \int_0^A \sigma_{z_2}\,dA \cong \int_0^A f_2(\bar{\sigma}_{r_2})\,dA + \epsilon_{z_2}\int_0^A \frac{2G}{1-\nu}\,dA + C_2\int_0^A \frac{2\nu G}{1-\nu}\,dA$$

in which the values of all of the terms on the right are known except ϵ_{z_2} and C_2. The application of the boundary conditions to $(\text{Eq. } 23b)_2$ and $(\text{Eq. } 24b)_2$ results in the following second approximations to the values of the constants.

$$(25a)_2 \qquad \epsilon_{z_2} \cong \bar{\epsilon}_{z_2} + \frac{-\int_0^1 f_2(\bar{\sigma}_{r_2})\,dA\int_0^1 \frac{2G}{1-\nu}\,dA + \int_0^1 f_1(\bar{\sigma}_{r_2})\,dA\int_0^1 \frac{2\nu G}{1-\nu}\,dA}{\left[\int_0^1 \frac{2G}{1-\nu}\,dA\right]^2 - \left[\int_0^1 \frac{2\nu G}{1-\nu}\,dA\right]^2}$$

$$(26a)_2 \qquad C_2 \cong \bar{C}_2 + \frac{-\int_0^1 f_1(\bar{\sigma}_{r_2})\,dA\int_0^1 \frac{2G}{1-\nu}\,dA + \int_0^1 f_2(\bar{\sigma}_{r_2})\,dA\int_0^1 \frac{2\nu G}{1-\nu}\,dA}{\left[\int_0^1 \frac{2G}{1-\nu}\,dA\right]^2 - \left[\int_0^1 \frac{2\nu G}{1-\nu}\,dA\right]^2}$$

Using the values obtained from these equations for the constants, a second approximation for σ_{r_2} may now be obtained from the following equations.

$$(23b)_2 \qquad 2A\sigma_{r_2} = \int_0^A f_1(\overline{\sigma_{r_2}})dA + \epsilon_{z_2}\int_0^A \frac{2\nu G}{1-\nu}dA + C_2\int_0^A \frac{2G}{1-\nu}dA$$

$$2\sigma_{r_2}\Big|_{A=0} = \epsilon_{z_2}\frac{2\nu G}{1-\nu}\Big|_{A=0} + C_2\frac{2G}{1-\nu}\Big|_{A=0}, \quad \text{Note } f_1(\sigma_{r_2})\Big|_{A=0} = 0$$

The value of σ_{r_2} obtained from the above equations may now be used to replace the value of $\overline{\sigma}_{r_2}$ used in the foregoing argument, and the process may be repeated, or, in some cases, this second approximation will be close enough without subsequent iterations.

With the value of σ_{r_2} known, the remaining stresses are determined from the following equations, in which all of the terms on the right are known.

$$(17)_2 \qquad \sigma_{\phi_2} = -\sigma_{r_2} + f_1(\sigma_{r_2}) + \frac{2\nu G}{1-\nu}\epsilon_{z_2} + \frac{2G}{1-\nu}C_2$$

$$(21)_2 \qquad \sigma_{z_2} = f_2(\sigma_{r_2}) + \frac{2G}{1-\nu}\epsilon_{z_2} + \frac{2\nu G}{1-\nu}C_2$$

As in the case of the stresses due to the thermal dilation, satisfactory accuracy can be achieved, when all of the terms discussed are evaluated at only a few radial positions, and the required intermediate points are graphically interpolated.

A semigraphical method for solving the set of equations which gives the stresses due to the residual strains will now be developed. The residual strains will be presumed to be known (graphical) functions of position.

The equations which apply to this case are repeated below.

$$\left.\begin{array}{ll}(17)_3 & \sigma_{\phi_3}+\sigma_{r_3}\\ (18)_3 & 2\frac{d}{dA}(A\sigma_{r_3})\end{array}\right\} = f_1(\sigma_{r_3}) - \frac{2G}{1-\nu}\int_0^A \frac{\epsilon^\circ_\phi - \epsilon^\circ_r}{2A}dA - \frac{2G}{1-\nu}(\epsilon^\circ_\phi + \nu\epsilon^\circ_z) + \frac{2\nu G}{1-\nu}\epsilon_{z_3} + \frac{2G}{1-\nu}C_3$$

$$(19)_3 \quad 2A\sigma_{r_3}\Big|_{A=0} = 0 \qquad (20)_3 \quad 2A\sigma_{r_3}\Big|_{A=1} = 0$$

$$(21)_3 \quad \sigma_{z_3} = f_2(\sigma_{r_3}) - \frac{2\nu G}{1-\nu}\int_0^A \frac{\epsilon^\circ_\phi - \epsilon^\circ_r}{2A}dA - \frac{2G}{1-\nu}(\nu\epsilon^\circ_\phi + \epsilon^\circ_z) + \frac{2G}{1-\nu}\epsilon_{z_3} + \frac{2\nu G}{1-\nu}C_3$$

$$(22)_3 \quad \int_0^1 \sigma_{z_3}dA = 0$$

The results of the integration of $(\text{Eq. } 18)_3$ and $(\text{Eq. } 21)_3$ are:

$$(23)_3 \quad 2A\sigma_{r_3} = \int_0^A f_1(\sigma_{r_3})dA - \int_0^A\left[\frac{2G}{1-\nu}\int_0^A \frac{\epsilon^\circ_\phi - \epsilon^\circ_r}{2A}dA\right]dA - \int_0^A \frac{2G}{1-\nu}(\epsilon^\circ_\phi + \nu\epsilon^\circ_z)dA + \epsilon_{z_3}\int_0^A \frac{2\nu G}{1-\nu}dA + C_3\int_0^A \frac{2G}{1-\nu}dA$$

$$(24)_3 \quad \int_0^A \sigma_{z_3}dA = \int_0^A f_2(\sigma_{r_3})dA - \int_0^A\left[\frac{2\nu G}{1-\nu}\int_0^A \frac{\epsilon^\circ_\phi - \epsilon^\circ_r}{2A}dA\right]dA - \int_0^A \frac{2G}{1-\nu}(\nu\epsilon^\circ_\phi + \epsilon^\circ_z)dA + \epsilon_{z_3}\int_0^A \frac{2G}{1-\nu}dA + C_3\int_0^A \frac{2\nu G}{1-\nu}dA$$

Note that $(\text{Eq. } 23)_3$ automatically satisfies the boundary condition: $2A\sigma_{r_3}\Big|_{A=0} = 0$, due to the limits of integration which were selected.

The application of the boundary conditions: $2A\sigma_{r_3}\Big|_{A=1} = 0$ and $\int_0^1 \sigma_{z_3}dA = 0$, to $(\text{Eq. } 23)_3$ and $(\text{Eq. } 24)_3$, in which $f_1(\sigma_{r_3})$ and $f_2(\sigma_{r_3})$ have been set equal to zero, results in the following first

approximations to the values of the constants denoted by $\bar{\epsilon}_{z_3}$ and $\bar{C}_3$.

$$(25)_3\ \bar{\epsilon}_{z_3} = \frac{\int_0^1 \frac{2G}{1-\nu}dA\left\{\int_0^1\left[\frac{2\nu G}{1-\nu}\int_0^A \frac{\epsilon_\phi^\circ-\epsilon_r^\circ}{2A}dA\right]dA+\int_0^1\frac{2G}{1-\nu}(\nu\epsilon_\phi^\circ+\epsilon_z^\circ)dA\right\}-\int_0^1\frac{2\nu G}{1-\nu}dA\left\{\int_0^1\left[\frac{2G}{1-\nu}\int_0^A\frac{\epsilon_\phi^\circ-\epsilon_r^\circ}{2A}dA\right]dA+\int_0^1\frac{2G}{1-\nu}(\epsilon_\phi^\circ+\nu\epsilon_z^\circ)dA\right\}}{\left[\int_0^1\frac{2G}{1-\nu}dA\right]^2-\left[\int_0^1\frac{2\nu G}{1-\nu}dA\right]^2}$$

$$(26)_3\ \bar{C}_3 = \frac{\int_0^1 \frac{2G}{1-\nu}dA\left\{\int_0^1\left[\frac{2G}{1-\nu}\int_0^A \frac{\epsilon_\phi^\circ-\epsilon_r^\circ}{2A}dA\right]dA-\int_0^1\frac{2G}{1-\nu}(\epsilon_\phi^\circ+\nu\epsilon_z^\circ)dA\right\}-\int_0^1\frac{2\nu G}{1-\nu}dA\left\{\int_0^1\left[\frac{2\nu G}{1-\nu}\int_0^A\frac{\epsilon_\phi^\circ-\epsilon_r^\circ}{2A}dA\right]dA+\int_0^1\frac{2G}{1-\nu}(\nu\epsilon_\phi^\circ+\epsilon_z^\circ)dA\right\}}{\left[\int_0^1\frac{2G}{1-\nu}dA\right]^2-\left[\int_0^1\frac{2\nu G}{1-\nu}dA\right]^2}$$

The values of the constants can be determined from the above equations, if the values of the terms are determined by graphical integration. Using these values for the constants, a first approximation to the value of the radial stress, denoted by $\bar{\sigma}_{r_3}$, may be obtained from the following equations:

$$(23a)\quad 2A\bar{\sigma}_{r_3} = -\int_0^A\left[\frac{2G}{1-\nu}\int_0^A\frac{\epsilon_\phi^\circ-\epsilon_r^\circ}{2A}dA\right]dA-\int_0^A\frac{2G}{1-\nu}(\epsilon_\phi^\circ+\nu\epsilon_z^\circ)dA+\bar{\epsilon}_{z_3}\int_0^A\frac{2\nu G}{1-\nu}dA+\bar{C}_3\int_0^A\frac{2G}{1-\nu}dA$$

$$2\bar{\sigma}_{r_3}\Big|_{A=0} = -\frac{2G}{1-\nu}(\epsilon_\phi^\circ+\nu\epsilon_z^\circ)\Big|_{A=0}+\bar{\epsilon}_{z_3}\frac{2\nu G}{1-\nu}\Big|_{A=0}+\bar{C}_3\frac{2G}{1-\nu}\Big|_{A=0},\quad \text{Note limit}_{A\to 0}\frac{\epsilon_\phi^\circ-\epsilon_r^\circ}{2A}<\infty$$

The resulting values of $\bar{\sigma}_{r_3}$ are now put into the neglected terms, $f_1(\sigma_{r_3})$ and $f_2(\sigma_{r_3})$, of $(\text{Eq. } 23)_3$ and $(\text{Eq. } 24)_3$, giving:

$$(23b)_3\quad 2A\sigma_{r_3}\cong\int_0^A f_1(\bar{\sigma}_{r_3})dA-\int_0^A\left[\frac{2G}{1-\nu}\int_0^A\frac{\epsilon_\phi^\circ-\epsilon_r^\circ}{2A}dA\right]dA-\int_0^A\frac{2G}{1-\nu}(\epsilon_\phi^\circ+\nu\epsilon_z^\circ)dA+\epsilon_{z_3}\int_0^A\frac{2\nu G}{1-\nu}dA+C_3\int_0^A\frac{2G}{1-\nu}dA$$

$$(24b)_3\quad \int_0^A\sigma_{z_3}dA\cong\int_0^A f_2(\bar{\sigma}_{r_3})dA-\int_0^A\left[\frac{2\nu G}{1-\nu}\int_0^A\frac{\epsilon_\phi^\circ-\epsilon_r^\circ}{2A}dA\right]dA-\int_0^A\frac{2G}{1-\nu}(\nu\epsilon_\phi^\circ+\epsilon_z^\circ)dA-\epsilon_{z_3}\int_0^A\frac{2G}{1-\nu}dA+C_3\int_0^A\frac{2\nu G}{1-\nu}dA$$

In these equations the values of all of the terms on the right are known except ϵ_{z_3} and C_3. The application of the boundary equations to $(\text{Eq. 23b})_3$ and $(\text{Eq. 24b})_3$ results in the following second approximations to the values of the constants.

$$(25a)_3 \quad \epsilon_{z_3} \cong \bar{\epsilon}_{z_3} + \frac{-\int_0^1 \frac{2G}{1-\nu} dA \int_0^1 f_2(\bar{\sigma}_{r_3}) dA + \int_0^1 \frac{2\nu G}{1-\nu} dA \int_0^1 f_1(\bar{\sigma}_{r_3}) dA}{\left[\int_0^1 \frac{2G}{1-\nu} dA\right]^2 - \left[\int_0^1 \frac{2\nu G}{1-\nu} dA\right]^2}$$

$$(26a)_3 \quad C_3 \cong \bar{C}_3 + \frac{-\int_0^1 \frac{2G}{1-\nu} dA \int_0^1 f_1(\bar{\sigma}_{r_3}) dA + \int_0^1 \frac{2\nu G}{1-\nu} dA \int_0^1 f_2(\bar{\sigma}_{r_3}) dA}{\left[\int_0^1 \frac{2G}{1-\nu} dA\right]^2 - \left[\int_0^1 \frac{2\nu G}{1-\nu} dA\right]^2}$$

Using the values obtained from these equations for the constants, a second approximation for σ_{r_3} may now be obtained from the following equations.

$$(23b)_3 \quad 2A\sigma_{r_3} = \int_0^A f_1(\bar{\sigma}_{r_3}) dA - \int_0^A \left[\frac{2G}{1-\nu} \int_0^A \frac{\epsilon_\phi^\circ - \epsilon_r^\circ}{2A} dA\right] dA - \int_0^A \frac{2G}{1-\nu} (\epsilon_\phi^\circ + \nu \epsilon_z^\circ) dA + \epsilon_{z_3} \int_0^A \frac{2\nu G}{1-\nu} dA + C_3 \int_0^A \frac{2G}{1-\nu} dA$$

$$2\sigma_{r_3}\Big|_{A=0} = -\frac{2G}{1-\nu} (\epsilon_\phi^\circ + \nu \epsilon_z^\circ)\Big|_{A=0} + \epsilon_{z_3} \frac{2\nu G}{1-\nu}\Big|_{A=0} + C_3 \frac{2G}{1-\nu}\Big|_{A=0}$$

The value of σ_{r_3} obtained from the above equations may now be used to replace the value of $\bar{\sigma}_{r_3}$ used in the foregoing argument, and the process may be repeated, or, as in the numerical case to be considered in Chapter VII, this second approximation will be close enough without subsequent iterations.

With the value of σ_{r_3} known, the remaining stresses are determined from the following equations, in which all of the terms on the right are known.

$$(17)_3 \qquad \sigma_{\phi_3} = -\sigma_{r_3} + f_1(\sigma_{r_3}) - \frac{2G}{1-\nu}\int_0^A \frac{\epsilon^\circ_\phi - \epsilon^\circ_r}{2A}dA - \frac{2G}{1-\nu}(\epsilon^\circ_\phi + \nu\epsilon^\circ_z) + \frac{2\nu G}{1-\nu}\epsilon_{z_3} + \frac{2G}{1-\nu}C_3$$

$$(21)_3 \qquad \sigma_{z_3} = f_2(\sigma_{r_3}) - \frac{2\nu G}{1-\nu}\int_0^A \frac{\epsilon^\circ_\phi - \epsilon^\circ_r}{2A}dA - \frac{2G}{1-\nu}(\nu\epsilon^\circ_\phi + \epsilon^\circ_z) + \frac{2G}{1-\nu}\epsilon_{z_3} + \frac{2\nu G}{1-\nu}C_3$$

A numerical example of this calculation, determining the stresses due to the residual strains, is given in Chapter VIII. As will be seen in that calculation, the method readily lends itself to tabular-graphical form. In that calculation, it will be seen that satisfactory accuracy may be obtained if the values of the terms are calculated at only a few radial positions, and the required intermediate points are graphically interpolated.

This chapter was devoted to the determination of the stresses existing at a given instant of time in an infinitely long solid isotropic cylinder, when all of the variables are functions of the radial position only. The equations which determine the stresses as a function of the thermal dilation, the boundary forces, and the residual strains, were presented. These equations were divided into three sets of equations, which gave the stresses due to the thermal dilation, the stresses due to the boundary forces, and the stresses due to the residual strains. Semi-graphical methods for the solution of each of these sets were then indicated.

CHAPTER IV

In this chapter, a theory of strength will be introduced and it will be indicated how this theory of strength may be used to determine the values of the residual strains as a function of position and time. Before the theory of strength is introduced, however, it is desirable that a recapitulation be made so that the function of this chapter in the total problem becomes more apparent.

The problem which is undertaken in Part I is the development of an analytical method for the prediction of the residual stresses induced in an infinitely long solid isotropic cylinder by a symmetrical quench. In Chapter I, a technique was presented for the determination of the temperature as a function of the radial position and time. In Chapter II, a theory, which is an extension of the ordinary theory of elasticity, was developed which included the effects of thermal dilation and residual strains upon the stresses existing in an isotropic body at any given time. This theory presumes that the material behaves elastically in the sense that Hooke's Law describes the changes of the strains which appear if the stresses on an element of the body are removed. Such effects as yielding or creep, by this definition, merely change the residual strain terms. In Chapter III, the theory of Chapter II is used to separately determine, at a given time, the stresses due to the thermal dilation, the stresses due to the boundary forces, and the stresses due to the residual strains, for the case of an infinitely long solid isotropic cylinder when all of the variables are functions of the radial position only.

The following notation will be used in this chapter:

Let: E	be Young's Modulus for unloading.
ν	be Poisson's Ratio for unloading.
G	$= E/2(1-\nu)$.
t	be the time.
$x,\ y,\ z$	be the local coordinates, parallel in direction to the local principle stresses.
$i,\ j,\ k$	be unit vectors in the x, y, and z directions.
$\sigma_x,\ \sigma_y,\ \sigma_z$	be the principal stresses.
	$= \frac{1}{3}(\sigma_x + \sigma_y + \sigma_z)$.
$(\sigma_x - \sigma)$ $(\sigma_y - \sigma)$ $(\sigma_z - \sigma)$	be the principal reduced stresses.
$\sigma_{y.p.}$	be the tensile stress at which the material will yield. (If such exists.)
k^2	$= (\sigma_x - \sigma)^2 + (\sigma_y - \sigma)^2 + (\sigma_z - \sigma)^2$ be a parameter proportional to the shear strain energy.
$\frac{2}{3}(\sigma_{y.p.})^2$	be the value of k^2 at which yielding commences.
$\epsilon_x,\ \epsilon_y,\ \epsilon_z$	be the principal strains.
$\epsilon_x^o,\ \epsilon_y^o,\ \epsilon_z^o$	be the principal residual strains.
$\frac{d\epsilon_x^o}{dt},\ \frac{d\epsilon_y^o}{dt},\ \frac{d\epsilon_z^o}{dt}$	be the principal residual strain rates.
V	be the shear strain energy.
$\underline{V}$	be the energy required to produce the residual strains.

If the residual strains are known, the stresses due to them can be determined, but the method of determining these residual strains has yet to be presented. The remaining part of the total problem is, therefore, the development of methods for either determining the changes of the residual strains as a function of time, in the terms of the temperature and the stresses which would have been present if those changes in residual strain had not taken place, or of determining the residual strain rates as a function of the stresses and temperature existing at a particular time.

There are obviously as many approaches to this problem as there are theories of strength. This is, however, a three dimensional stress problem, hence, for example, the maximum tension theory of strength may be eliminated, since it makes no pretence of describing three dimensional yielding. In addition, it must be remembered that, in Chapter II, certain restrictions on the elastic (unloading) properties of the material were necessary. It will be instructive to examine certain of the types of stress strain relationships for simple tension which satisfy these restrictions, as a preliminary to the introduction of a theory of strength. The restrictions are that there are <u>known</u> values of E, ν, and $2G = E/(1 + \nu)$, which are unique functions of the temperature (or more generally, which are unique functions of position and time but which are independent of the stress level) and which relate, through Hooke's Law, the changes in the strains with the changes in the stresses, which occur in an element of the body if the stresses are <u>removed</u> from that element, but no other changes take place.

The simplest type of stress strain relationship which satisfies these restrictions is illustrated in (Fig. 2). Mild steel at moderate temperatures closely approximates this curve, if the upper yield is neglected and the flat portion of the yield is not exceeded.

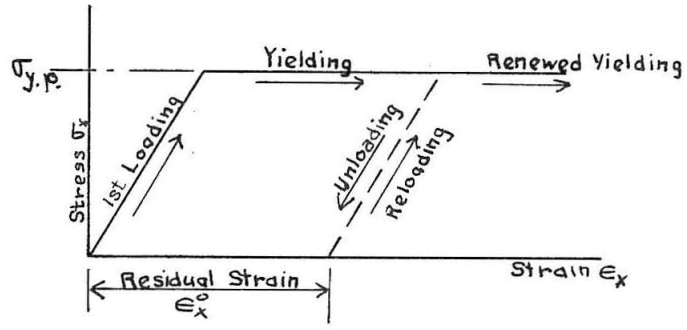

(Fig. 2)

This type of stress strain relationship, where the yield point, E, and ν are functions of temperature, is because of its simplicity particularly adapted to the solution of the outlined problem. This is the type of relationship assumed in the numerical computations of Chapter VII and is the one to which most of the succeeding development will be devoted.

Another type of stress strain relationship, which satisfies the restrictions, is indicated in (Fig. 3a). It is approximated by materials in which strain hardening is apparent, such as aluminum or stainless steel at ordinary temperatures.

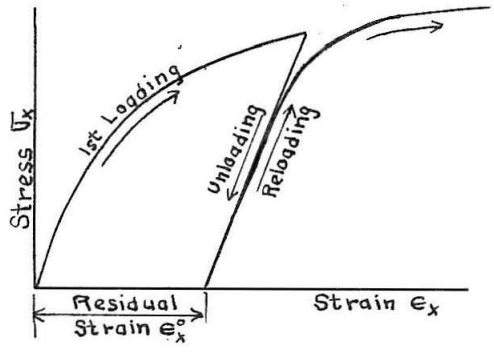

(Fig. 3a)

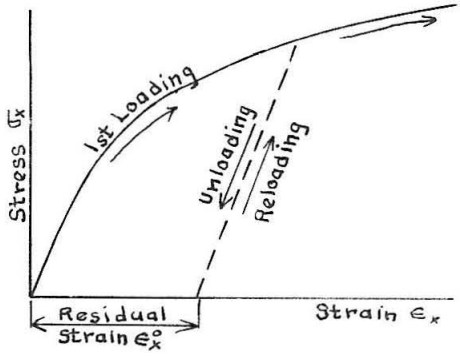

(Fig. 3b)

Depending upon the material and the temperature, (Fig. 3a) may or may not be idealized into (Fig. 3b). This strain hardening type will be discussed briefly in the succeeding developments. The required computations, using this type of relationship, are more difficult.

Such materials as pitch, or metals at high temperature, may be approximated by a completely different type of stress strain relationship. For rapid loading or unloading, the material is presumed to behave elastically with E, ν, and G being functions of temperature, but for sustained loads the residual strain rate is presumed to be a function of the stress level and the temperature. For pure tension, the relationship may be expressed as: $\frac{d\epsilon_x^o}{dt} = f(\sigma_x, T)$. This type of stress strain relationship is indicated in (Fig. 4).

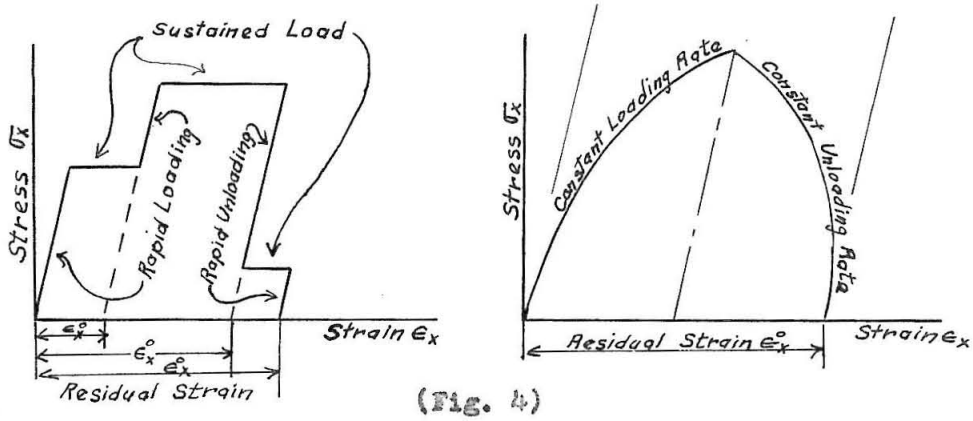

(Fig. 4)

This type of stress strain relationship is most ideally adapted to use in conjunction with the theory of Chapter II. Because of this fact, this type will be discussed in the succeeding developments. This type of relationship is particularly useful in computing the amount of residual stress relief due to tempering or other stress relief heat treatment, and is also applicable to cases where creep is the dominant factor.

The first step in the selection of a theory of strength is the selection of the parameter, in addition to the temperature, whose value is presumed to indicate whether yielding takes place, or whose value determines the rate of yielding. In the case of simple tension, to which the foregoing stress strain curves apply, the obvious parameter is the tensile stress. For three dimensional stress problems, however, the maximum tensile stress has been shown to be an unsatisfactory criterion. The parameters most commonly used in three dimensional stress problems are the shear strain energy and the maximum shear stress. While the results from the use of either of these parameters differ only slightly, it is commonly accepted* that the shear strain energy (or Mises-Hencky criterion) corresponds most closely to the experimental results obtained using polycrystalline materials, where macroscopic isotropy is assumed due to the smallness and random orientation of the crystals. This is particularly fortunate, since this criterion is mathematically more suitable for the problem at hand than the maximum shear criterion.

The second step in the selection of a theory of strength is the determination, if yielding takes place, of the relative proportions of the principal residual strain increments. Again the mathematically most suitable theory* is the one now accepted as being the most accurate for polycrystalline materials, where macroscopic isotropy is assumed due to the smallness and random orientation of the crystals. This theory

---

* Nadai, "Plasticity", contains a good discussion of the different theories of strength and plastic flow. The reader is referred to this text as a background for this chapter.

presumes that the principal residual strain increments are proportional to the principal reduced stresses and are in the same direction. This implies that the sum of the principal residual strains is zero.

The mathematical application of this theory of strength to the problem at hand will now be discussed in relation to the foregoing types of simple tension stress strain relationships. Most of the succeeding development will be devoted to the first type, approximated by mild steel at moderate temperatures, since this type will be assumed in the numerical computations of Chapter VII.

Assuming that the stress strain relationship for simple tension is of the type indicated in (Fig. 2), the modified Hooke's Law of Chapter II, neglecting thermal dilation, may be written in the form:

$$E(\epsilon_x - \epsilon_x^\circ) = (1+\nu)\sigma_x - 3\nu\sigma$$

$$E(\epsilon_y - \epsilon_y^\circ) = (1+\nu)\sigma_y - 3\nu\sigma$$

$$E(\epsilon_z - \epsilon_z^\circ) = (1+\nu)\sigma_z - 3\nu\sigma$$

$$\therefore\ E(\epsilon - \epsilon^\circ) = (1-2\nu)\sigma$$

where: $\sigma = \frac{1}{3}(\sigma_x+\sigma_y+\sigma_z)$

$\epsilon = \frac{1}{3}(\epsilon_x+\epsilon_y+\epsilon_z)$

$\epsilon^\circ = \frac{1}{3}(\epsilon_x^\circ+\epsilon_y^\circ+\epsilon_z^\circ)$

The shear strain energy may now be written in the following form.

$$V = \underbrace{\tfrac{1}{2}\left[\sigma_x(\epsilon_x-\epsilon_x^\circ) + \sigma_y(\epsilon_y-\epsilon_y^\circ) + \sigma_z(\epsilon_z-\epsilon_z^\circ)\right]}_{\text{Total strain energy}} - \underbrace{1\tfrac{1}{2}\sigma(\epsilon-\epsilon^\circ)}_{\text{dilation strain energy}}$$

$$= \frac{1}{2E}\left\{\sigma_x\left[(1+\nu)\sigma_x - 3\nu\sigma\right] + \sigma_y\left[(1+\nu)\sigma_y - 3\nu\sigma\right] + \sigma_z\left[(1+\nu)\sigma_z - 3\nu\sigma\right] - 3(1-2\nu)\sigma^2\right\}$$

By suitable manipulation, this may be written in the following form.

$$V = \frac{1+\nu}{2E}\left[(\sigma_x-\sigma)^2+(\sigma_y-\sigma)^2+(\sigma_z-\sigma)^2\right]$$

By the assumption of the theory of strength, V may never exceed a certain value. If V tends to exceed this value, yielding takes place. This value is readily determined from the yield point in simple tension, and is:

$$V_{y.p.} = \frac{2}{3}\frac{1+\nu}{2E}\sigma_{y.p.}^2$$

Therefore the limiting value of the function,

$$k^2 = \left[(\sigma_x-\sigma)^2+(\sigma_y-\sigma)^2+(\sigma_z-\sigma)^2\right] \quad , \quad \text{is} \quad k^2_{y.p.} = \frac{2}{3}\sigma_{y.p.}^2$$

The significance of the proportionality of the principal residual strain increments to the principal reduced stresses will now be investigated. If $\underline{V}$ is the energy required to produce the residual strains, the differential increment of work done in yielding is:

$$d\underline{V} = \sigma_x d\epsilon_x^\circ + \sigma_y d\epsilon_y^\circ + \sigma_z d\epsilon_z^\circ$$

$$= (\sigma_x-\sigma)d\epsilon_x^\circ + (\sigma_y-\sigma)d\epsilon_y^\circ + (\sigma_z-\sigma)d\epsilon_z^\circ - 3\sigma d\epsilon^\circ$$

Now if ϵ° (defined to be $\frac{1}{3}(\epsilon_x^\circ + \epsilon_y^\circ + \epsilon_z^\circ)$) is assumed to be zero (the residual strains result in zero volume change), then the increment of

work done in yielding may be written in the following vector form.

$$d\underline{V} = \left[(\sigma_x-\sigma)\underline{i} + (\sigma_y-\sigma)\underline{j} + (\sigma_z-\sigma)\underline{K}\right] \circ \left[d\epsilon_x^o\,\underline{i} + d\epsilon_y^o\,\underline{j} + d\epsilon_z^o\,\underline{K}\right]$$

The requirement of the theory of strength that $d\epsilon_x^o : d\epsilon_y^o : d\epsilon_z^o$ as $(\sigma_x - \sigma) : (\sigma_y - \sigma) : (\sigma_z - \sigma)$, therefore, implies that the foregoing vectors are parallel. This maximizes $d\underline{V}$ in terms of a given magnitude of the vector strain increment. It is further implied that the proportionality of the reduced stresses and the strain increments is based upon the assumption that ϵ^o is zero, rather than vice versa.

A finite difference technique for determining the residual strains as a function of time will now be indicated on the basis of these developments. It is assumed that, at time t, the values of the residual strains are known. At time $t + \Delta t$, it is assumed that the stresses due to the thermal dilation and the stresses due to the boundary forces are known. Using the residual strains present at time t, the stresses due to these residual strains at time $t + \Delta t$ are then computed. The reduced stresses corresponding to the sum of the stresses due to these three factors, and the value of the function $k^2 = \left((\sigma_x - \sigma)^2 + (\sigma_y - \sigma)^2 + (\sigma_z - \sigma)^2\right)$ are then determined at time $t + \Delta t$.

The following technique is then used to estimate the values of the residual strain increments in the interval Δt. Modifications to the estimate, made possible by the knowledge of the results of previous time interval computations, should be included to increase the accuracy of the estimate. Subject to these modifications, it is assumed that everywhere

k^2 exceeds $\frac{2}{3}\sigma^2_{y.p.}$, yielding will take place. It is also assumed that the residual strain increments due to this yielding will be proportional to the foregoing reduced stresses. For the purpose of estimating these increments, it will be further assumed that these increments of the residual strains do not affect the total strains. With this further assumption, the following relationships relating the changes of the reduced stresses to the increments of the residual strains are valid.

$$2G\,\Delta\epsilon_x^\circ = -\Delta(\sigma_x - \sigma)$$

$$2G\,\Delta\epsilon_y^\circ = -\Delta(\sigma_y - \sigma)$$

$$2G\,\Delta\epsilon_z^\circ = -\Delta(\sigma_z - \sigma)$$

Wherever k^2 exceeds $\frac{2}{3}\sigma^2_{y.p.}$, the changes of the reduced stresses and the corresponding increments of the residual strains, required to cause k^2 to match $\frac{2}{3}\sigma^2_{y.p.}$, may then be estimated from the following equations.

$$2G\,\Delta\epsilon_x^\circ = -\Delta(\sigma_x - \sigma) = \left(1 - \sqrt{\frac{\frac{2}{3}\sigma^2_{y.p.}}{k^2}}\right)(\sigma_x - \sigma)$$

$$2G\,\Delta\epsilon_y^\circ = -\Delta(\sigma_y - \sigma) = \left(1 - \sqrt{\frac{\frac{2}{3}\sigma^2_{y.p.}}{k^2}}\right)(\sigma_y - \sigma)$$

$$2G\,\Delta\epsilon_z^\circ = -\Delta(\sigma_z - \sigma) = \left(1 - \sqrt{\frac{\frac{2}{3}\sigma^2_{y.p.}}{k^2}}\right)(\sigma_z - \sigma)$$

The stresses due to these estimated residual strain increments are then computed. Due to the grossness of the assumption that the total strains are a constant, these stresses, added to the previous stresses may not be expected to give a satisfactory agreement between k^2 and $\frac{2}{3}\sigma^2_{y.p.}$ over the region in which yielding was assumed. The agreement will,

however, be much better than was achieved with the value of k^2 from the previous stresses only, and may be improved still more by determining a constant which when multiplied by the estimated residual strain increments and the stresses due to these increments results in the best match between k^2 and $\frac{2}{3}\sigma^2_{y.p.}$ over the assumed region of yielding.

With the restriction that the ratio of the residual strain increments in each coordinate direction does not change, the results of this first estimate are used, in much the same fashion, to determine a new estimate of the required residual strain increments. The results of this second estimate should give a still closer match between k^2 and $\frac{2}{3}\sigma^2_{y.p.}$. With two independent solutions for the stresses due to the estimated values of the residual strain increments, this match may be further improved by utilizing a linear combination of these two solutions.

This process of successive approximations to the required residual strain increments may be, if necessary, continued. As the number of independent solutions becomes larger, the use of a linear combination of these solutions becomes more important. k^2 and $\frac{2}{3}\sigma^2_{y.p.}$ can be exactly matched at the same number of positions as there are linearly independent solutions due to successive estimates of the required residual strain increments. When a satisfactory match between k^2 and $\frac{2}{3}\sigma^2_{y.p.}$ is obtained, the required values of the residual strains at the time $t + \Delta t$ are known. The entire process is then repeated for the next time interval. In this manner, the complete solution vs. time is obtained.

The foregoing discussion applies in toto to the case where the mate-

rial has a stress strain relationship for simple tension of the form (Fig. 3) indicated for strain hardening materials. The only difference is that the parameter, $\frac{2}{3}\sigma^2_{y.p.}$ (the maximum value of the function $k^2 = \left((\sigma_x - \sigma)^2 + (\sigma_y - \sigma)^2 + (\sigma_z + \sigma)^2\right)$ which the material may sustain without yielding) must now be considered to be a function of the residual strain-temperature history, including the values of the assumed residual strain increments in the time interval Δt. A discussion of suitable approximations for this functional dependence is beyond the scope of this thesis.

When the material has a stress strain relationship of the type indicated in (Fig. 4), which is mathematically similar to slow viscous fluid flow, the technique is even simpler. It is assumed that the residual strains and the total stresses are known at time t. These stresses, together with the temperature, determine the residual strain rate. This residual strain rate is presumed to act unchanged for the time interval Δt, at the end of which time the total stresses are computed. These stresses, at time $(t + \Delta t)$, determine the residual strain rate in the succeeding time interval. The process is repeated until the complete solution is built up. The simplest functional dependence between the stresses and the residual strain rates (mathematically identical to slow viscous fluid flow) is:

$$\frac{d\epsilon^\circ_x}{dt} = \mu(\sigma_x - \sigma) \quad , \quad \frac{d\epsilon^\circ_y}{dt} = \mu(\sigma_y - \sigma) \quad , \quad \frac{d\epsilon^\circ_z}{dt} = \mu(\sigma_z - \sigma)$$

where μ is an experimentally determined function of the temperature,

analogous to viscosity. A discussion of more complicated relationships, such as would be involved in creep with strain hardening, is beyond the scope of this thesis.

In Chapter II, it was indicated how the stresses due to the thermal dilation, the stresses due to the boundary forces, and the stresses due to known values of the residual strains, could be determined. It was indicated that, while the stresses due to known values of the residual strains could be determined, the values of the residual strains were unknown. It was further indicated that the values of the residual strains could be determined only if additional information, in the form of a theory of strength, was introduced. In this Chapter, certain theories of strength were presented, and it was indicated how these theories could be applied to determine the values of the residual strains as a function of position and time.

It may be noted here that the developments of this Chapter are more restrictive, in the sense of the required assumptions, than are those of Chapter II. Hence the utility of Chapter II is not limited by the applicability of the developments of this Chapter, but rather, it is limited by the ability, by any method or through any theory of strength, to determine the residual strains.

PART II

The application of the developments of PART I to the following problem, neglecting end effects:

"Determine the residual stresses induced by quenching, from 600 °C. in still water at ambient temperature, a previously normalized solid steel cylinder, 5 cm. in diameter by 40 cm. long. The composition of the steel is as follows: 0.30% C., 0.20% Si., 0.75% Mn., 0.051% P., and 0.030% S.".

This particular problem corresponds to the experimental residual stress determination performed by H. Bucholtz and H. Buhler (3), who used the techniques developed by Sachs (1) for their determination.

CHAPTER V

This chapter will be devoted to the determination of the temperature distribution, as a function of the position and time, for this case of a 5 cm. diameter mild steel cylinder, quenched from 600 °C. in still water at ambient temperature.

The first step in this determination is the selection of the values of the pertinent variables, as a function of temperature, from the literature. This problem of selection is complicated by the fact that the values of the required parameters are not available for the particular composition of steel used in the experimental residual stress determination for this case. Fortunately the parameters are only slightly influenced by small changes of composition, hence reasonably accurate values of these parameters may be obtained from weighted averages of the values of these parameters for steels of neighboring composition.

Table I contains a summary of the assumed values of the pertinent parameters as a function of the temperature. A discussion of the selection of these values follows the table. The results are presumed to approximate the values which would have been obtained from a previously normalized steel of the following composition: 0.30% C., 0.20% Si., 0.75% Mn., 0.051% P., and 0.030% S..

The notation used in this chapter is the same as that used in CHAPTER I

Table I

The assumed values of the pertinent parameters as a function of the temperature.

Parameter	Units	Temperature °C						
		0	100	200	300	400	500	600
c_p	cal./gm. °C.	0.110	0.117	0.124	0.133	0.144	0.161	0.182
k	cal./cm. °C. sec.	0.124	0.121	0.116	0.109	0.101	0.092	0.083
ρ	gm./cm.^{3}	7.85 @ 20°C.	7.84	7.80	7.76	7.73	7.70	7.67
a	cm.^{2}/sec.	0.144	0.132	0.120	0.106	0.091	0.074	0.059
h	cal./cm.^{2} sec. °C.	0.028	0.028	0.028 0.078	0.078	0.078	0.078	0.078
k $\log_{10}$ e/hr.$_1$		0.77	0.75	0.72	0.675 0.243	0.226	0.205	0.185
$2a\Delta t/r_1^2(\Delta x)^2 = 2a\Delta t/(\Delta r)^2$ for $\Delta t/(\Delta r)^2 = 8$ sec./cm.^{2}		2.30	2.11	1.92	1.70	1.46	1.18	0.95
$2a\Delta t/r_1^2(\Delta x)^2 = 2a\Delta t/(\Delta r)^2$ for $\Delta t/(\Delta x)^2 = 4.8$ sec./cm.^{2}		1.38	1.27	1.15	1.02	0.87	0.71	0.57

The data used in the estimation of c_p is given in (Fig. 5). The assumed values for the specific heat are given by the curve, which was obtained by taking a smoothed weighted average of the specific heats of pure iron and of three steels, whose compositions are in the neighborhood of the desired composition.

The data used in the estimation of k is given in (Fig. 6). The assumed values for the conductivity are given by the curve, which was obtained by taking a smoothed weighted average of the conductivities of two steels, whose compositions bracket the desired composition.

The values of ρ, the specific weight, were obtained by calculation from the thermal expansion data developed in (Fig. 7), assuming that the specific weight at 20 °C. is 7.85 gm./cm.^{3}. The values were obtained from the relationship:

$$\rho = 7.85/(1 + \epsilon_{20}^{T})^3 \qquad \text{gm./cm.}^3$$

The data used in the estimation of ϵ_{20}^{T} is given in (Fig. 7). The assumed values of the thermal expansion are given by the curve, which was obtained by taking a smoothed weighted average of the thermal expansions of three steels, whose compositions are in the neighborhood of the desired composition. This thermal expansion data will also be used in the stress calculation of Chapter VI.

It is apparent, from the spread of the original data in these figures, that c_p, k, and ϵ_{20}^{T} are relatively insensitive to composition. An estimate of the accuracy of their assumed values, without knowing the accuracy of the original data, is difficult. Considering the spread of

Data from "Metals Handbook" 1948 Ed. p313

Code:
1 Pure Iron
2 0.23% C., 1.51% Mn., 0.105% Cu.
3 0.415% C., 0.643% Mn.
4 0.23% C., 0.635% Mn.

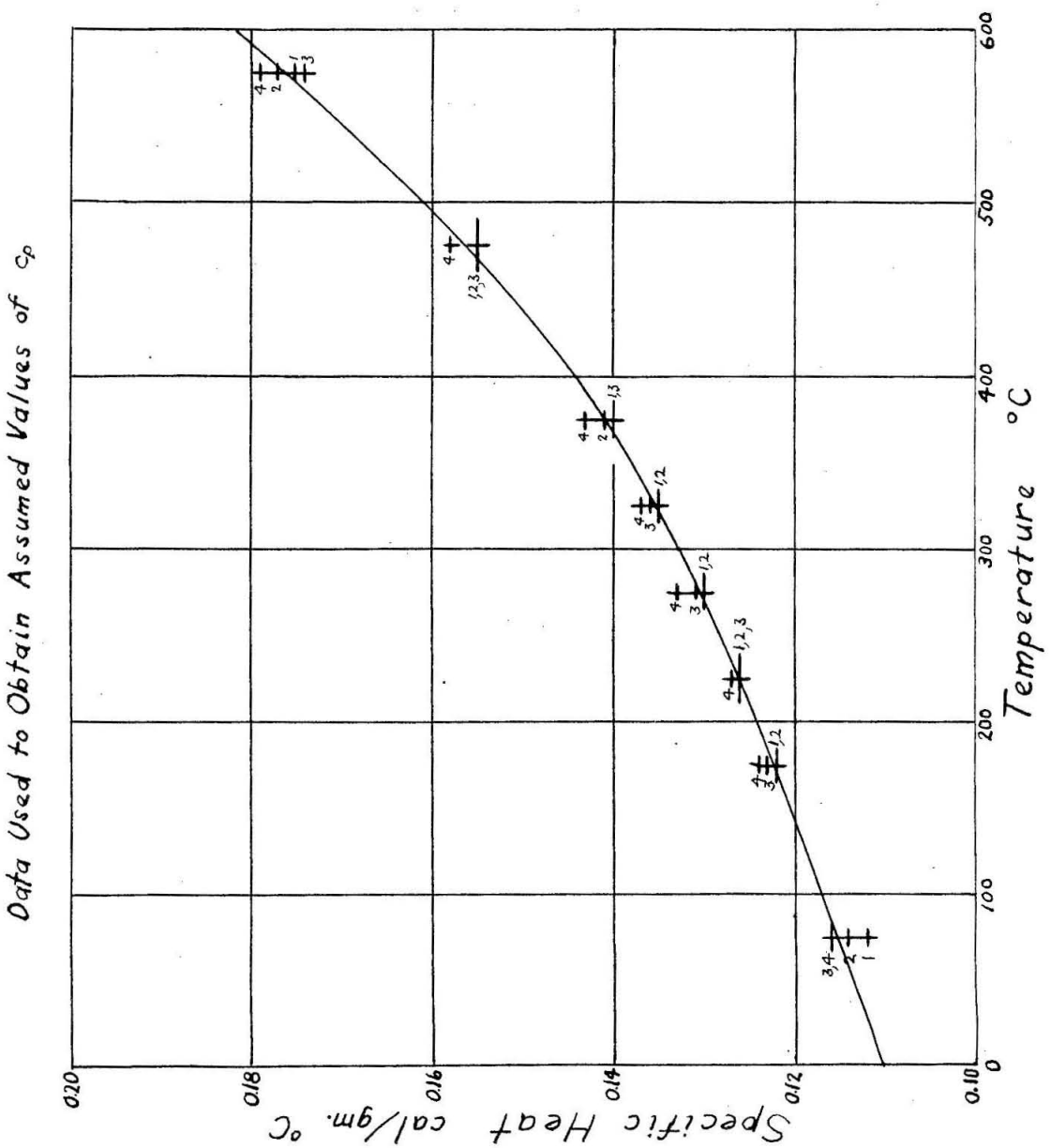

(Fig. 5)

Data from "Metals Handbook" 1948 Ed. p 314
Code: 1 0.23% C., 0.635% Mn., 0.074% Ni., 0.13% Cu., trace Cr.
2 0.415% C., 0.643% Mn., 0.063% Ni., 0.12% Cu., trace Cr.

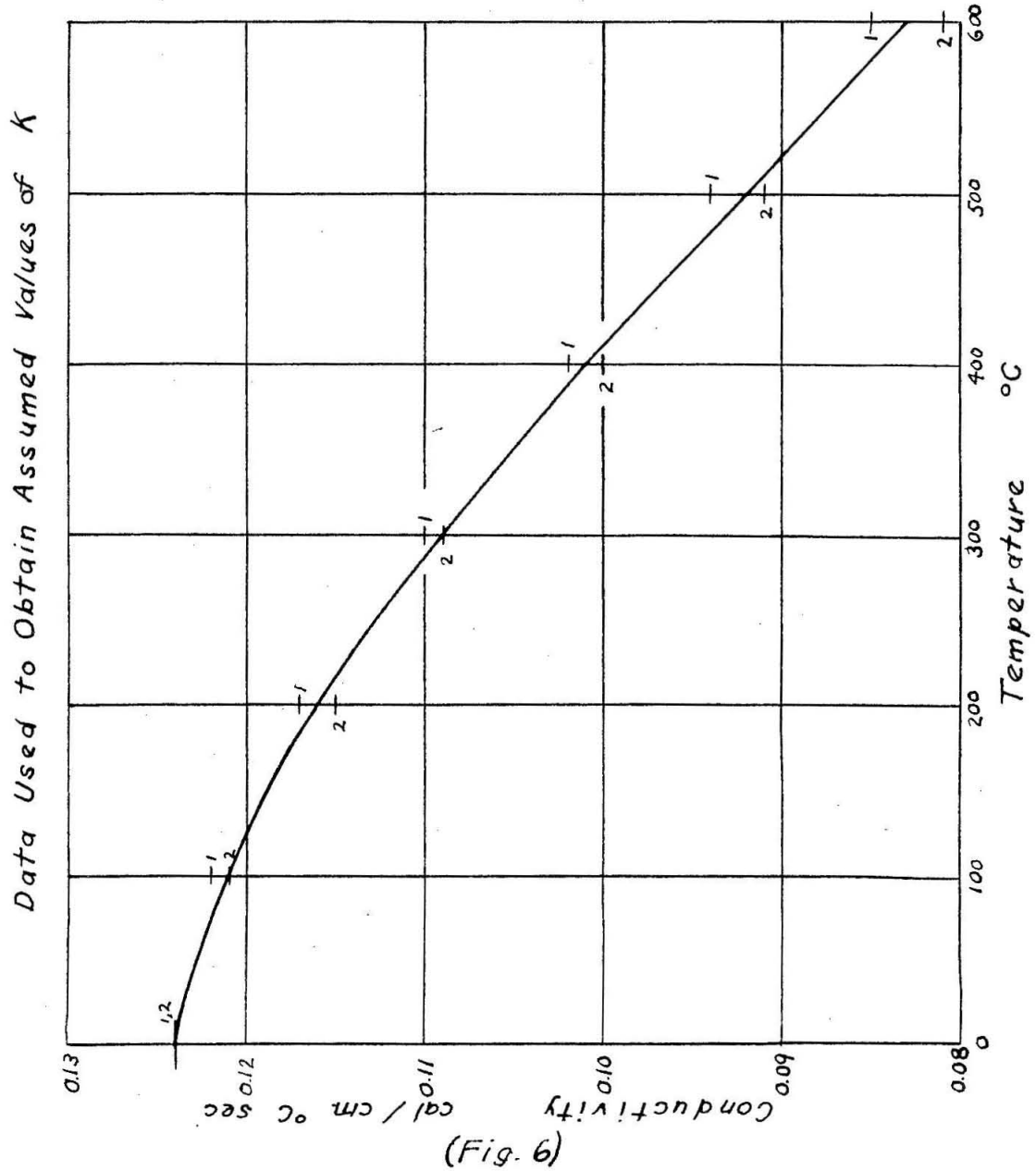

(Fig. 6)

Data Used to Obtain Assumed Values of ϵ_{20}^{T}

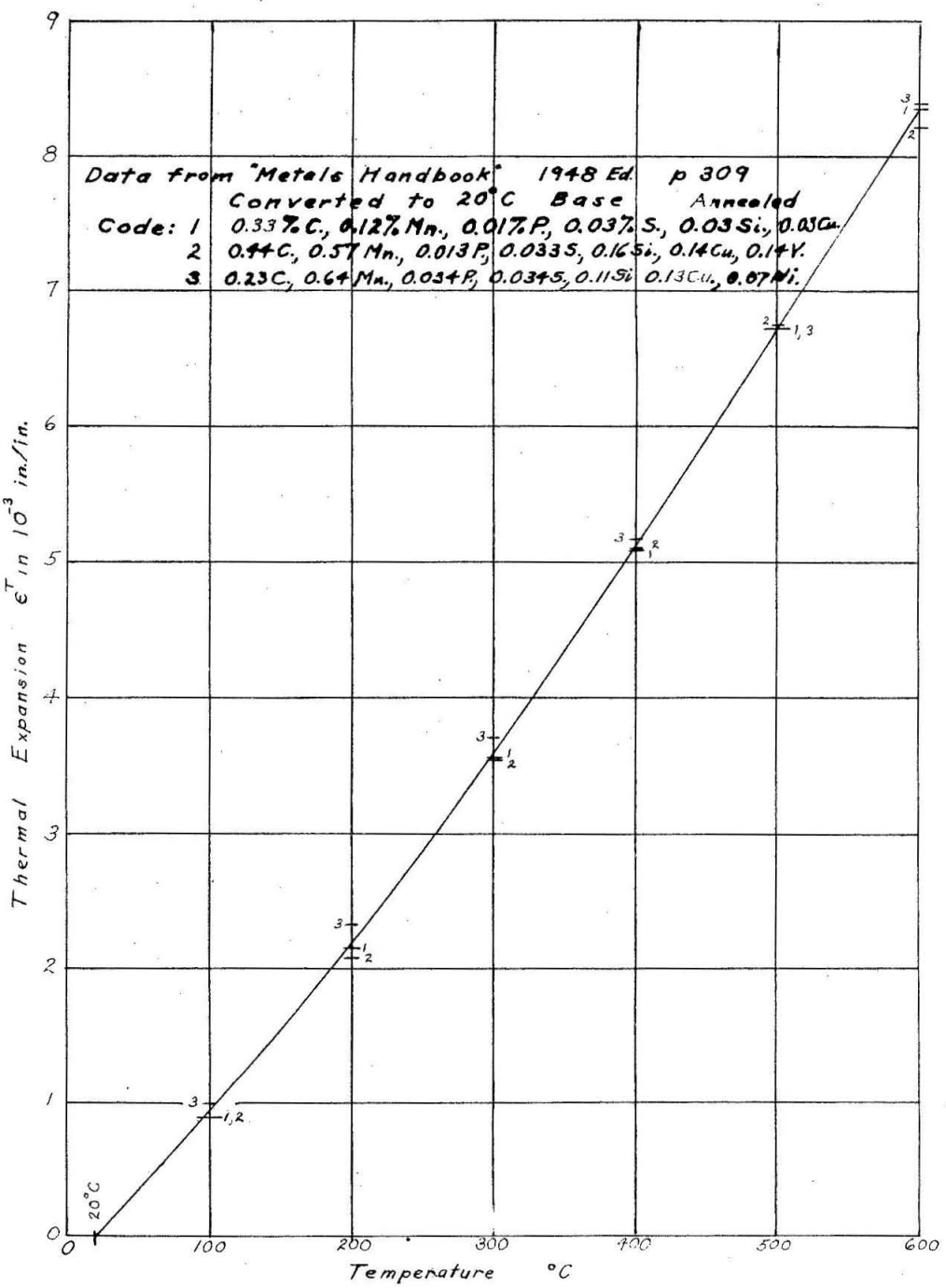

(Fig. 7)

the original data only, an accuracy of the order of 2% appears reasonable.

The estimation of the boundary layer conductivity is, however, more difficult, due to the lack of data. Most of the data appearing in the literature relates to hardenability calculations, and is of an empirical nature. The most highly developed of this type of calculation is that of M. A. Grossman and his associates (13). In their calculations, an empirical constant value of h/k is assigned to different quenching mediums under different conditions, for all steels, and an empirical constant value of the thermal diffusivity a is given to all steels. On the basis of these assumptions, the temperature distribution versus time is computed, neglecting the heat of transformation. The hardenability is then related to the half temperature time, or the time this calculation indicates is required for the temperature at a point to be reduced by one half. Such a calculation is successful since whether or not a steel will harden is largely a function of the cooling rate at a temperature near the knee of the isothermal time temperature, or S, curve, and the empirical parameters are so chosen that this calculation of the half temperature time is suitably related to the cooling velocity at this temperature. It is, however, apparent that values of h used in such a calculation have little meaning for the particular computation under consideration.

A. Rose (14), in 1940, made a literature survey of the data from which values of h, as a function of temperature, could be calculated. Of all the data he reports, only the experimental results of N. B. Pilling and T. D. Lynch (15) correspond at all closely to the case under

consideration. The results of Pilling and Lynch's experiments are presented in the form of a center temperature versus time curve for a 6.5 mm. by 50 mm. Ni. plus 5% Si. cylinder quenched in still water at ambient temperature. Based upon A. Rose's analysis of this data, the following values of the boundary layer conductivity, as a function of the specimen surface temperature, for a quench into still water at ambient temperature, are assumed.

Temperature Range °C	h cal./cm.^{2} sec. °C.
20 - 300	0.028
300 - 700	0.078
700 - up	0.037

The discontinuities in this data are based upon the fact that the mode of cooling changes with the temperature in fairly distinct steps, which are visible to the eye. The highest temperature range represents cooling through a steam jacket without fluid contact and consequently has a low value. The middle range represents vigorous boiling with fluid contact and high convection currents and has the highest value. The lower range represents conduction and convection without boiling and has a low value. As seen in (Fig. 8), the transition at 300 °C. was slightly smoothed in order to avoid anomalies in the temperature solution due to the difference equation approximations.

The accuracy of these values for the boundary layer conductivity is open to question because the cylinder on which these values were determined is 1/8 the size of the cylinder involved in this computation. The data of A. Rose (14), which is all for small specimens, indicates

that the boundary layer conductivity is a drastic function of the bulk temperature and velocity of the water. The bulk temperature particularly affects the surface temperature at which the transition in the mode of cooling occurs. In view of this, and in the light of ordinary fluid-solid heat transfer theory, it may be expected that the value of h is a function of the following factors:

1) The surface temperature of the body being quenched.
2) The bulk temperature of the coolant.
3) The local coolant velocity.
4) The thickness of the heated, or boundary, layer.
5) The surface condition of the body.
6) The availability of the nuclei for the start of vapor bubbles.
7) The pressure.

Considerations of this type indicate that there is not only a size effect but that in the experimental case, which this calculation matches, the value of h may have varied by a fairly large factor over the length of the cylinder.

The assumption of the value of the boundary layer conductivity may, therefore, be considered to be the most critical assumption in the temperature problem. This will be discussed again in Chapter VIII when the results of the calculated values of the residual stresses are compared with the results of the experimental determination of Bucholtz and Buhler.

The values of the pertinent parameters have now been selected as a function of temperature. The temperature, as a function of position and time may now be determined by the application of the techniques developed in Chapter I. (Fig. 8) indicates, to a reduced scale, the complete graphical set-up used to obtain the solution of the temperature problem. This figure also indicates a sample calculation for the interval from $t = 7$ to $t = 9$ seconds. The necessary tabular computations accompanying this sample calculation are indicated in Table II. The calculation was carried out through a total of 37 seconds; or until the temperature gradient became comparatively small. During the first five seconds of this calculation, the radius was divided up into $n = 5$ equal intervals, and the time interval was $\frac{1}{3}$ second. At five seconds, the number n was changed to 5 and the value of Δt was increased to 2 seconds. At the end of 31 seconds, the value of Δt was decreased to 1.2 seconds, in order to decrease the value of the multiplier $2a\Delta t/(\Delta r)^2$ from approximately 1.5 to 1.0 .

The results of this calculation were cross plotted as temperature versus time for various radial positions, in order to check the continuity of the solution. The final results were then plotted, (Fig. 9) , for $t = 1, 2, 4, 8, 16$, and 32 seconds against the new variable $A = x^2 = r^2/r_1^2$. (Fig. 9) represents the temperature distributions which are used in the stress problem.

Complete Set-up for the Solution of the Temperature Distribution vs Time

A Sample Calculation for the Time Interval t=7 to t=9 sec is Illustrated if this Figure is used in conjunction with Table II

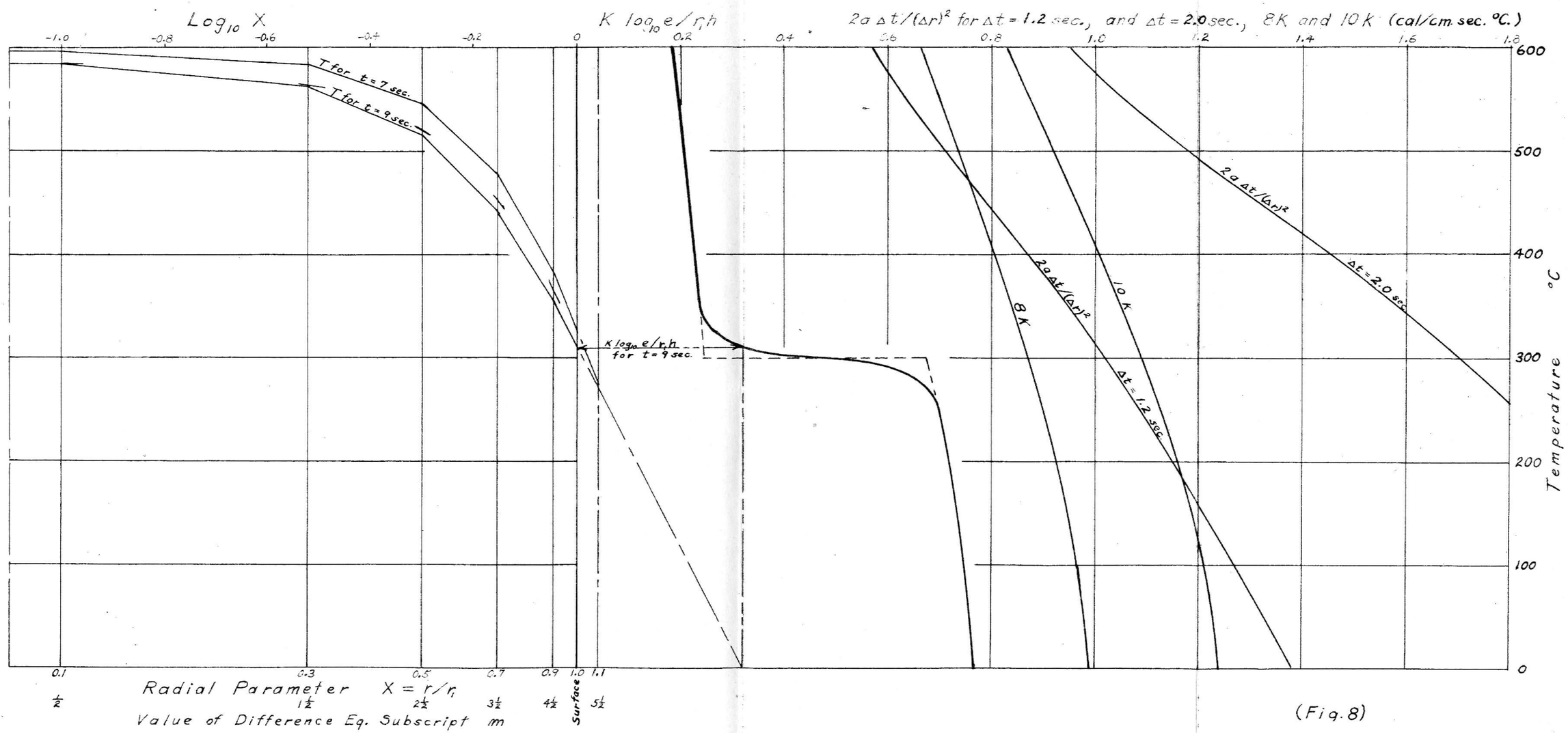

(Fig. 8)

Table II

The necessary tabular computations accompanying the sample calculation of (Fig. 8).

t	Δt	j	Parameter	Value of m: ½	1½	2½	3½	4½	5½
7 sec.	2 sec.	11	T_m	596.2	583.9	546.2	478.2	381.7	282.0
			k_m	.0834	.0846	.0879	.0941	.1025	.1104
			$k_{m+1}-k_{m-1}$	.0012	.0045	.0095	.0146	.0163	--
			$8k_m$	.667	.676	.7035	.752	.820	--
			$T_{m+1}-T_{m-1}$	-12.3	-50.0	-105.7	-164.5	-196.2	--
			$B_m = (k_{m+1}-k_{m-1})(T_{m+1}-T_{m-1})/8k_m$	-.022	-.333	-1.43	-3.20	-3.90	--
			$A_m = \frac{1}{2}\left[(T_{m+1}-2T_m+T_{m-1}) + \frac{1}{2m}(T_{m+1}-T_{m-1})\right]$	-12.8	-21.0	-27.0	-26.5	-13.4	--
			$A_m + B_m$	-12.8	-21.3	-28.4	-29.7	-17.3	--
			$C_m = 2a\Delta t/(\Delta r)^2$	-.959	-.986	-1.070	-1.240	-1.505	--
			$T_{m,12}-T_{m,11} = C_m(A_m+B_m)$	-12.3	-21.0	-30.4	-36.8	-26.0	--
9 sec.	2 sec.	12	$T_m = T_{m,11} + (T_{m,12}-T_{m,11})$	583.9	562.9	515.8	441.4	355.7	277.4

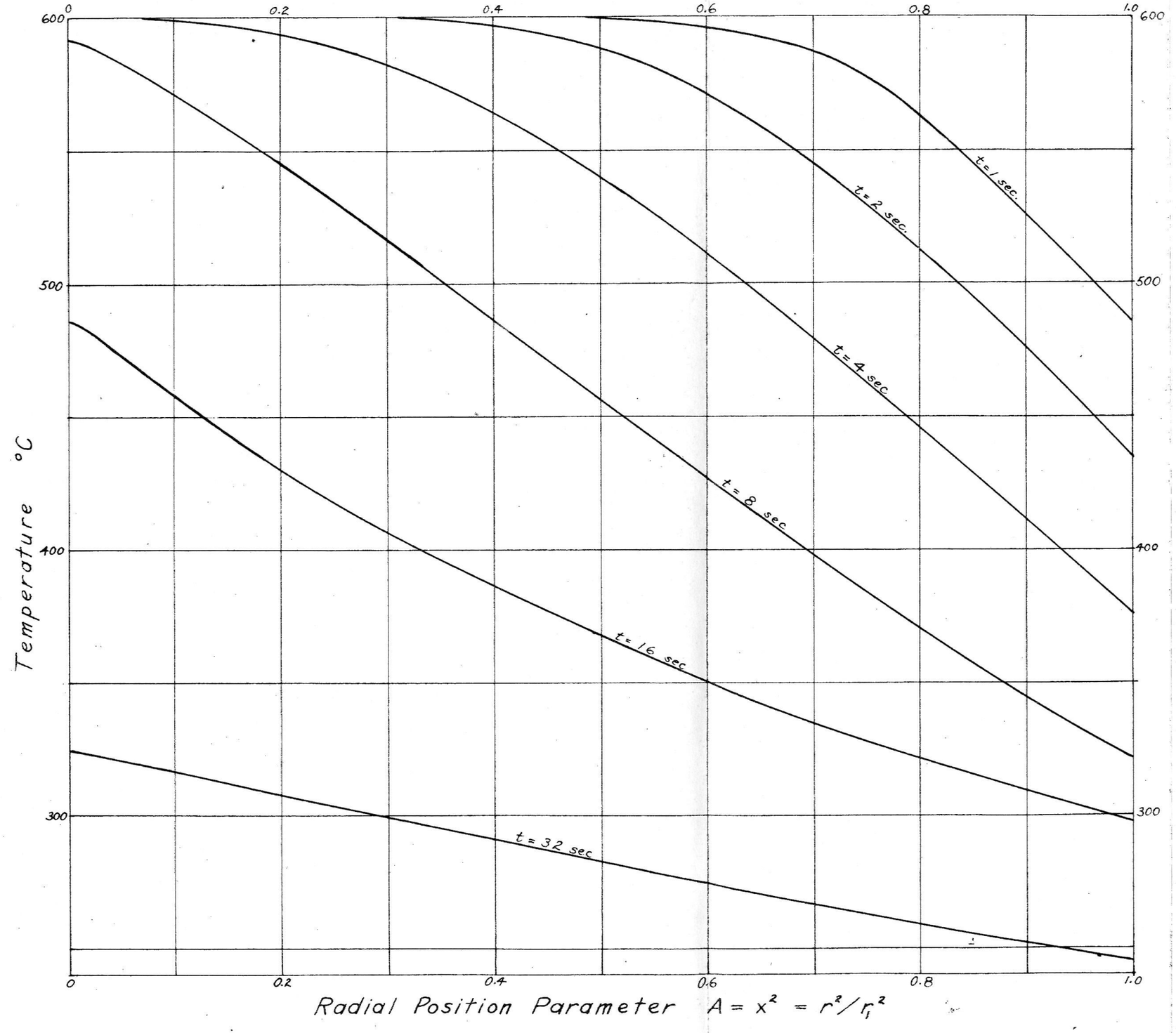

Final Results

Temperature versus

Radial Position for

Various Values of Time

(Fig. 9)

CHAPTER VI

This chapter will be devoted to the determination of the stresses due to the thermal dilation, as a function of the position and the time, for the case of a 5 cm. diameter mild steel cylinder which is subjected to the temperature distribution versus time indicated in (Fig. 9). This temperature distribution corresponds to a quench from 600 °C. in still water at ambient temperature. Since the boundary forces are zero, the results of this computation will represent the stresses which would have been present in the cylinder if no yielding had taken place. The techniques of solution and the notation used will be those of Chapter III.

The first step in this determination is the selection of the values of the pertinent variables, as a function of the temperature, from the literature.

The value of the linear component of the thermal dilation (thermal expansion), ϵ_{20}^{T} , was selected in Chapter V and is presented in (Fig. 7).

The selection of values of E , G , and $\nu = (E/2G) - 1$, is, however, more difficult. The articles of F. L. Everett and J. Miklowitz (16) and G. Verse (17) contain not only original determinations of E and G , but also show comparisons of their results with those of previous investigators. The bibliographies of these articles are virtually inclusive of the work done in this field. These references indicate that the values of E and G , while not particularly sensitive to composition,

are sensitive to the techniques by which they are determined. This is particularly evident when values of ν are calculated from values of E and G which were determined by different techniques. As ν is an important parameter in the calculation under consideration, and as the experimental determinations of Everett and Miklowitz are the only ones specifically designed to obtain reliable values of ν, the results of their experimental work is assumed in the computation under consideration. Their values of E and G were determined by unloading in combined bending and torsion. Since these values were determined simultaneously, the resulting value of ν may be presumed to be more reliable than when (as in the other available determinations) the values of E and G are determined by different techniques on different specimens. Furthermore, the technique of unloading corresponds to the definitions for E and G which were specified in Chapter II. The composition and the heat treatment of the steel used in this determination of the elastic constants (nominal S.A.E. 1020 -- hot rolled) deviates appreciably from the steel assumed in the calculation under consideration (nominal S.A.E. 1030 -- normalized), but, in lieu of better data, this divergence must be accepted.

This data of Everett and Miklowitz is presented as values of E and G at ambient temperature, 200 °F., 400 °F., 600 °F., 800 °F., and 1000 °F. For use in the computation under consideration, the intermediate points were plotted with extreme care in (Fig. 10) in such a manner that the resulting value of $\nu = (E/2G) - 1$ formed a smooth curve. The values of E and 2G were graphically extrapolated from 1000 °F. (537.78 °C.) to 600 °C. From the curves of (Fig. 10), the values of

the parameters: ν , $E/1-\nu$, $2G/1-\nu$, and $2\nu G/1-\nu$ were computed and plotted in (Fig. 11). The derivative $d/dT(1/2G)$ was graphically determined from the curve $1/2G$, which was obtained from the value of $2G$, (Fig. 10). This derivative is plotted in (Fig. 12).

The technique used in determining the stresses due to the thermal dilation will now be indicated through the aid of a sample calculation. In this sample calculation, the stresses due to the thermal dilation corresponding to the temperature distribution, (Fig. 9), for $t = 4$ seconds will be computed.

The equations to be solved were developed in Chapter III, but will be presented again here for convenience. The equations to be solved are:

$$(25)_1 \qquad \epsilon_{z_1} = \frac{\int_0^1 \frac{E}{1-\nu}\epsilon^T dA}{\int_0^1 \frac{E}{1-\nu} dA} + \frac{\int_0^1 f_1(\sigma_{r_1})dA \int_0^1 \frac{2\nu G}{1-\nu} dA - \int_0^1 f_2(\sigma_{r_1})dA \int_0^1 \frac{2G}{1-\nu} dA}{\int_0^1 \frac{E}{1-\nu} dA \left[\int_0^1 \frac{2G}{1-\nu} dA - \int_0^1 \frac{2\nu G}{1-\nu} dA\right]}$$

$$(26)_1 \qquad C_1' = \frac{-\int_0^1 f_1(\sigma_{r_1})dA + \int_0^1 f_2(\sigma_{r_1})dA}{\int_0^1 \frac{2G}{1-\nu} dA - \int_0^1 \frac{2\nu G}{1-\nu} dA}$$

$$(23)_1 \qquad 2A\sigma_{r_1} = \int_0^A f_1(\sigma_{r_1})dA - \int_0^A \frac{E}{1-\nu}\epsilon^T dA + \epsilon_{z_1}\int_0^A \frac{E}{1-\nu} dA + C_1'\int_0^A \frac{2G}{1-\nu} dA$$

$$(17a)_1 \qquad \sigma_{\phi_1} = -\sigma_{r_1} + f_1(\sigma_{r_1}) - \frac{E}{1-\nu}\epsilon^T + \epsilon_{z_1}\frac{E}{1-\nu} + C_1'\frac{2G}{1-\nu}$$

$$(21a)_1 \qquad \sigma_{z_1} = f_2(\sigma_{r_1}) - \frac{E}{1-\nu}\epsilon^T + \epsilon_{z_1}\frac{E}{1-\nu} + C_1'\frac{2\nu G}{1-\nu}$$

Data from F. Everett and J. Miklowitz "Poisson's Ratio at High Temperature" Journal of Applied Physics 15 592 - 598 1944

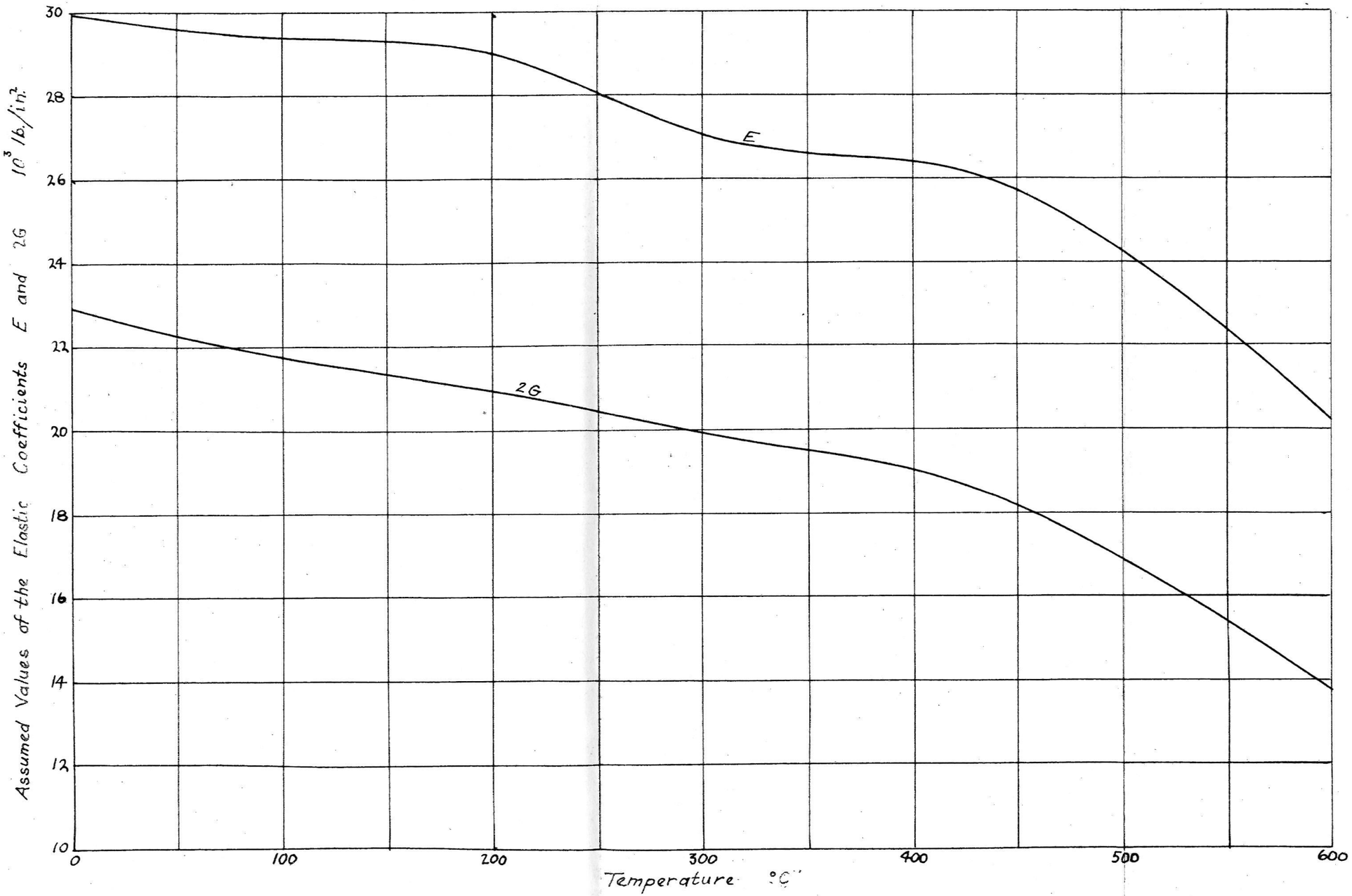

Nominal S.A.E. 1020 Hot Rolled E & G. determined by unloading in combined torsion and bending

(Fig. 10)

Functions derived from the assumed values of E & 2G

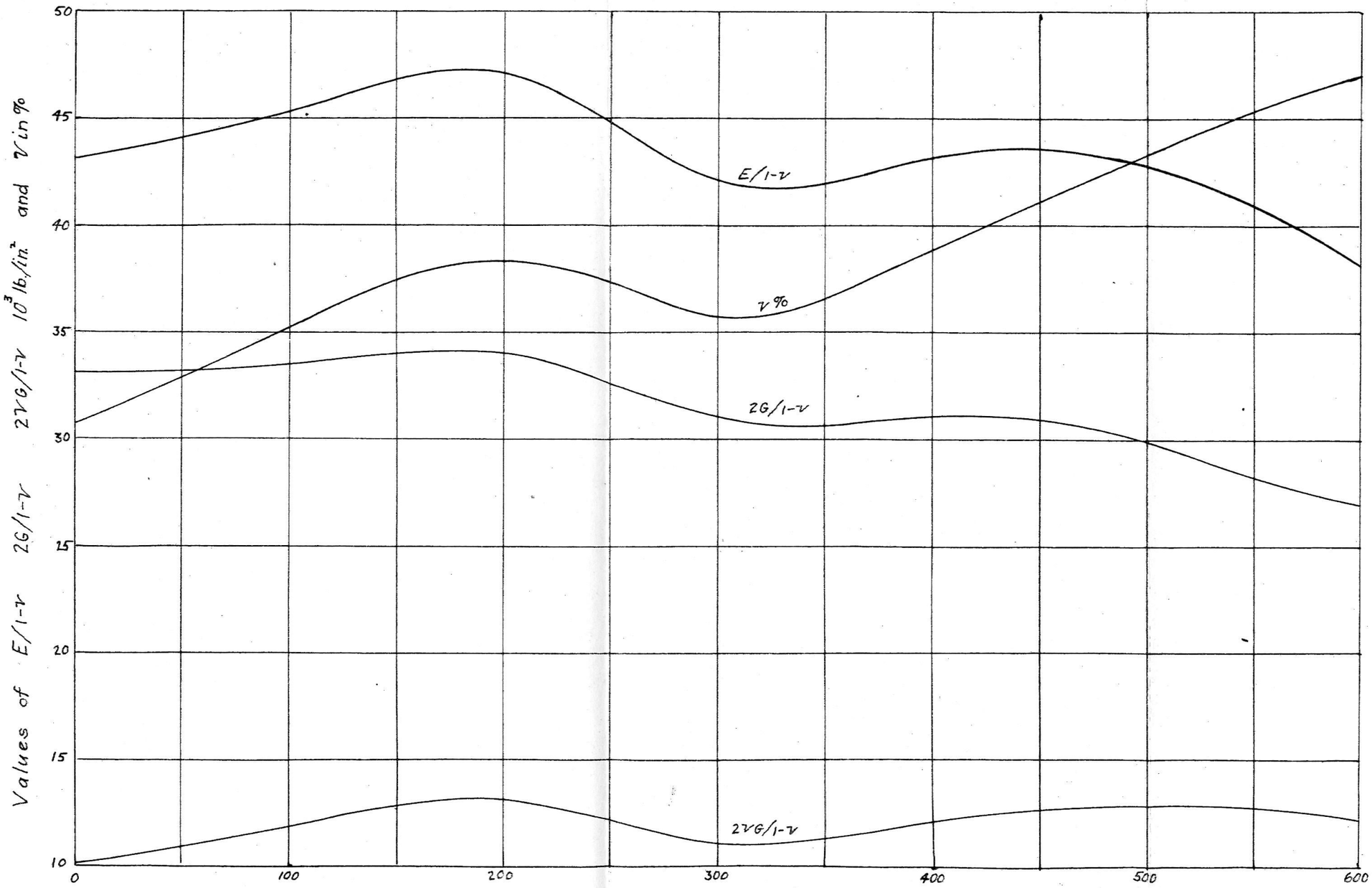

(Fig. 11)

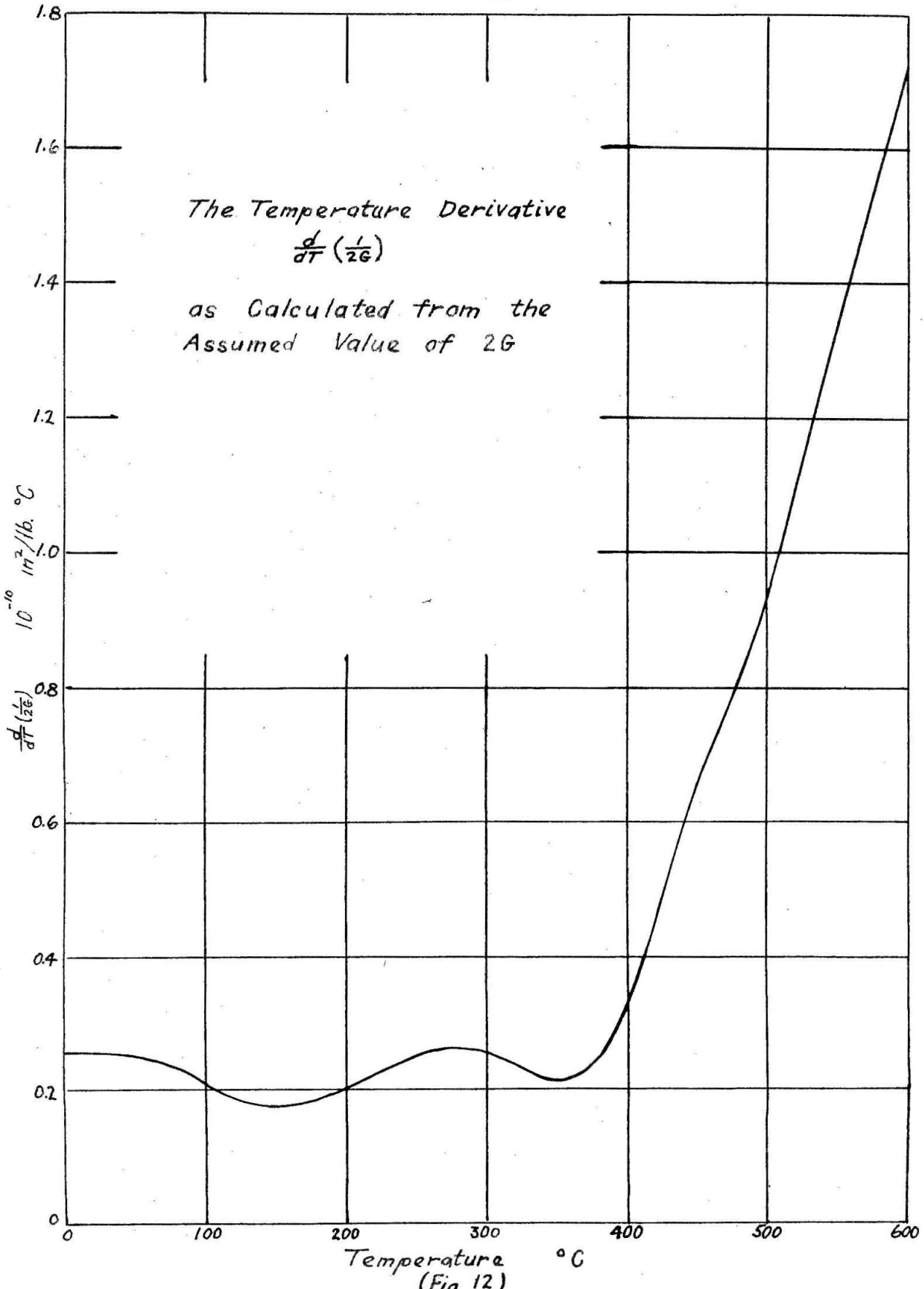
The Temperature Derivative
$\frac{d}{dT}\left(\frac{1}{2G}\right)$
as Calculated from the
Assumed Value of 2G
$\frac{d}{dT}\left(\frac{1}{2G}\right)$ 10^{-10} $in^2/lb.\ °C$
1.8
1.6
1.4
1.2
1.0
0.8
0.6
0.4
0.2
0
0
100
200
300
400
500
600
Temperature °C

(Fig. 12)

SAMPLE CALCULATION - STRESS DUE THERMAL DILATION

$t = 4$ sec

Required Tabular Data and Calculations

$A = r^2/r_1^2$	From Previous Solution for Temp. Distribution	Known Function of Temperature	$\epsilon^T = \epsilon^T_{20} - \epsilon^T_{20}\big\vert_{A=0}$	Known Function of Temperature	Graphically Perform $\int_0^A \frac{E}{1-\nu}\epsilon^T dA$	Perform Indicated Product	Graphically Perform $\int_0^A ③ dA$
A	T	ϵ^T_{20}	ϵ^T	④ $\frac{E}{1-\nu}$	$\int_0^A ④ dA$	$-\frac{E}{1-\nu}\epsilon^T$	$\int_0^A ③ dA$
in^2/in^2	°C	10^{-3} in/in	10^{-3} in/in	10^6 lb/in²	10^6 lb/in²	10^3 lb/in²	10^3 lb/in²
0	600	8.35	0	38.15	0	0	0
0.2	594	8.245	- .105	38.55	7.65	4.05	.28
0.4	564.5	7.76	- .59	40.29	15.61	23.75	2.72
0.6	511.5	6.90	-1.45	42.47	23.89	61.6	11.02
0.8	446	5.85	-2.50	43.61	32.53	109.0	27.96
0.9	411.5	6.30	-3.05	43.42	36.89	132.5	39.98
1.0	376	4.74	-3.61	42.62	41.20	153.8	54.24

$$\bar{\epsilon}_{z_1} = \frac{-\int_0^1 ③ dA}{\int_0^1 ④ dA} = \frac{-54.24\times10^3}{41.2\times10^6} = -1.3165\times10^{-3}$$

	Perform Product $\bar{\epsilon}_{z_1} \times \int_0^A \frac{E}{1-\nu} dA$	$2A\bar{\sigma}_{r_1} = \int_0^A ③ dA + \bar{\epsilon}_{z_1}\int_0^A ④ dA$
	$\bar{\epsilon}_{z_1}\int_0^A ④ dA$	$2A\bar{\sigma}_{r_1}$
	10^3 lb/in²	10^3 lb/in²
0	0	0
0.2	-10.07	- 9.79
0.4	-20.55	-17.83
0.6	-31.43	-20.41
0.8	-42.8	-14.84
0.9	-48.55	- 8.57
1.0	-54.25	0

$$2\bar{\sigma}_{r_1}\Big\vert_{A=0} = \frac{E}{1-\nu}\bar{\epsilon}_{z_1}\Big\vert_{A=0} = 38.15\times10^6 \times (-1.3165\times10^{-3}) = -50.2\times10^3$$

$\bar{\sigma}_{r_1} = \frac{2A\bar{\sigma}_{r_1}}{2A}$ $A\neq0$	Known Function of Temperature ⑤ $\frac{2G}{1-\nu}$	Graphically Perform $\int_0^A ⑤ dA$	Known Function of Temperature ⑥ $\frac{2\nu G}{1-\nu}$	Graphically Perform $\int_0^A ⑥ dA$	From Graphical Differentiation of Temp. Distribution $\frac{dT}{dA}$	From Graphical Differentiation of $\frac{1}{2G}$ vs T $\frac{d}{dT}\left(\frac{1}{2G}\right)$	$\frac{d}{dA}\left(\frac{1}{2G}\right) = \frac{d}{dT}\left(\frac{1}{2G}\right)\frac{dT}{dA}$	Perform Product $\frac{1}{\bar{\sigma}_{r_1}}\frac{d}{dA}\left(\frac{1}{2G}\right)$ B	Graphically Perform $\int_0^A B\,dA$	Perform Product $\frac{2G}{1-\nu}\int_0^A B\,dA$ ①	Graphically Perform $\int_0^A ① dA$	Perform Product $\frac{2\nu G}{1-\nu}\int_0^A B\,dA$ ②	Graphically Perform $\int_0^A ② dA$
10^3 lb/in²	10^6 lb/in²	10^6 lb/in²	10^6 lb/in²	10^6 lb/in²	°C	$10^{-10}\frac{in^2}{lb\,°C}$	10^{-8} in²/lb	10^{-5} in/in	10^{-5} in/in	10^3 lb/in²	10^3 lb/in²	10^3 lb/in²	10^3 lb/in²
-25.1	26.95	0	12.20	0	0	1.72	0	0	0	0	0	0	0
-24.45	27.07	5.395	12.30	2.405	-81.5	1.675	- 1.365	33.38	1.825	.494	.025	.225	.012
-22.3	27.78	10.87	12.67	4.905	-219.	1.455	- 3.11	69.4	13.745	3.82	.423	1.74	.184
-17.01	29.02	16.53	12.90	7.475	-307.5	1.025	- 3.15	53.6	26.595	7.72	1.587	3.43	.709
- 9.28	30.93	23.55	12.66	10.050	-340.5	.636	- 2.165	20.1	34.075	10.53	3.437	4.31	1.500
- 4.76	31.09	26.66	12.27	11.300	-351.5	.405	- 1.423	6.77	35.355	10.99	4.517	4.335	1.935
0	30.94	29.76	11.70	12.504	-357.5	.238	- .85	0	35.655	11.02	5.619	4.12	2.36

$$C_1' = \frac{-\int_0^1 ① dA + \int_0^1 ② dA}{\int_0^1 ⑤ dA - \int_0^1 ⑥ dA} = \frac{-5.619\times10^3 + 2.36\times10^3}{29.76\times10^6 - 12.504\times10^6} = -0.1889\times10^{-3}$$

$$\epsilon_{z_1} = \bar{\epsilon}_{z_1} + \frac{\int_0^1 ① dA\int_0^1 ⑥ dA - \int_0^1 ⑧ dA\int_0^1 ⑤ dA}{\int_0^1 ④ dA\left[\int_0^1 ⑤ dA - \int_0^1 ⑥ dA\right]}$$

$$= -1.3165\times10^{-3} + \frac{5.619\times12.504 - 2.36\times29.76}{41.20\left[29.76 - 12.504\right]}\times10^{-3} = -1.3163\times10^{-3}$$

	Perform Product $\epsilon_{z_1} \times \frac{E}{1-\nu}$	Perform Product $\epsilon_{z_1}\int_0^A ④ dA$	Perform Product $C_1' \times \frac{2G}{1-\nu}$	Perform Product $C_1' \times \int_0^A \frac{2G}{1-\nu} dA$	Perform Product $C_1' \times \frac{2\nu G}{1-\nu}$	$2A\bar{\sigma}_{r_1} = \int_0^A ① dA + \int_0^A ③ dA + \epsilon_{z_1}\int_0^A ⑤ dA + C_1'\int_0^A ⑤ dA$
A	ϵ_{z_1} ④	$\epsilon_{z_1}\int_0^A ④ dA$	C_1' ⑤	$C_1'\int_0^A ⑤ dA$	C_1' ⑥	$2A\bar{\sigma}_{r_1}$
in^2/in^2	10^3 lb/in²	10^3 lb/in²	10^5 lb/in²	10^3 lb/in²	10^3 lb/in²	10^3 lb/in²
0	- 50.2	0	- 5.09	0	- 2.305	0
0.2	-50.7	- 10.07	- 5.11	- 1.019	- 2.32	-10.784
0.4	-53.0	-20.53	- 5.24	- 2.053	- 2.39	-19.44
0.6	-55.9	- 31.4	- 5.49	- 3.12	- 2.49	-21.913
0.8	-57.3	- 42.8	- 5.84	- 4.45	- 2.39	-15.853
0.9	-57.1	-48.5	- 5.87	- 5.035	- 2.315	- 9.038
1.0	-56.05	-54.23	- 5.84	- 5.62	- 2.21	0 (4.009)

$$2\bar{\sigma}_{r_1}\Big\vert_{A=0} = \epsilon_{z_1}④\Big\vert_{A=0} C_1'⑤\Big\vert_{A=0} = -502\times10^{-3} - 5.09\times10^{-3} = -55.29\times10^{-3}$$

$\bar{\sigma}_{r_1} = \frac{2A\bar{\sigma}_{r_1}}{2A}$ $A\neq0$	$\bar{\sigma}_{\phi_1} = ① + ③ - ⑦ + \epsilon_{z_1}④ + C_1'⑥$	$\bar{\sigma}_{z_1} = ② + ③ + \epsilon_{z_1}④ + C_1'⑥$
$\bar{\sigma}_{r_1}$ ⑦	$\bar{\sigma}_{\phi_1}$	$\bar{\sigma}_{z_1}$
10^3 lb/in²	10^3 lb/in²	10^3 lb/in²
-27.695	-27.695	-52.51
-26.96	-29.31	-48.75
-24.3	- 6.37	-29.90
-18.75	+26.18	+ 6.69
- 9.91	66.30	53.62
- 5.02	85.54	77.42
0	102.93	99.66

The Set of Equations Solved in this Sample Calculation are:

$$2\frac{d}{dA}(A\bar{\sigma}_{r_1}) = \bar{\sigma}_{\phi_1} + \bar{\sigma}_{r_1}$$

$$\simeq \frac{2G}{1-\nu}\int_0^A \bar{\sigma}_{r_1}\frac{d}{dA}\left(\frac{1}{2G}\right)dA - \frac{E}{1-\nu}\epsilon^T + \frac{E}{1-\nu}\epsilon_{z_1} + \frac{2G}{1-\nu}C_1'$$

$$A\bar{\sigma}_{r_1}\Big\vert_{A=0} = 0$$

$$A\bar{\sigma}_{r_1}\Big\vert_{A=1} = 0$$

$$\bar{\sigma}_{z_1} = \frac{2\nu G}{1-\nu}\int_0^A \bar{\sigma}_{r_1}\frac{d}{dA}\left(\frac{1}{2G}\right)dA - \frac{E}{1-\nu}\epsilon^T + \frac{E}{1-\nu}\epsilon_{z_1} + \frac{2\nu G}{1-\nu}C_1'$$

$$\int_0^1 \bar{\sigma}_{z_1} dA = 0$$

where ϵ_{z_1} and C_1' are constants and remainder of terms on right hand side, except $\bar{\sigma}_{r_1}$, are Known graphical functions of A.

(Table III)

SAMPLE CALCULATION $t = 4$ sec

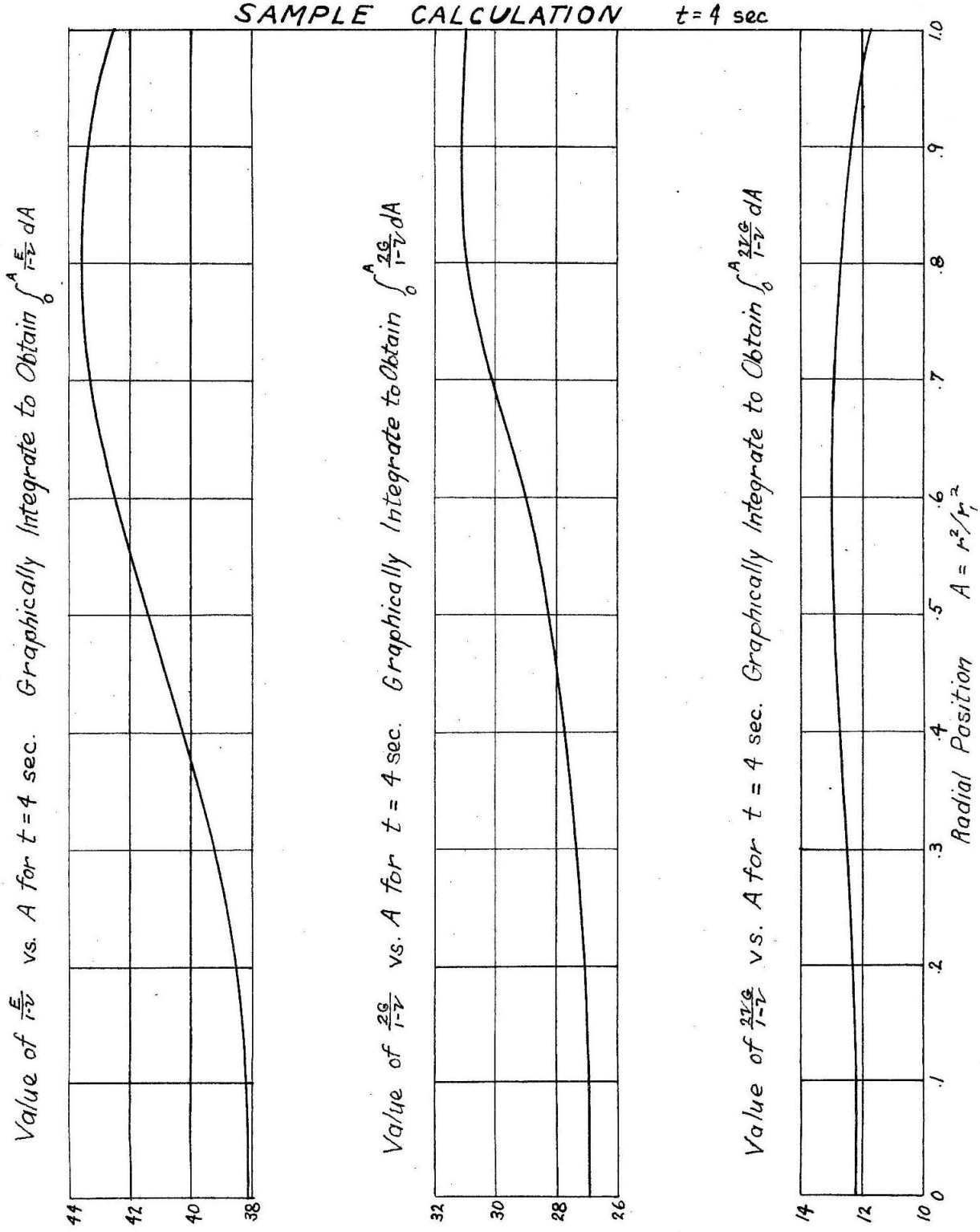

(Fig. 13)

Value of $-\frac{E}{1-\nu}\epsilon^T$, $f_1(\bar{\sigma}_{r_1})$, $f_2(\bar{\sigma}_{r_1})$ vs A for $t = 4$ sec. Graphically Integrate to Obtain $-\int_0^A \frac{E}{1-\nu}\epsilon^T dA$, $\int_0^A f_1(\bar{\sigma}_{r_1})dA$, and $\int_0^A f_2(\bar{\sigma}_{r_1})dA$

$f_1(\bar{\sigma}_{r_1})$ and $f_2(\bar{\sigma}_{r_1})$ are determined from graphical integral $\int_0^A \bar{\sigma}_{r_1} \frac{d}{dA}\left(\frac{1}{2G}\right) dA$

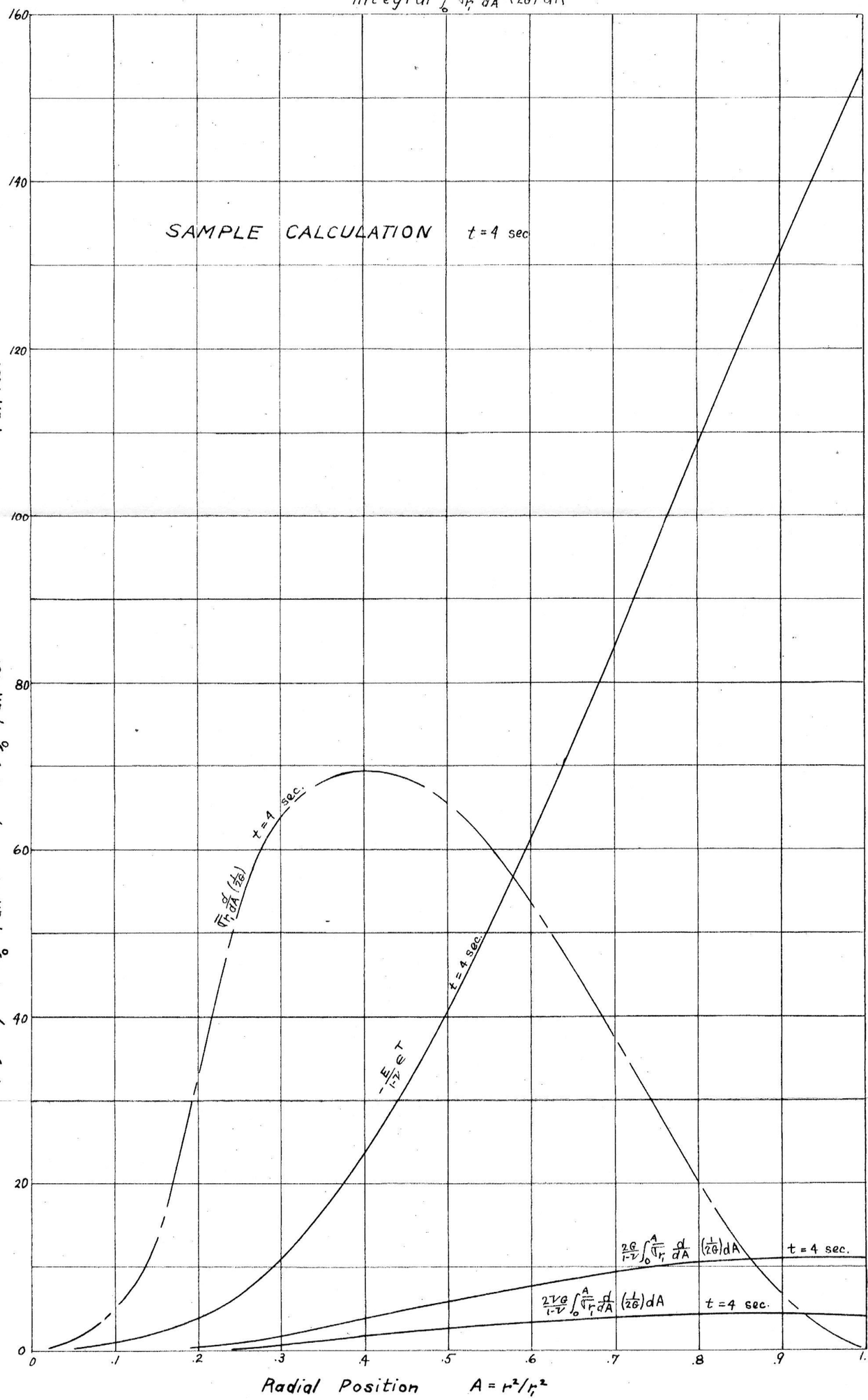

(Fig. 14)

(Table III) contains the necessary numerical aspects of this sample calculation. Referring to this table, all of the parameters are evaluated at $A = 0$, 0.2 , 0.4 , 0.6 , 0.8 , 0.9 and 1.0. These positions are arbitrarily selected as the minimum number which will give the necessary accuracy for the graphical interpolation of the values of the parameters. The extra position, $A = 0.9$, is added because of the greater initial temperature gradient near the surface. The temperature of each of these positions, at $t = 4$ sec., is obtained from (Fig. 9), and is recorded in (Table III). The corresponding values of $E/(1-\nu)$, $2G/(1-\nu)$ and $2\nu G/(1-\nu)$, obtained from (Fig. 11), are recorded in (Table III) and plotted in (Fig. 13) as a function of A. The values of $\int_0^A \frac{E}{1-\nu} dA$, $\int_0^A \frac{2G}{1-\nu} dA$, and $\int_0^A \frac{2\nu G}{1-\nu} dA$ are determined, for these positions, by the graphical integration of the curves of (Fig. 13), and are recorded in (Table III). The corresponding values of ϵ_{20}^T, determined from (Fig. 7), $d/dT(1/2G)$, determined from (Fig. 12), and dT/dA , determined by graphical differentiation of (Fig. 9), are also recorded in (Table III). The values of the products $\frac{E}{1-\nu}\epsilon^T = \frac{E}{1-\nu}(\epsilon_{20}^T - \epsilon_{20}^T\Big|_{A=0})$ and $\frac{d}{dA}(\frac{1}{2G}) = \frac{d}{dT}(\frac{1}{2G})\frac{dT}{dA}$ are determined for these positions and are recorded in (Table III). $\frac{E}{1-\nu}\epsilon^T$ is plotted in (Fig. 14) and the value $\int_0^A \frac{E}{1-\nu}\epsilon^T dA$, at these positions, is determined by graphical integration and is recorded in (Table III).

A first approximation to the values of ϵ_{z_1} and C_1' is then obtained from $(\text{Eq. } 25)_1$ and $(\text{Eq. } 26)_1$ by assuming that $f_1(\sigma_{r_1}) = f_2(\sigma_{r_1}) = 0$. This approximation is:

$$\bar{\epsilon}_{z_1} = \frac{\int_0^1 \frac{E}{1-\nu}\epsilon^T dA}{\int_0^1 \frac{E}{1-\nu} dA} = 1.3165 \times 10^{-3} \text{ in/in} \quad \text{and} \quad \bar{C}_1' = 0$$

A first approximation to σ_{r_1}, denoted by $\bar{\sigma}_{r_1}$, is then obtained for these positions from $(\text{Eq. } 23)_1$ by assuming that $f_1(\sigma_{r_1}) = 0$. This approximation is:

$$2A\bar{\sigma}_{r_1} = -\int_0^A \frac{E}{1-\nu}\epsilon^T dA + \bar{\epsilon}_{z_1}\int_0^A \frac{E}{1-\nu}dA$$

These values of $\bar{\sigma}_{r_1}$ are used to form the function $\bar{\sigma}_{r_1}\frac{d}{dA}(\frac{1}{2G})$, which is plotted in (Fig. 14). The function $\int_0^A \bar{\sigma}_{r_1}\frac{d}{dA}(\frac{1}{2G})dA$ is then obtained, for these positions, by graphical integration, and is recorded in (Table III). The functions:

$$f_1(\bar{\sigma}_{r_1}) = \frac{2G}{1-\nu}\int_0^A \bar{\sigma}_{r_1}\frac{d}{dA}(\frac{1}{2G})dA \quad \text{and} \quad f_2(\bar{\sigma}_{r_1}) = \frac{2\nu G}{1-\nu}\int_0^A \bar{\sigma}_{r_1}\frac{d}{dA}(\frac{1}{2G})dA$$

are then obtained for these positions and are recorded in (Table III) and plotted in (Fig. 14). The values of the functions $\int_0^A f_1(\bar{\sigma}_{r_1})dA$ and $\int_0^A f_2(\bar{\sigma}_{r_1})dA$, are then obtained by graphical integration, for these positions, and are recorded in (Table III).

A second, and in this case final, approximation to ϵ_{z_1} and C_1' is then obtained from $(\text{Eq. } 25)_1$ and $(\text{Eq. } 26)_1$, by replacing $f_1(\sigma_{r_1})$ and $f_2(\sigma_{r_1})$ by $f_1(\bar{\sigma}_{r_1})$ and $f_2(\bar{\sigma}_{r_1})$ respectively. These approximations are:

$$\epsilon_{z_1} \cong \bar{\epsilon}_{z_1} + \frac{\int_0^1 f_1(\bar{\sigma}_{r_1})dA\int_0^1 \frac{2\nu G}{1-\nu}dA - \int_0^1 f_2(\bar{\sigma}_{r_1})dA\int_0^1 \frac{2G}{1-\nu}dA}{\int_0^1 \frac{E}{1-\nu}dA\left[\int_0^1 \frac{2G}{1-\nu}dA - \int_0^1 \frac{2\nu G}{1-\nu}dA\right]} = -1.3163\times10^{-3}\ \text{in/in}$$

$$C_1' \cong \frac{-\int_0^1 f_1(\bar{\sigma}_{r_1})dA + \int_0^1 f_2(\bar{\sigma}_{r_1})dA}{\int_0^1 \frac{2G}{1-\nu}dA - \int_0^1 \frac{2\nu G}{1-\nu}dA} = -0.1889\times10^{-3}\ \text{in/in}$$

These values of the constants are used to obtain a second, and in this case final, approximation to the values of the stresses at these positions. The values of the stresses are obtained from the equations:

$$2A\sigma_{r_1} \cong \int_0^A f_1(\bar{\sigma}_{r_1})dA - \int_0^A \frac{E}{1-\nu}\epsilon^T dA + \epsilon_{z_1}\int_0^A \frac{E}{1-\nu}dA + C_1'\int_0^A \frac{2G}{1-\nu}dA$$

$$\sigma_{\phi_1} \cong -\sigma_{r_1} + f_1(\bar{\sigma}_{r_1}) - \frac{E}{1-\nu}\epsilon^T + \epsilon_{z_1}\frac{E}{1-\nu} + C_1'\frac{2G}{1-\nu}$$

$$\sigma_{z_1} \cong f_2(\bar{\sigma}_{r_1}) - \frac{E}{1-\nu}\epsilon^T + \epsilon_{z_1}\frac{E}{1-\nu} + C_1'\frac{2\nu G}{1-\nu}$$

The question of whether a third approximation is required is easily settled in this case. The second approximation for σ_{r_1} differed from the first by a maximum factor of about 10%. Therefore, it may be expected that the third approximation will differ from the second by a maximum factor of approximately 1%. A factor of 10% is somewhat large, in this case, but a factor of 1% is better than the input data, hence a third approximation is unecessary.

The values of the stresses due to the thermal dilation were calculated in a similar manner to the sample calculation for $t = 1$, 2, 4, 8, 16 and 32 seconds. The results of these calculations are plotted in (Fig. 15) and (Fig. 16). A cross plot (not shown) of the stresses at the surface and at the center versus time indicates that $t = 4$ seconds corresponds approximately to the most severe surface stresses, and that $t = 8$ seconds corresponds approximately to the most severe center stresses. On this basis it may be presumed that no appreciable yielding takes place after 8 seconds, until t approaches infinity, at which

time the stresses due to the residual strains present at $t = 8$ seconds may cause yielding. It follows, therefore, that it is unnecessary to go beyond 8 seconds in the determination of the yielding due to the stresses of thermal dilation. The reduced stresses due to the thermal dilation are plotted in (Fig. 17) and (Fig. 18) for $t = 1, 2, 4$, and 8 seconds.

(Fig. 19) shows the value of k^2, a parameter proportional to the shear strain energy, due to the stresses of thermal dilation, for $t = 1, 2, 4$, and 8 seconds. On the same figure, for comparative purposes, the maximum value which k^2 may assume whithout the material yielding is indicated. This set of curves is introduced at this point in order to indicate the amount of yielding required. The discussion of the assumption of the value of the yield point, as a function of the temperature, is deferred to Chapter VII.

Plot of Circumferential Stress σ_ϕ, due to Thermal Dilation Versus Radial Position $A = (r/r_i)^2$ for Various Elapsed Times

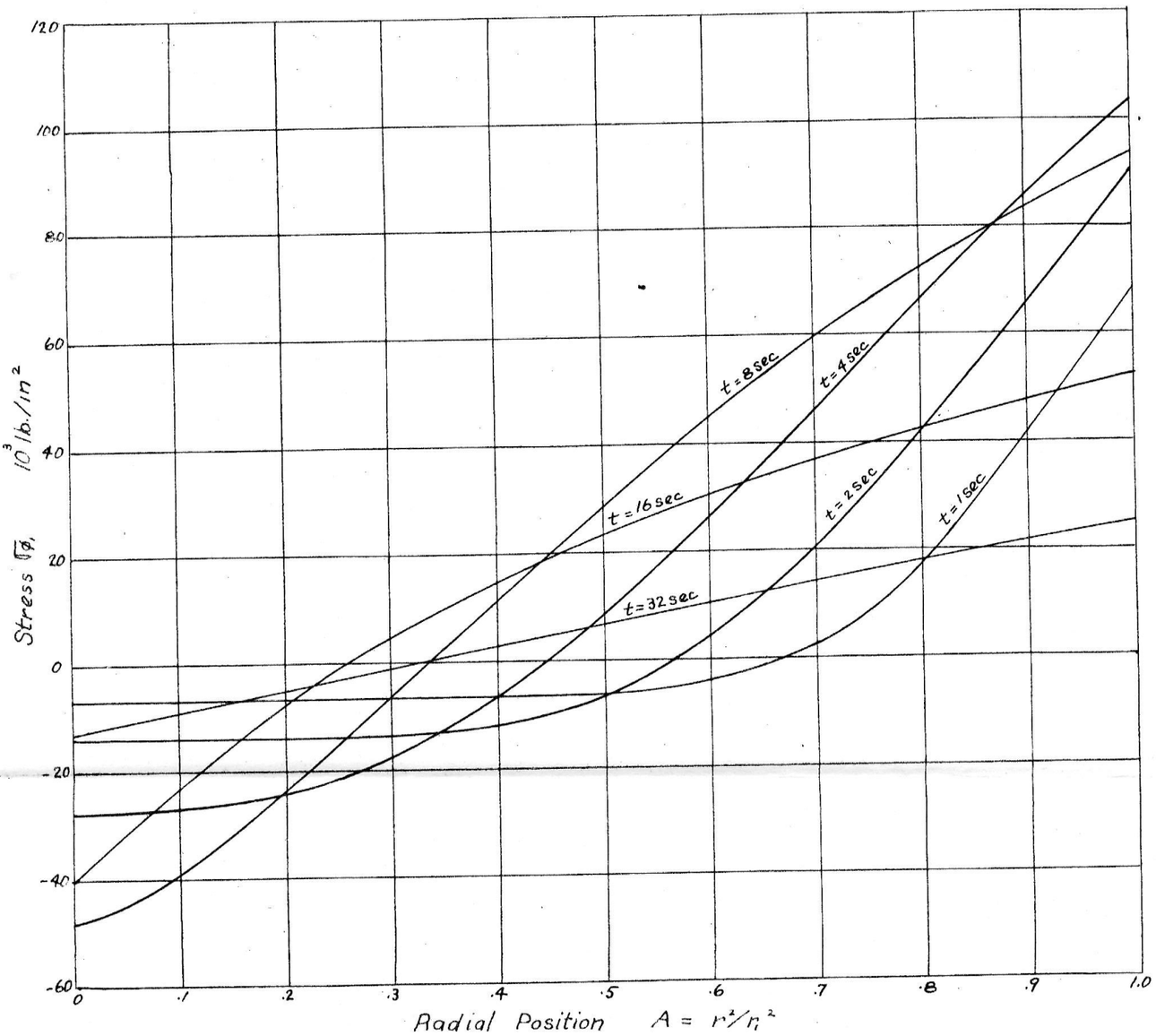

Plot of Radial Stress σ_{r_i} due to Thermal Dilation Versus Radial Position $A = (r/r_i)^2$ for Various Elapsed Times

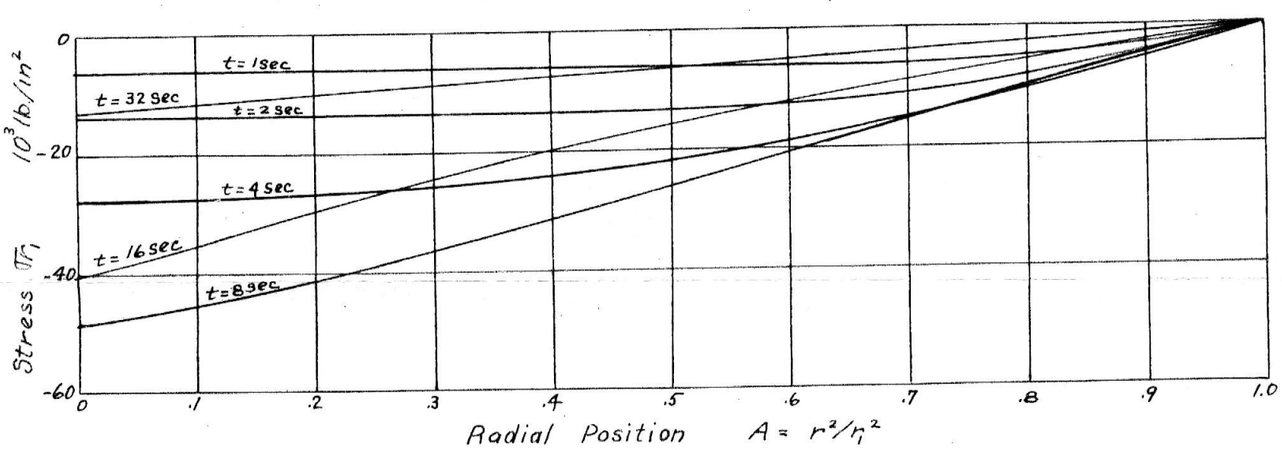

(Fig. 15)

Plot of Axial Stress σ_z, due to Thermal Dilation versus Radial Position $A = (r/r_1)^2$ for various Elapsed Times

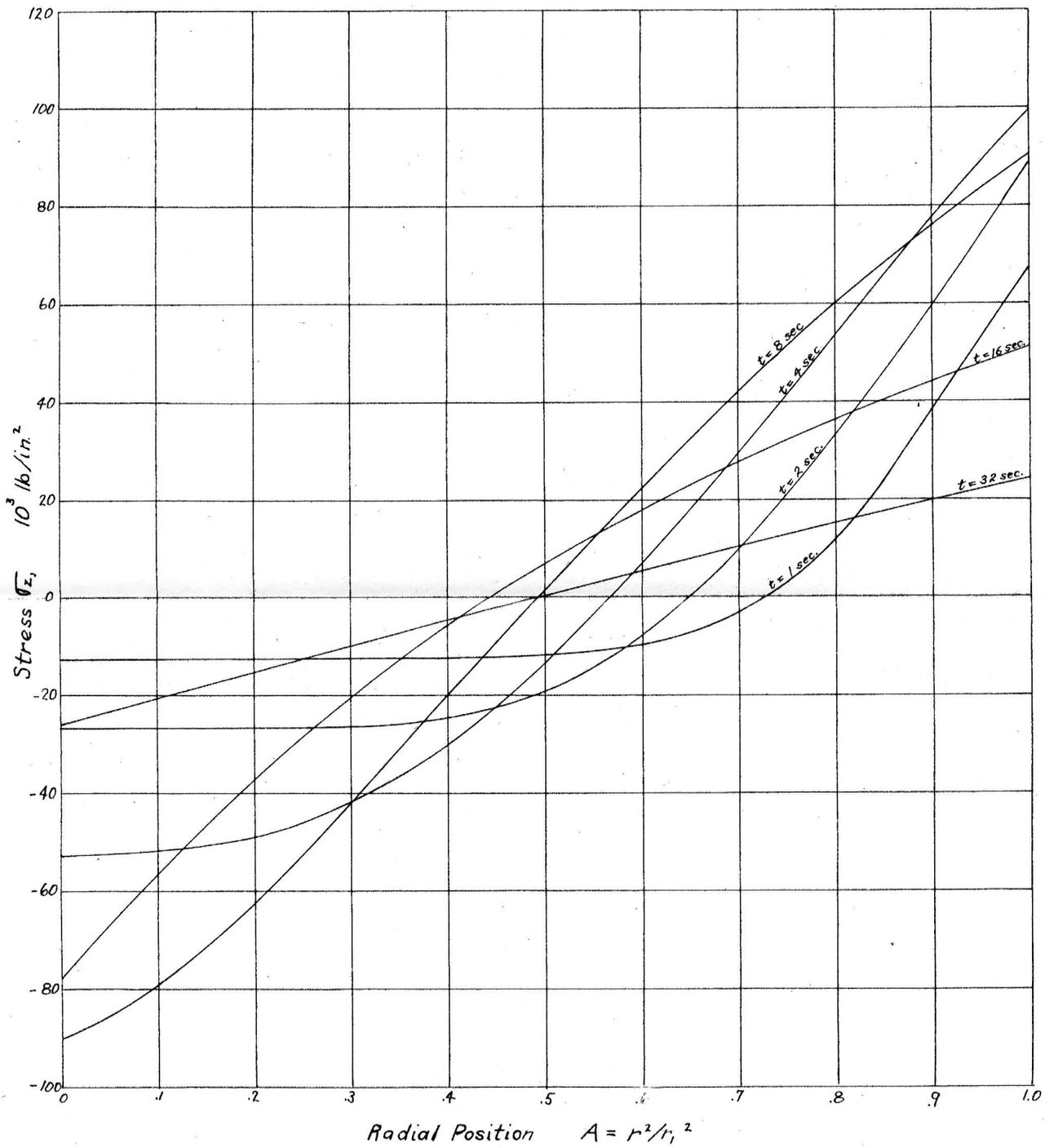

(Fig. 16)

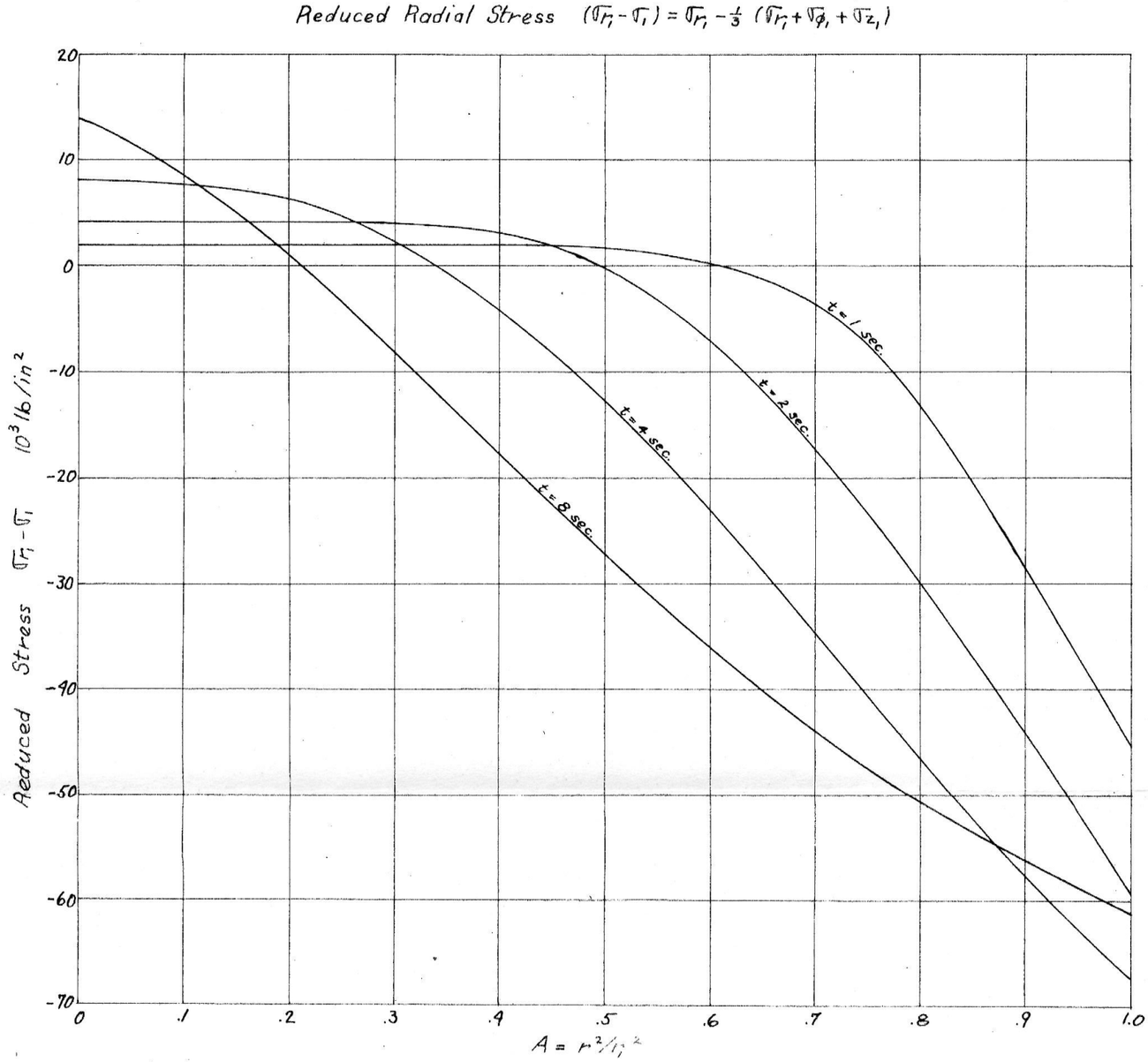

Plots of Reduced Stresses Due to Thermal Dilation vs. Radial Position $A=(r/r_1)^2$ for Various Elapsed Times

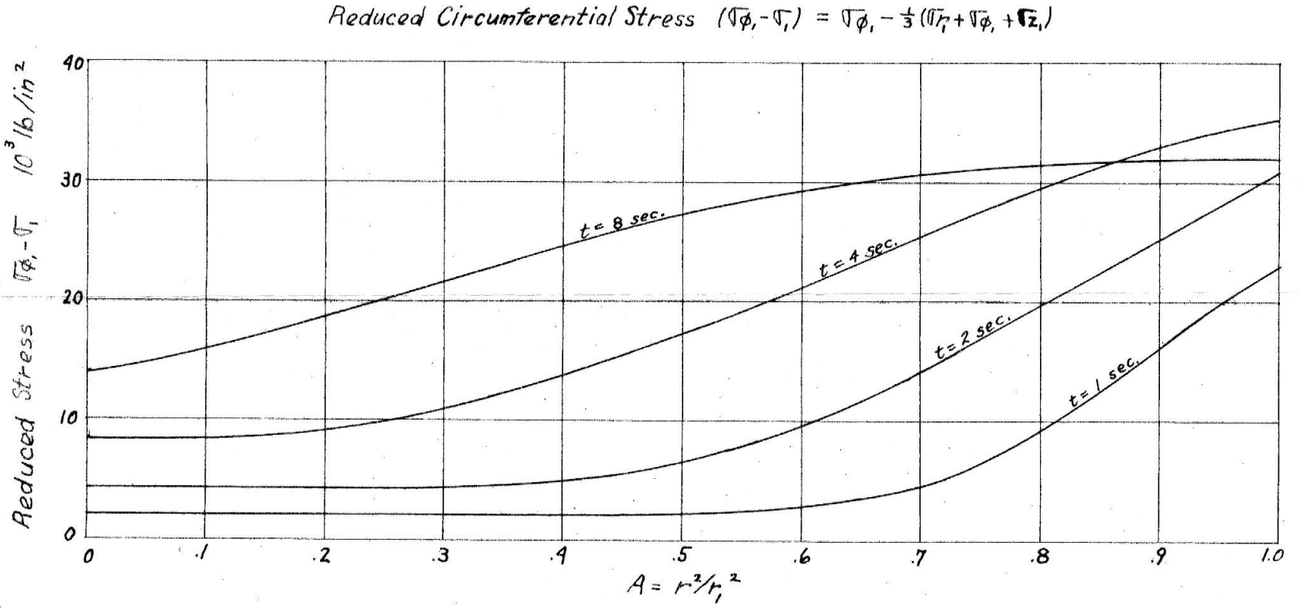

(Fig. 17)

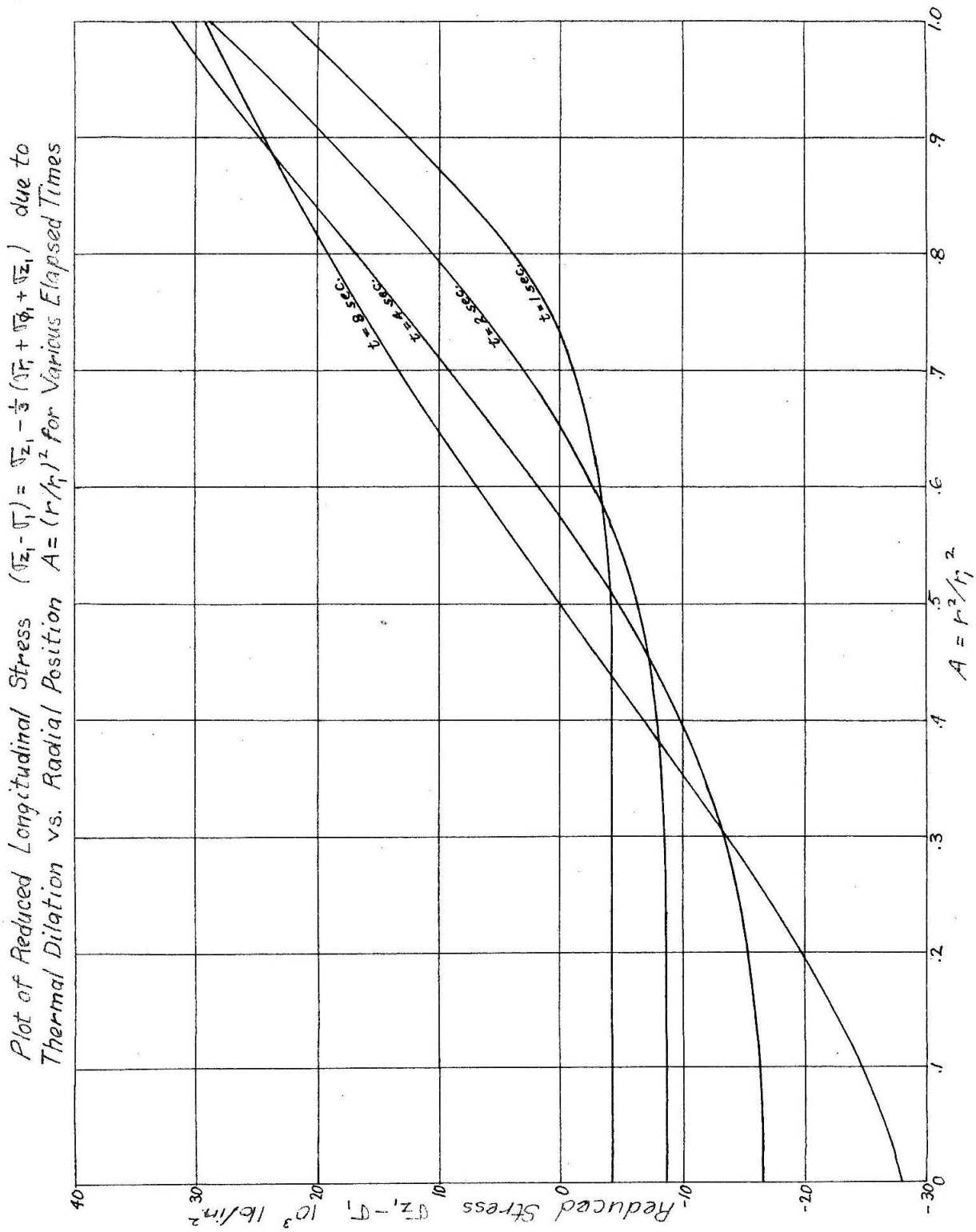
Plot of Reduced Longitudinal Stress $(\bar{\sigma}_{z_1} - \bar{\sigma}_1) = \bar{\sigma}_{z_1} - \frac{1}{3}(\bar{\sigma}_{r_1} + \bar{\sigma}_{\phi_1} + \bar{\sigma}_{z_1})$ due to Thermal Dilation vs. Radial Position $A = (r/r_1)^2$ for Various Elapsed Times
Reduced Stress $\bar{\sigma}_{z_1} - \bar{\sigma}_1$ 10^3 lb/in^2
$A = r^2/r_1^2$
$t_1 = 8$ sec.
$t_1 = 4$ sec.
$t_1 = 2$ sec.
$t_1 = 1$ sec.
40
30
20
10
0
-10
-20
-30
0
.1
.2
.3
.4
.5
.6
.7
.8
.9
1.0

(Fig. 18)

Plot of $K^2 = [(\sigma_{r_1} - \sigma_1)^2 + (\sigma_{\phi_1} - \sigma_1)^2 + (\sigma_{z_1} - \sigma_1)^2]$ Due to Thermal Dilation Versus Radial Position $A = r^2/r_1^2$ for Various Values of Elapsed Time.

The Term K^2 is Proportional to the Shear Strain Energy.

Comparative Plot of $\frac{2}{3}\sigma_{y.p.}^2$ Versus Radial Position $A = r^2/r_1^2$ for Various Values of Elapsed Time

The Term $\frac{2}{3}\sigma_{y.p.}^2$ Corresponds to the Limiting Value which K^2 may take without the Material Yielding

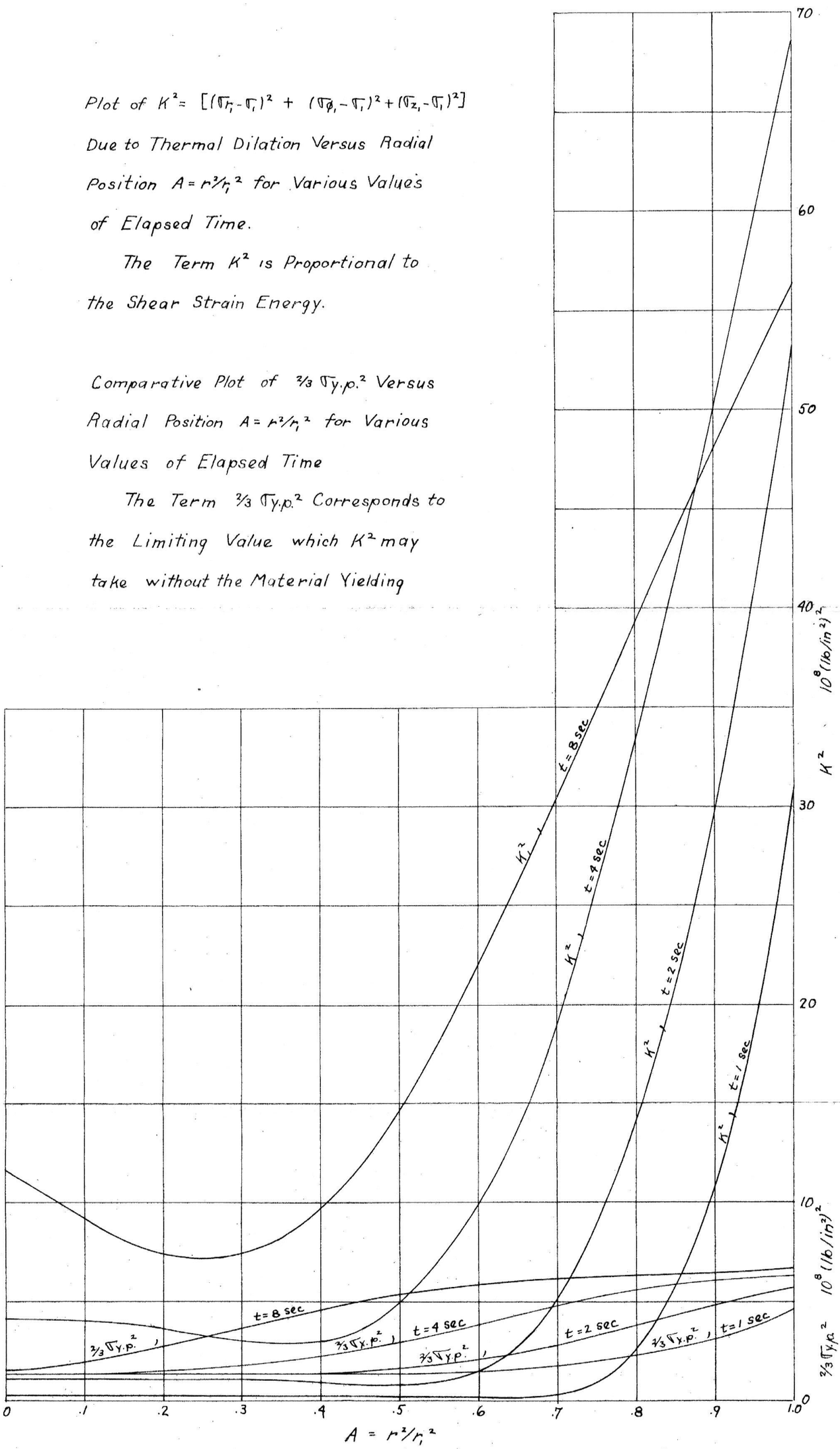

(Fig. 19)

In this chapter a complete sample calculation of the stresses due to the thermal dilation at $t = 4$ seconds was presented. Graphical plots of the stresses versus radial position, resulting from this and similar calculations, were presented for $t = 1, 2, 4, 8, 16,$ and 32 seconds. It was indicated that $t = 8$ seconds corresponds, for purposes of calculation, to the last time at which yielding, caused by the stresses due to the thermal dilation, occurs. Graphical plots of the reduced stresses and of k^2 for $t = 1, 2, 4,$ and 8 seconds were then presented. The stresses due to the thermal dilation, as t becomes large, approach zero.

CHAPTER VII

This chapter will be devoted to the determination of the values of the residual strains, and the stresses due to these residual strains, as a function of the radial position and time, for the case of a 5 cm. diameter mild steel cylinder quenched from 600 °C in still water at ambient temperature. The techniques for the determination of the stresses due to known values of the residual strains were developed in Chapter III. The techniques used in the determination of the values of the residual strains were developed in Chapter IV. The notation used will be that used in these two chapters.

The values of all of the necessary parameters, as a function of the temperature, were assumed in Chapter VI, with the exception of the yield point. Bucholtz and Buhler (3), who made the experimental determination of the final residual stresses for the case under consideration, also determined some of the properties of the steel under consideration. The results of their short time tensile tests are presented in (Table IV).

Table IV

Stahl St 50 mit 0.30% C., 0.20% Si., 0.75% Mn., 0.051% P., and 0.030%S.

Pruf-temperatur °C.	Streck-grenze kg/mm^2	Zug-festigkeit kg/mm^2	Dehnung (l=10 d) %	Ein-schurung %
20	35.6	57.3	23.7	64
150	34.6	61.9	13.7	68
300	22.9	60.3	21.0	50
450	20.2	41.9	22.5	66
550	14.1	29.0	42.0	75

These values of the yield point are the values assumed in the problem under consideration. They are plotted in (Fig. 20) together with the derived parameter $\frac{2}{3}\sigma^2_{y.p.}$, which represents the maximum value which k^2 may assume without yielding occurring.

It is known that the results of a short time tensile test of mild steel at elevated temperatures has the form indicated below.

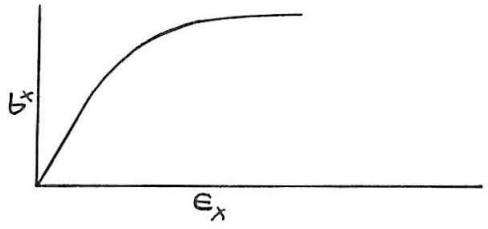

In order to make the solution as simple as possible, and because there is no better available data, it is necessary to replace this with an approximate curve of the form indicated below.

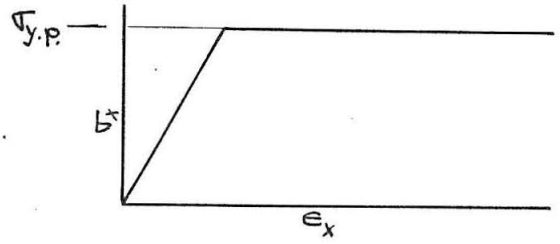

It is further assumed that what is nominally reported as a "yield point" in such a short time tensile test corresponds to the value which should be assigned to the yield point in the simplified curve. Such an assumption at temperatures in the vicinity of 600 °C. is open to some question, but in lieu of better data it will be accepted here. This factor will be discussed again in Chapter VIII, particularly in relation to "creep" at these temperatures, when the calculated values of the final residual stresses are compared with the experimental results of Bucholtz and Buhler (3).

Reference (3)

Assumed Value of Yield Point $\sigma_{y.p.}$ and $\frac{2}{3}\sigma^2_{y.p.}$

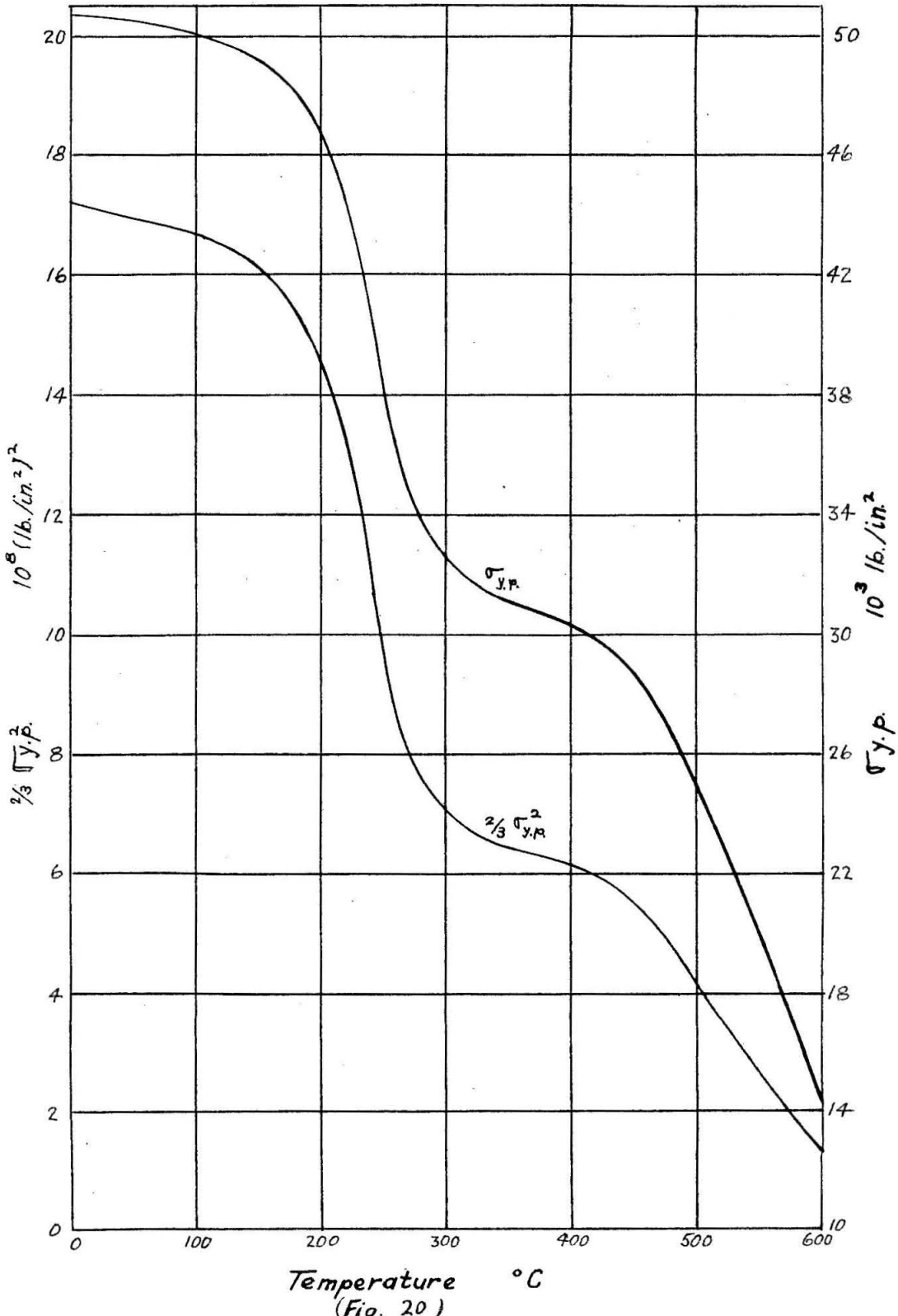

(Fig. 20)

The techniques required to determine the residual strains and the stresses due to these residual strains, as a function of the position and time, will now be illustrated with the aid of a sample calculation. In this sample calculation, the residual strains will be computed at $t = 4$ seconds, based upon a knowledge of the residual strains present at $t = 2$ seconds. This particular sample calculation is chosen because it illustrates two artifices which may sometimes be employed to reduce the labor involved in the calculation per time step.

The sequence of steps in this sample calculation will be as follows:

(1) The stresses in the body at $t = 4$ seconds, due to the residual strains present at $t = 2$ seconds, will be computed.

(2) These stresses will be combined with the previously computed stresses at $t = 4$ seconds due to the thermal dilation to form the total reduced stresses present at 4 seconds, assuming that no additional yielding takes place.

(3) The function k^2 will be formed, and the increments of the residual strains in the interval from 2 to 4 seconds will be estimated. These increments will be added to the residual strains present at 2 sec. (This later is not a necessary step, but is convenient since the total residual strains are usually more regular than the increments, and hence, require fewer points to plot.)

(4) The first artifice will then be introduced. In this particular case the dominant estimated values of the residual strains will occur near the surface and near the center, with an intermediate region in which

there will be little or no yielding. The estimated values of the residual strains will, therefore, be divided into estimated residual strains near the surface and near the center. Linear combinations of the stresses due to these factors will allow a perfect match between k^2 and $\frac{2}{3}\tau^2_{y.p.}$ at both the surface and the center, where the residual strains will have their maximum value.

(5) The stresses due to the assumed values of the residual strains near the surface and due to the assumed values of the residual strains near the center will then be computed.

(6) A linear combination of the solutions to (5) will be made which matches k^2 and $\frac{2}{3}\tau^2_{y.p.}$ at the surface and at the center. It will be found that this does not result in a satisfactory match in the intermediate regions. In most cases this would mean that another estimation of the values of the residual strains would be needed, but in this case, the second artifice may be introduced. This artifice consists in noticing that the residual strain ratios at $t = 2$ seconds are nearly the same as the required ratios of the increments of the residual strains. Hence the stresses, at $t = 4$ seconds, due to the residual strains present at $t = 2$ seconds, may be used as a third independent solution, as long as it represents a minor part of the combination. Using a linear combination of these three independent solutions, k^2 and $\frac{2}{3}\tau^2_{y.p.}$ are matched at three points, resulting in a satisfactory match over the entire region. The fact that the possibility of this artifice exists indicates that a longer time interval could have been used.

For convenience in exposition, the discussion of the sample calculation will be divided into three sections, which are not precisely in the foregoing sequence. These sections are:

(a) The determination of the stresses at $t = 4$ seconds, due to the residual strains present at $t = 2$ seconds, due to the estimated residual strains present near the surface, and due to the estimated residual strains present near the center.

(b) The estimation of the residual strains present at $t = 4$ seconds and the separation of this estimate into residual strains present near the surface and near the center.

(c) The use of a linear combination of the three independent solutions to (a) to satisfactorily match k^2 and $\frac{2}{3}\sigma_{y.p.}^2$ over the entire region.

Section (a) will now be discussed in detail. It must be remembered that in the sequence of steps in this sample calculation, the estimation of the values of the residual strains precedes the determination of the stresses due to them.

The equations necessary to solve section (a) were developed in Chapter III, but will be presented again for convenience. The equations to be solved are:

$$(25)_3 \quad \epsilon_{z_3} = \left\{ \int_0^1 \frac{2G}{1-\nu} dA \left[\int_0^1 \left(\frac{2\nu G}{1-\nu} \int_0^A \frac{\epsilon_\phi^\circ - \epsilon_r^\circ}{2A} dA \right) dA + \int_0^1 \frac{2G}{1-\nu} (\nu \epsilon_\phi^\circ + \epsilon_z^\circ) dA - \int_0^1 f_2(\sigma_{r_3}) dA \right] \right.$$

$$\left. - \int_0^1 \frac{2\nu G}{1-\nu} dA \left[\int_0^1 \left(\frac{2G}{1-\nu} \int_0^A \frac{\epsilon_\phi^\circ - \epsilon_r^\circ}{2A} dA \right) dA + \int_0^1 \frac{2G}{1-\nu} (\epsilon_\phi^\circ + \nu \epsilon_z^\circ) dA - \int_0^1 f_1(\sigma_{r_3}) dA \right] \right\} \div$$

$$\left\{ \left[\int_0^1 \frac{2G}{1-\nu} dA \right]^2 - \left[\int_0^1 \frac{2\nu G}{1-\nu} dA \right]^2 \right\}$$

$$(26)_3 \quad C_3 = \left\{ \int_0^1 \frac{2G}{1-\nu} dA \left[\int_0^1 \left(\frac{2G}{1-\nu} \int_0^A \frac{\epsilon_\phi^\circ - \epsilon_r^\circ}{2A} dA \right) dA + \int_0^1 \frac{2G}{1-\nu} (\epsilon_\phi^\circ + \nu \epsilon_z^\circ) dA - \int_0^1 f_1(\sigma_{r_3}) dA \right] \right.$$

$$\left. - \int \frac{2\nu G}{1-\nu} dA \left[\int_0^1 \left(\frac{2\nu G}{1-\nu} \int_0^A \frac{\epsilon_\phi^\circ - \epsilon_r^\circ}{2A} dA \right) dA + \int_0^1 \frac{2G}{1-\nu} (\nu \epsilon_\phi^\circ + \epsilon_z^\circ) dA - \int_0^1 f_2(\sigma_{r_3}) dA \right] \right\} \div$$

$$\left\{ \left[\int_0^1 \frac{2G}{1-\nu} dA \right]^2 - \left[\int_0^1 \frac{2\nu G}{1-\nu} dA \right]^2 \right\}$$

$$(23)_3 \quad 2A\sigma_{r_3} = \int_0^A f_1(\sigma_{r_3}) dA - \int_0^A \left(\frac{2G}{1-\nu} \int_0^A \frac{\epsilon_\phi^\circ - \epsilon_r^\circ}{2A} dA \right) dA - \int_0^A \frac{2G}{1-\nu} (\epsilon_\phi^\circ + \nu \epsilon_z^\circ) dA$$

$$+ \epsilon_{z_3} \int_0^A \frac{2\nu G}{1-\nu} dA + C_3 \int_0^A \frac{2G}{1-\nu} dA$$

$$(17)_3 \quad \sigma_{\phi_3} = -\sigma_{r_3} + f_1(\sigma_{r_3}) - \frac{2G}{1-\nu} \int_0^A \frac{\epsilon_\phi^\circ - \epsilon_r^\circ}{2A} dA - \frac{2G}{1-\nu} (\epsilon_\phi^\circ + \nu \epsilon_z^\circ) + \epsilon_{z_3} \frac{2\nu G}{1-\nu} + C_3 \frac{2G}{1-\nu}$$

$$(21)_3 \quad \sigma_{z_3} = f_2(\sigma_{r_3}) - \frac{2\nu G}{1-\nu} \int_0^A \frac{\epsilon_\phi^\circ - \epsilon_r^\circ}{2A} dA - \frac{2G}{1-\nu} (\nu \epsilon_\phi^\circ + \epsilon_z^\circ) + \epsilon_{z_3} \frac{2G}{1-\nu} + C_3 \frac{2\nu G}{1-\nu}$$

(Table V) contains the necessary numerical aspects of the sample calculation for $t = 4$ seconds required to solve (Section a). Since a similar calculation was outlined in Chapter III, the discussion which follows will presume that (Table V) is nearly self-explanatory. The first, second and third rows, respectively, of (Table V) give the numerical computations necessary to determine the stresses, at $t = 4$ seconds, due to the residual strains present at $t = 2$ seconds, the estimated residual strains present near the surface, and the estimated residual strains present near the center. (Fig. 21) and (Fig. 22) give the plots of the parameters (in addition to those already determined in the sample calculation of Chapter VI) whose integral values are required in (Table V) for the calculation of the stresses due to the estimated strains present near the surface.

The sequence of the major steps presented in (Table V) is as follows. A first estimate of the values of ϵ_{z_3} and C_3, denoted by $\bar{\epsilon}_{z_3}$ and $\bar{C}_3$, is obtained from $(\text{Eq. } 25)_3$ and $(\text{Eq. } 26)_3$, assuming that $f_1(\sigma_{r_3})$ and $f_2(\sigma_{r_3})$ are equal to zero. Using these values for $\bar{\epsilon}_{z_3}$ and $\bar{C}_3$, a first estimate of σ_{r_3}, denoted by $\bar{\sigma}_{r_3}$, is obtained from $(\text{Eq. } 23)_3$, in which $f_1(\sigma_{r_3})$ is assumed to be equal to zero. Using this value for $\bar{\sigma}_{r_3}$, the functions $f_1(\bar{\sigma}_{r_3})$ and $f_2(\bar{\sigma}_{r_3})$ are formed. A second estimate of the values of the constants ϵ_{z_3} and C_3 is then obtained from $(\text{Eq. } 23)_3$, in which $f_1(\sigma_{r_3})$ and $f_2(\sigma_{r_3})$ have been replaced by the known functions, $f_1(\bar{\sigma}_{r_3})$ and $f_2(\bar{\sigma}_{r_3})$. Using these values for ϵ_{z_3} and C_3, a second estimate of σ_{r_3} is obtained from $(\text{Eq. } 23)_3$, in which $f_1(\sigma_{r_3})$ has been replaced by the

known function $f_1(\bar{\sigma}_{r_3})$. In this case the second estimate is accepted as being accurate enough. Values of σ_{ϕ_3} and σ_{z_3} are obtained from $(\text{Eq. } 17)_3$ and $(\text{Eq. } 21)_3$, in which $f_1(\sigma_{r_3})$ and $f_2(\sigma_{r_3})$ have been replaced by $f_1(\bar{\sigma}_{r_3})$ and $f_2(\bar{\sigma}_{r_3})$.

These steps may be readily followed in (Table V).

SAMPLE CALCULATION - STRESS DUE TO RESIDUAL STRAIN - Required Tabular Data and Calculations - t=4 sec

This Illustrates the Technique Required to Approximate to Any Required Degree of Accuracy, the Values of Residual Strains which Satisfy the Law: $\left\{\frac{d\epsilon_r^\circ}{dt} : \frac{d\epsilon_\phi^\circ}{dt} : \frac{d\epsilon_z^\circ}{dt}\right\}$ *as* $(\bar\sigma_r-\bar\sigma):(\bar\sigma_\phi-\bar\sigma):(\bar\sigma_z-\bar\sigma)\}$
and which Result in Stresses which Satisfy the Following Form of the Mises-Hencky Criterion: $[(\bar\sigma_r-\bar\sigma)^2+(\bar\sigma_\phi-\bar\sigma)^2+(\bar\sigma_z-\bar\sigma)^2] \leq \frac{2}{3}\bar\sigma_{y.p.}^2$ *where* $\bar\sigma_{y.p.}=\bar\sigma_{y.p.}(T)$ *is the Yield Point in Simple Tension*

	$A=r^2/r_1^2$	From Previous Solution for Temp. Distribution	Known Function of Temperature - (Previously Determined)	(Previously Determined)	(Previously Determined)	(Previously Determined)	(See Left Column)			Perform Indicated Subtraction	Perform Indicated Division	Graphically Perform $\int_0^A \frac{\epsilon_\phi^\circ-\epsilon_r^\circ}{2A}dA$	Perform Product $-\frac{2G}{1-\nu}\times\int_0^A\frac{\epsilon_\phi^\circ-\epsilon_r^\circ}{2A}dA$	Graphically Perform $\int_0^A\left\{-\frac{2G}{1-\nu}\int_0^A\frac{\epsilon_\phi^\circ-\epsilon_r^\circ}{2A}dA\right\}dA$	Perform Product $-\frac{2\nu G}{1-\nu}\times\int_0^A\left\{-\frac{2G}{1-\nu}\int_0^A\frac{\epsilon_\phi^\circ-\epsilon_r^\circ}{2A}dA\right\}dA$	Graphically Perform $\int_0^A\left\{-\frac{2\nu G}{1-\nu}\int_0^A\frac{\epsilon_\phi^\circ-\epsilon_r^\circ}{2A}dA\right\}dA$	Perform Product $-\frac{2G}{1-\nu}\times\epsilon_\phi^\circ$	Graphically Perform $\int_0^A\left[-\frac{2G}{1-\nu}\epsilon_\phi^\circ\right]dA$	Perform Product $-\frac{2\nu G}{1-\nu}\times\epsilon_\phi^\circ$	Graphically Perform $\int_0^A\left[-\frac{2\nu G}{1-\nu}\epsilon_\phi^\circ\right]dA$	Perform Product $-\frac{2\nu G}{1-\nu}\times\epsilon_z^\circ$	Graphically Perform $\int_0^A\left[-\frac{2\nu G}{1-\nu}\epsilon_z^\circ\right]dA$	Perform Product $-\frac{2G}{1-\nu}\times\epsilon_z^\circ$	Graphically Perform $\int_0^A\left[-\frac{2G}{1-\nu}\epsilon_z^\circ\right]dA$	$\bar C_3=\left\{\int_0^1\left[\int_0^A\frac{2\nu G}{1-\nu}dA\right]^2dA-\left[\int_0^1\frac{2\nu G}{1-\nu}dA\right]^2\right\}\Big/$ $-\int_0^1\frac{2G}{1-\nu}dA\left[\int_0^A\frac{2\nu G}{1-\nu}dA\right]+\int_0^1\frac{2G}{1-\nu}dA\int_0^1\left[\int_0^A\frac{2\nu G}{1-\nu}dA\right]dA$ $\left\{\int_0^1\left[\int_0^A\frac{2G}{1-\nu}dA\right]^2-\left[\int_0^1\frac{2\nu G}{1-\nu}dA\right]^2\right\}$	$\bar\epsilon_{z_3}=\int_0^1\left[-\frac{2\nu G}{1-\nu}\epsilon_z^\circ\right]dA+\int_0^1\frac{2G}{1-\nu}dA\int_0^1\left[\frac{2\nu G}{1-\nu}\epsilon_z^\circ\right]dA$ $-\int_0^1\frac{2G}{1-\nu}dA\int_0^1\left[\frac{2\nu G}{1-\nu}\epsilon_z^\circ\right]dA+\int_0^1\frac{2\nu G}{1-\nu}dA\int_0^1\left[\frac{2G}{1-\nu}\epsilon_z^\circ\right]dA$ $\left\{\int_0^1\left[\frac{2G}{1-\nu}dA\right]^2-\left[\int_0^1\frac{2\nu G}{1-\nu}dA\right]^2\right\}$
	A	T	$\frac{2G}{1-\nu}$	$\int_0^A\frac{2G}{1-\nu}dA$	$\frac{2\nu G}{1-\nu}$	$\int_0^A\frac{2\nu G}{1-\nu}dA$	ϵ_r°	ϵ_ϕ°	ϵ_z°	$\epsilon_\phi^\circ-\epsilon_r^\circ$	(6) $\frac{\epsilon_\phi^\circ-\epsilon_r^\circ}{2A}$	(8) $\int_0^A$(6)dA	(2) $-\frac{2G}{1-\nu}$(8)	$\int_0^A$(2)dA	(20) $-\frac{2\nu G}{1-\nu}$(8)	$\int_0^A$(20)dA	(3) $-\frac{2G}{1-\nu}\epsilon_\phi^\circ$	$\int_0^A$(3)dA	(30) $-\frac{2\nu G}{1-\nu}\epsilon_\phi^\circ$	$\int_0^A$(30)dA	(4) $-\frac{2\nu G}{1-\nu}\epsilon_z^\circ$	$\int_0^A$(4)dA	(40) $-\frac{2G}{1-\nu}\epsilon_z^\circ$	$\int_0^A$(40)dA		
	in^2/in^2	°C	10^6 lb/in²	10^6 lb/in²	10^6 lb/in²	10^6 lb/in²	10^{-3} in/in	10^{-3} in/in	10^{-3} in/in	10^{-3} in/in	10^{-3} in/in	10^{-3} in/in	10^3 lb/in²	10^{-3} in/in	10^3 lb/in²	10^{-3} lb/in²	10^3 lb/in²	10^{-3} lb/in²	10^3 lb/in²	10^{-3} lb/in²	10^3 lb/in²	10^{-3} lb/in²	10^3 lb/in²	10^{-3} lb/in²		
$\epsilon_r^\circ,\epsilon_\phi^\circ,\epsilon_z^\circ$ from values of $t=2$ sec	0	600	26.95	0	12.30	0	0	0	0	0	0	0	0	0	0	0	0	0	0	0	0	0	0	0	$\bar C_3=\frac{12.504(-9.220)-29.76(-12.584)}{(29.76)^2-(12.504)^2}\times10^{-3}$ $=0.34315\times10^{-3}$	$\bar\epsilon_{z_3}=\frac{12.504(-12.584)-29.76(-9.929)}{(29.76)^2-(12.504)^2}\times10^{-3}$ $=0.18946\times10^{-3}$
	0.2	594	27.07	5.395	12.30	2.105	0	0	0	0	0	0	0	0	0	0	0	0	0	0	0	0	0	0	0	
	0.4	564.5	27.78	10.87	12.67	4.905	0	0	0	0	0	0	0	0	0	0	0	0	0	0	0	0	0	0	0	
	0.6	511.5	29.02	16.53	12.90	7.475	0	0	0	0	0	0	0	0	0	0	0	0	0	0	0	0	0	0	0	
	0.8	446	30.93	23.55	12.66	10.050	-1.145	.658	.487	1.803	1.127	.0968	-2.993	-.183	-1.224	-.073	-20.35	-1.73	-8.33	-.695	-6.16	-.48	-15.07	-.62		
	0.9	411.5	31.09	26.66	12.27	11.300	-1.960	1.025	.935	2.985	1.658	.2363	-7.35	-.683	-2.900	-.277	-31.87	-9.34	-12.58	-1.24	-11.34	-1.34	-29.08	-2.80		
	1.0	376	30.94	29.76	11.70	12.504	-2.912	1.400	1.512	4.312	2.156	.4273	-13.22	-1.701	-5.000	-.669	-93.30	-8.10	-16.38	-2.69	-17.69	-2.78	-46.80	-6.57		
$\epsilon_r^\circ,\epsilon_\phi^\circ,\epsilon_z^\circ$ Estimated total yield neglecting center	0	same as above	same as above	same as above	same as above	same as above	0	0	0	0	0	0	0	0	0	0	0	0	0	0	0	0	0	0	$\bar C_3=\frac{12.504(-17.334)-29.76(-22.072)}{(29.76)^2-(12.504)^2}\times10^{-3}$ $=0.60347\times10^{-3}$	$\bar\epsilon_{z_3}=\frac{12.504(-22.072)-29.76(-17.339)}{(29.76)^2-(12.504)^2}\times10^{-3}$ $=0.32890\times10^{-3}$
	0.2						0	0	0	0	0	0	0	0	0	0	0	0	0	0	0	0	0	0	0	
	0.4						0	0	0	0	0	0	0	0	0	0	0	0	0	0	0	0	0	0	0	
	0.6						-.544	.466	.098	1.010	.842	.0700	-2.03	-.112	-.90	-.047	-13.523	-1.025	-6.011	-.468	-1.269	-.063	-2.849	-.195		
	0.8						-1.769	1.018	.751	2.787	1.742	.3310	-10.24	-1.238	-4.19	-.518	-31.487	-5.528	-12.888	-2.371	-9.508	-1.061	-23.228	-2.602		
	0.9						-2.488	1.299	1.189	3.787	2.104	.5240	-16.29	-2.554	-6.43	-1.049	-40.386	-9.118	-15.939	-3.816	-14.589	-2.263	-36.966	-5.590		
	1.0						-3.344	1.560	1.684	4.804	2.402	.7495	-23.19	-4.522	-8.77	-1.789	-48.266	-13.573	-18.252	-5.533	-19.703	-3.977	-52.103	-10.012		
$\epsilon_r^\circ,\epsilon_\phi^\circ,\epsilon_z^\circ$ Estimated center yield	0	same as above	same as above	same as above	same as above	same as above	.174	.174	-.348	0	0	0	0	0	0	0	-4.689	0	-2.123	0	4.246	0	9.379	0	$\bar C_3=\frac{12.504(1.334)-29.76(-.769)}{(29.76)^2-(12.504)^2}\times10^{-3}$ $=0.059371\times10^{-3}$	$\bar\epsilon_{z_3}=\frac{12.504(-.769)-29.76(1.341)}{(29.76)^2-(12.504)^2}\times10^{-3}$ $=-0.067905\times10^{-3}$
	0.2						.088	.131	-.219	.043	.108	.0109	-.295	-.019	-.134	-.009	-3.596	-.849	-1.611	-.387	2.694	.715	5.928	1.598		
	0.4						0	0	0	0	0	.0228	-.633	-.119	-.289	-.055	0	-1.205	0	-.549	0	.951	0	2.112		
	0.6						0	0	0	0	0	.0228	-.662	-.246	-.294	-.114	0	-1.205	0	-.549	0	.951	0	2.112		
	0.8						0	0	0	0	0	.0228	-.705	-.374	-.289	-.172	0	-1.205	0	-.549	0	.951	0	2.112		
	0.9						0	0	0	0	0	.0228	-.709	-.445	-.280	-.200	0	-1.205	0	-.549	0	.951	0	2.112		
	1.0						0	0	0	0	0	.0228	-.705	-.515	-.267	-.227	0	-1.205	0	-.549	0	.951	0	2.112		

Table V

SAMPLE CALCULATION (continued) $t = 4$ sec

	A	Perform Product $\bar{C}_3 \times \int_0^A \frac{2G}{1-\nu} dA$	Perform Product $\bar{\epsilon}_{z_3} \times \int_0^A \frac{2\nu G}{1-\nu} dA$	$2A\bar{\sigma}_{r_3} = \int_0^A ② dA + \int_0^A ③ dA + \int_0^A ④ dA + \bar{C}_3 \int_0^A \frac{2G}{1-\nu} dA + \bar{\epsilon}_{z_3} \int_0^A \frac{2\nu G}{1-\nu} dA$	$2\bar{\sigma}_{r_3}\big\|_{A=0} = ②\big\|_{A=0} + ③\big\|_{A=0} + ④\big\|_{A=0} + \bar{C}_3 \frac{2G}{1-\nu}\big\|_{A=0} + \bar{\epsilon}_{z_3} \frac{2\nu G}{1-\nu}\big\|_{A=0}$	$\bar{\sigma}_{r_3} = \frac{2A\bar{\sigma}_{r_3}}{2A}$ $A \neq 0$	(Previously Determined)	Perform Product $\bar{\sigma}_{r_3} \times \frac{d}{dA}\left(\frac{1}{2A}\right)$	Graphically Perform $\int_0^A ⑤ dA \left(\frac{1}{2A}\right)$	Perform Product $\frac{2G}{1-\nu} \int_0^A ⑥ dA \left(\frac{1}{2A}\right)$	Graphically Perform $\int_0^A ① dA \left(\frac{1}{2A}\right)$	Perform Product $\frac{2\nu G}{1-\nu} \int_0^A ⑩ dA \left(\frac{1}{2A}\right)$	Graphically Perform $\int_0^A ⑩ dA \left(\frac{1}{2A}\right)$	$C_3 = \bar{C}_3 + \frac{\int_0^{'} \frac{2\nu G}{1-\nu} dA \int_0^{'} ⑩ dA - \int_0^{'} \frac{2G}{1-\nu} dA \int_0^{'} ⑩ dA}{\left[\int_0^{'} \frac{2G}{1-\nu} dA\right]^2 - \left[\int_0^{'} \frac{2\nu G}{1-\nu} dA\right]^2}$	$\epsilon_{z_3} = \bar{\epsilon}_{z_3} + \frac{\int_0^{'} \frac{2\nu G}{1-\nu} dA \int_0^{'} ⑩ dA - \int_0^{'} \frac{2G}{1-\nu} dA \int_0^{'} ⑩ dA}{\left[\int_0^{'} \frac{2G}{1-\nu} dA\right]^2 - \left[\int_0^{'} \frac{2\nu G}{1-\nu} dA\right]^2}$	Perform Product $C_3 \frac{2G}{1-\nu}$	Perform Product $C_3 \times \int_0^A \frac{2G}{1-\nu} dA$	Perform Product $C_3 \times \frac{2\nu G}{1-\nu}$	Perform Product $\epsilon_{z_8} \times \frac{2\nu G}{1-\nu}$	Perform Product $\epsilon_{z_3} \times \int_0^A \frac{2\nu G}{1-\nu}$	Perform Product $\epsilon_{z_3} \times \frac{2G}{1-\nu}$	$2A\bar{\sigma}_{r_3} = \int_0^A ① dA + \int_0^A ② dA + \int_0^A ③ dA + \int_0^A ④ dA + \int_0^A ⑤ dA + \int_0^A ⑥ dA$	$2\bar{\sigma}_{r_3}\big\|_{A=0} = ① + ② + ③ + ④ + ⑤ + ⑥$	$\bar{\sigma}_{r_3} = \frac{2A\bar{\sigma}_{r_3}}{2A}$ $A \neq 0$	$\bar{\sigma}_{\phi_3} = ① + ② + ③ + ④ + ⑤ + ⑥ - ⑦$	$\bar{\sigma}_{z_3} = ⑪ + ⑳ + ㉚ + ㊵ + ㊿ + ⑥⓪$
		⑥ $C_3 \frac{2G}{1-\nu}$	$\int_0^A ⑥ dA$	⑥⓪ $C_3 \frac{2\nu G}{1-\nu}$	⑤ $\epsilon_{z_8} \frac{2\nu G}{1-\nu}$	$\int_0^A ⑤ dA$	50 $\epsilon_{z_3} \frac{2G}{1-\nu}$	$2A\bar{\sigma}_{r_3}$	$2\bar{\sigma}_{r_3}\big\|_{A=0} = 13.009 \times 10^{-3}$	⑦ $\bar{\sigma}_{r_3}$	$\bar{\sigma}_{\phi_3}$	$\bar{\sigma}_{z_3}$
	in^2/in^2	10^3 lb/in²	10^3 lb/in²	10^3 lb/in²	10^3 lb/in²	10^3 lb/in²	10^3 lb/in²	10^3 lb/in²		10^3 lb/in²	10^{-8} in²/lb	10^{-5} in/in	10^{-5} in/in	10^3 lb/in²	10^3 lb/in²	10^3 lb/in²	10^3 lb/in²	10^3 lb/in²									
$\epsilon_r^\circ, \epsilon_\phi^\circ, \epsilon_z^\circ$ from values of $t = 2$ sec	0	0	0	0	$2\bar{\sigma}_{r_3} = 11.550 \times 10^{-3}$	5.775	0	0	0	0	0	0	0	$C_3 = .034315 \times 10^{-3} + \frac{12.504(-.6010) - 29.76(-1.6010)}{29.76^2 - 12.504^2} \times 10^{-3} = 0.39699 \times 10^{-3}$	$\epsilon_{z_3} = 0.18946 \times 10^{-3} + \frac{12.504(-.6010) - 29.76(-.6698)}{29.76^2 - 12.504^2} \times 10^{-3} = 0.18935 \times 10^{-3}$	10.699	0	4.843	2.310	0	5.103	0	$2A\bar{\sigma}_{r_3} = 13.009 \times 10^{-3}$	6.805	6.804	9.946
	0.2	1.857	.456	2.307		5.768	-1.365	-7.87	-.674	-.1825	-.0090	-.0829	-.0042			10.747	2.142	4.883	2.329	.455	5.126	2.588		6.470	6.423	9.926
	0.4	3.730	.929	4.659		5.824	-3.110	-18.112	-3.239	-.9000	-.1102	-.410	-.0497			11.028	4.315	5.030	2.399	.929	5.260	5.134		6.418	6.109	9.880
	0.6	5.672	1.416	7.088		5.907	-3.150	-18.607	-7.129	-2.070	-.9097	-.919	-.1818			11.521	6.562	5.121	2.443	1.415	5.495	7.572		6.310	5.584	9.697
	0.8	8.081	1.904	7.592		4.745	-2.165	-10.273	-10.156	-3.140	-.9330	-1.280	-.9072			12.279	9.349	5.023	2.397	1.903	5.857	7.926		4.954	-23.911	-14.663
	0.9	9.147	2.141	4.925		2.736	-1.423	-3.893	-10.858	-3.375	-1.2608	-1.330	-.5383			12.342	10.582	4.871	2.323	2.140	5.887	5.098		2.832	-92.102	-35.132
	1.0	10.312	2.369	0		0	-0.850	0	-11.026	-3.910	-1.6010	-1.290	-.6699			12.283	11.819	4.645	2.218	2.368	5.858	0		0	-63.122	-58.967
$\epsilon_r^\circ, \epsilon_\phi^\circ, \epsilon_z^\circ$ Estimated total yield neglecting center	0	0	0	0	$2\bar{\sigma}_{r_3} = 20.278 \times 10^{-3}$	10.139	0	0	0	0	0	0	0	$C_3 = 0.60347 \times 10^{-3} + \frac{12.504(-1.138) - 29.76(-2.4963)}{29.76^2 - 12.504^2} \times 10^{-3} = 0.68583 \times 10^{-3}$	$\epsilon_{z_3} = 0.32890 \times 10^{-3} + \frac{12.504(-2.4963) - 29.76(-1.138)}{29.76^2 - 12.504^2} \times 10^{-3} = 0.33253 \times 10^{-3}$	18.483	0	8.367	4.057	0	8.962	0	$2\bar{\sigma}_{r_3}\big\|_{A=0} = 22.540 \times 10^{-3}$	11.270	11.270	17.329
	0.2	3.256	.791	4.047		10.118	-1.365	-13.811	-.877	-.237	-.0105	-.108	-.0048			18.565	3.700	8.436	4.090	.800	9.002	4.489		11.223	11.195	17.330
	0.4	6.560	1.613	8.173		10.216	-3.110	-31.772	-5.617	-1.560	-.058	-.712	-.1210			19.052	7.455	8.689	4.213	1.631	9.238	9.028		11.285	10.920	17.215
	0.6	9.975	2.459	11.234		9.362	-3.150	-29.990	-12.005	-3.484	-.569	-1.599	-.3485			19.903	11.337	8.847	4.290	2.486	9.650	12.059		10.049	-6.187	7.193
	0.8	14.212	3.305	9.690		6.056	-2.165	-13.111	-16.904	-5.074	-1.932	-2.077	-.7190			21.213	16.151	8.683	4.210	3.342	10.285	10.234		6.396	-37.282	-23.915
	0.9	16.085	3.717	5.867		3.259	-1.423	-9.638	-17.269	-5.367	-1.957	-2.118	-.9295			21.322	18.281	8.415	4.080	3.758	10.338	6.147		3.915	-59.695	-92.700
	1.0	17.959	4.113	0		0	-0.850	0	-17.969	-5.905	-2.496	-2.044	-1.138			21.220	20.910	8.029	3.891	4.158	10.288	0		0	-71.953	-62.857
$\epsilon_r^\circ, \epsilon_\phi^\circ, \epsilon_z^\circ$ Estimated center yield	0	0	0	0	$2\bar{\sigma}_{r_3} = 0.1940 \times 10^{-3}$	+0.0970	0	0	0	0	0	0	0	$C_3 = 0.05371 \times 10^{-3} + \frac{12.504(.0115) - 29.76(.0273)}{29.76^2 - 12.504^2} \times 10^{-3} = 0.05354 \times 10^{-3}$	$\epsilon_{z_3} = -0.067905 \times 10^{-3} + \frac{12.504(.0273) - 29.76(.0115)}{29.76^2 - 12.504^2} \times 10^{-3} = -0.067906 \times 10^{-3}$	1.441	0	.652	-.828	0	-1.830	0	$2\bar{\sigma}_{r_3}\big\|_{A=0} = 0.170 \times 10^{-3}$	+.085	+.085	6.078
	0.2	.2933	-.1633	-.018		-.045	-1.365	.0614	.0028	.0008	0	.0003	0			1.447	.288	.657	-.835	-.163	-1.838	-.023		-.058	-.476	3.002
	0.4	.5910	-.3331	-.115		-.199	-3.110	.9978	.0583	.0162	.0019	.0074	.0006			1.485	.581	.677	-.860	-.333	-1.886	-.129		-.155	+.163	-1.963
	0.6	.8988	-.5076	-.109		-.091	-3.150	.2867	.1384	.0402	.0071	.0179	.0032			1.557	.884	.690	-.876	-.508	-1.971	-.117		-.098	.151	-1.557
	0.8	1.2804	-.6824	-.030		-.019	-2.165	.0411	.1701	.0526	.0166	.0215	.0073			1.653	1.259	.677	-.860	-.682	-2.100	-.034		-.021	.162	-1.690
	0.9	1.4993	-.7673	-.017		-.009	-1.923	.0128	.1731	.0538	.0220	.0212	.0094			1.662	1.425	.656	-.833	-.767	-2.111	-.019		-.011	.185	-1.719
	1.0	1.6181	-.8491	0		0	-0.850	0	.1735	.0537	.0273	.0203	.0115			1.659	1.591	.635	-.795	-.849	-2.101	0		0	.208	-1.723

Table V (cont.)

SAMPLE CALCULATION - STRESS DUE TO RESIDUAL STRAIN - $t = 4$ sec.

SAMPLE SET OF CURVES

These curves, and those in (Fig. 22) represent the factors whose value and whose integral value are required for the calculation represented in the second row of the tabular data sheet (Table V); Stress due to assumed values of ϵ_r°, ϵ_ϕ°, and ϵ_z° near surface.

Values of: $\frac{2G}{1-\nu}\epsilon_\phi^\circ$, $\frac{2\nu G}{1-\nu}\epsilon_\phi^\circ$, $\frac{2G}{1-\nu}\epsilon_z^\circ$, and $\frac{2\nu G}{1-\nu}\epsilon_z^\circ$ vs. A for $t = 4$ sec. Graphically integrate these curves for required integral values.

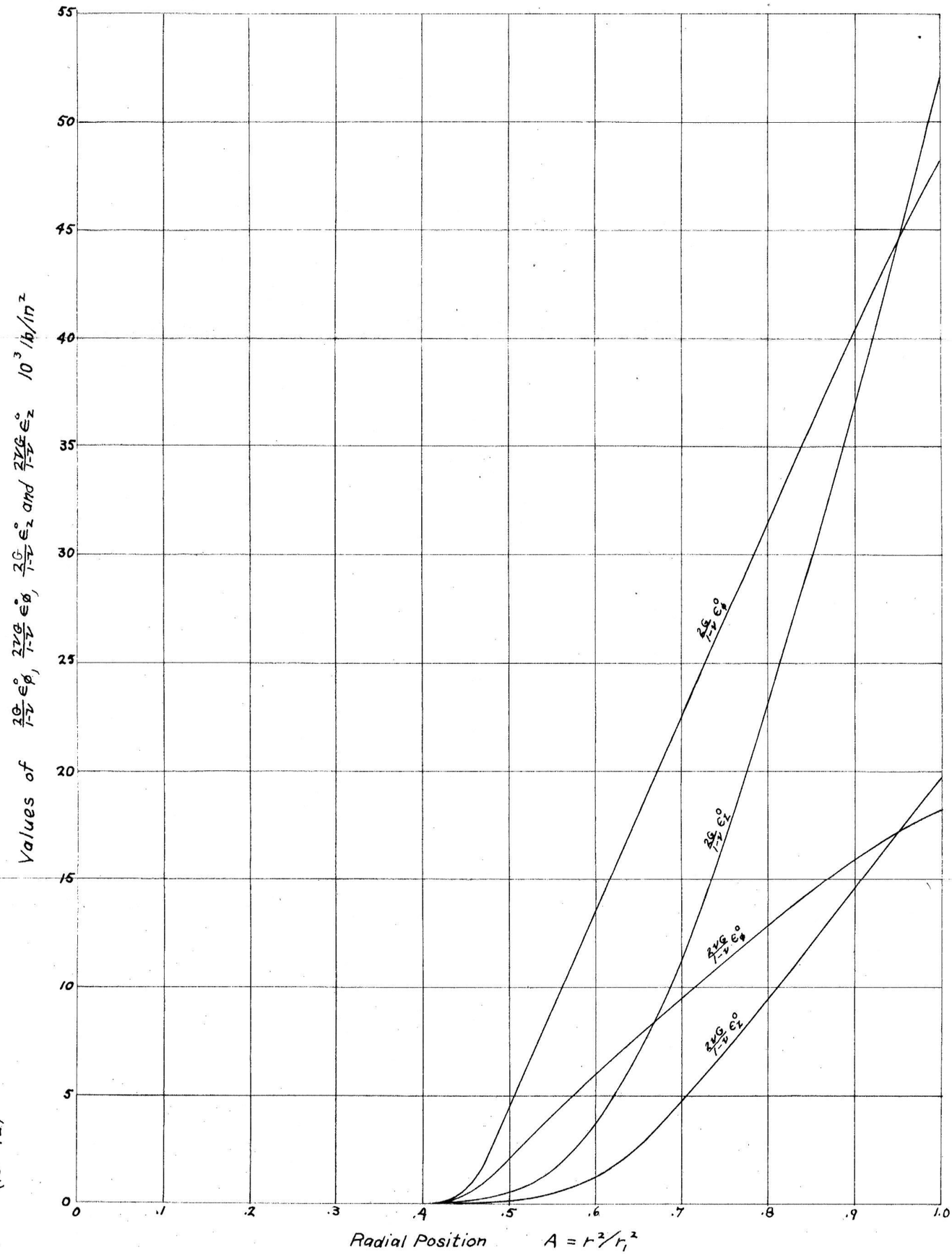

(Fig. 21)

SAMPLE CALCULATION - STRESSES DUE TO RESIDUAL STRAINS $t = 4$ sec

SAMPLE SET OF CURVES (Cont.)

Values of: $\frac{2G}{1-\nu}\int_0^A \frac{\epsilon_\phi^\circ - \epsilon_r^\circ}{2A}\,dA$, $\frac{2\nu G}{1-\nu}\int_0^A \frac{\epsilon_\phi^\circ - \epsilon_r^\circ}{2A}\,dA$, $f_1(\bar{\sigma}_{r_3}) = \frac{2G}{1-\nu}\int_0^A \bar{\sigma}_{r_3}\frac{d}{dA}\left(\frac{1}{2G}\right)dA$ and $f_2(\bar{\sigma}_{r_3}) = \frac{2\nu G}{1-\nu}\int_0^A \bar{\sigma}_{r_3}\frac{d}{dA}\left(\frac{1}{2G}\right)dA$ vs. A for $t = 4$ sec.

Graphically integrate these curves for required integral values.

$\frac{2G}{1-\nu}\int_0^A \frac{\epsilon_\phi^\circ - \epsilon_r^\circ}{2A}\,dA$, $\frac{2\nu G}{1-\nu}\int_0^A \frac{\epsilon_\phi^\circ - \epsilon_r^\circ}{2A}\,dA$, and $f_1(\bar{\sigma}_{r_3})$, $f_2(\bar{\sigma}_{r_3})$ are determined from the graphical integrals of $\frac{\epsilon_\phi^\circ - \epsilon_r^\circ}{2A}$ and $\bar{\sigma}_{r_3}\frac{d}{dA}\left(\frac{1}{2\theta}\right)$

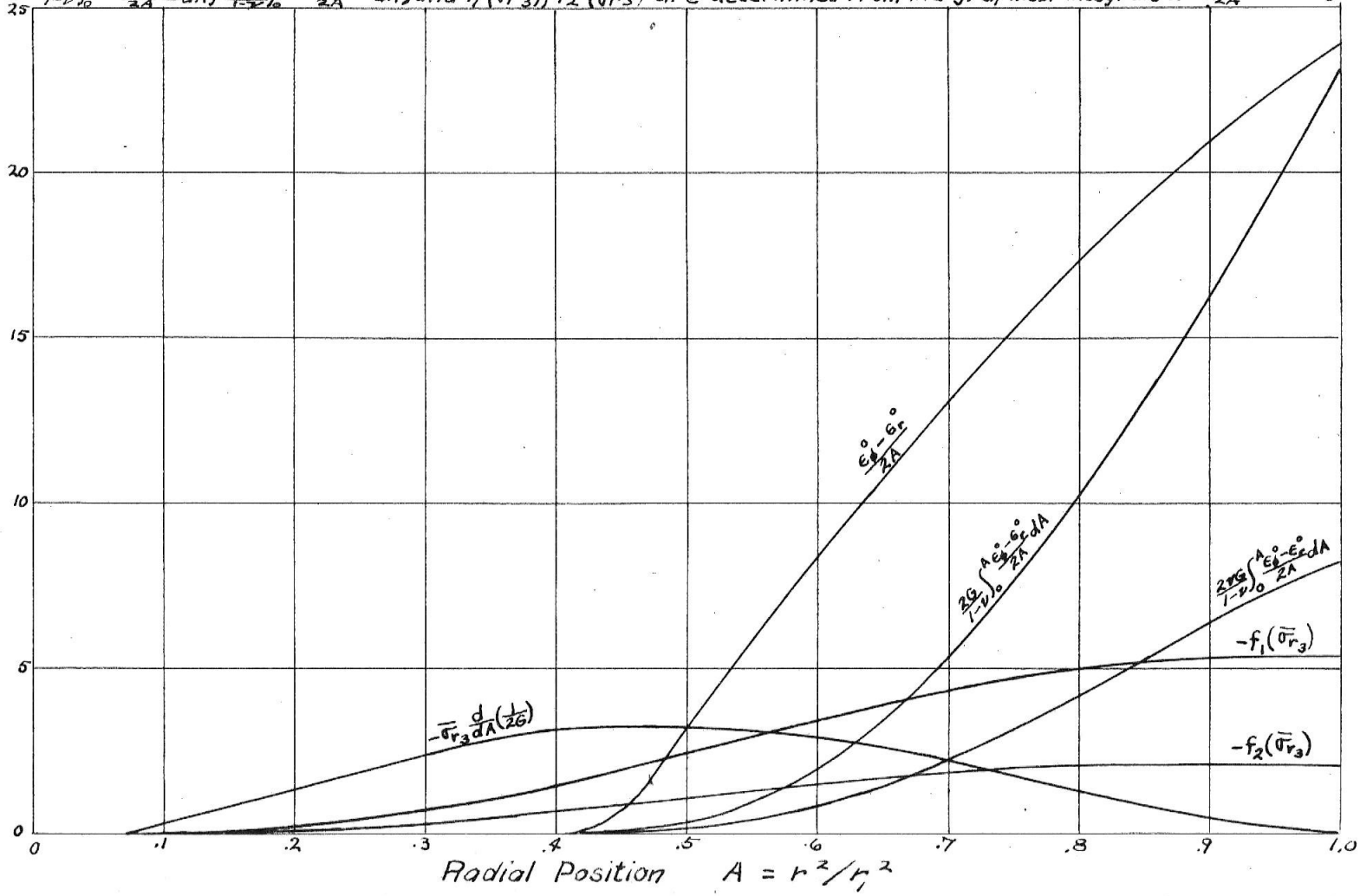

Values of: $\frac{2G}{1-\nu}\int_0^A \frac{\epsilon_\phi^\circ - \epsilon_r^\circ}{2A}\,dA$, $\frac{2\nu G}{1-\nu}\int_0^A \frac{\epsilon_\phi^\circ - \epsilon_r^\circ}{2A}\,dA$, $f_1(\bar{\sigma}_{r_3})$ and $f_2(\bar{\sigma}_{r_3})$, 10^3 lb/in^2 $\frac{\epsilon_\phi^\circ - \epsilon_r^\circ}{2A}$ and $\bar{\sigma}_{r_3}\frac{d}{dA}\left(\frac{1}{2G}\right)$, 10^{-4} in/in

(Fig. 22)

(Table VI) represents the numerical calculations corresponding to (Section b) of the sample calculation: the estimation of the residual strains present at $t = 4$ seconds, and the separation of this estimate into residual strains present near the surface and near the center. It is to be remembered that in the actual sequence of the calculation, this step precedes the calculations represented in the 2nd and 3rd rows of (Table V). The basis for this calculation was presented in Chapter IV.

Referring to (Table VI), the previously determined stresses at $t = 4$ seconds due to the thermal dilation and due to the residual strains present at $t = 2$ seconds are recorded. The reduced stresses due to these two factors are then computed, and their sum is recorded. The value of $\frac{2}{3}\sigma^2_{y.p.}$, the maximum value of the function k^2 which it is assumed that the material can sustain without yielding, is then determined from (Fig. 20), and the known temperature distribution (Table IV) at $t = 4$ seconds. The changes in the reduced stresses required to match k^2 and $\frac{2}{3}\sigma^2_{y.p.}$, at the points where k^2 is the larger, are then computed from the relationships:

$$\Delta(\sigma_r - \sigma) = -\left(1 - \sqrt{\frac{\frac{2}{3}\sigma^2_{y.p.}}{k^2}}\right)(\sigma_r - \sigma)$$

$$\Delta(\sigma_\phi - \sigma) = -\left(1 - \sqrt{\frac{\frac{2}{3}\sigma^2_{y.p.}}{k^2}}\right)(\sigma_\phi - \sigma)$$

$$\Delta(\sigma_z - \sigma) = -\left(1 - \sqrt{\frac{\frac{2}{3}\sigma^2_{y.p.}}{k^2}}\right)(\sigma_z - \sigma)$$

The increments of the residual strains are then computed on the basis of

the assumption that the total strains of any element of the body remain constant. With this assumption, the estimated values of the residual strain increments are given by the following relationships.

$$\Delta\epsilon_r^o = -\frac{1}{2G}\Delta(\sigma_r - \sigma) \quad , \quad \Delta\epsilon_\phi^o = -\frac{1}{2G}\Delta(\sigma_\phi - \sigma) \text{ and } \quad \Delta\epsilon_z^o = -\frac{1}{2G}\Delta(\sigma_z - \sigma)$$

The value of $2G$, appearing above, is obtained from (Fig. 10) and the known temperature distribution (Table IV) at $t = 4$ seconds.

These estimated increments of the residual strains are then added to the residual strains present at $t = 2$ seconds, giving the estimated residual strains at $t = 4$ seconds. For this case, these estimated residual strains are separated, as indicated in (Table VI), into the estimated residual strains near the surface and near the center. The stresses due to these estimated residual strains were calculated in (Table V).

SAMPLE CALCULATION (continued)

t = 4 sec

This illustrates the method of estimating the required values of Residual Strain

	A	$\sigma_{r_1}, \sigma_{\phi_1}, \sigma_{z_1}$ from Stresses due to Thermal Dilation			$-\sigma_1$	$\sigma_{r_3}, \sigma_{\phi_3}, \sigma_{z_3}$ from Stresses of t=4 due to $\epsilon_r^\circ, \epsilon_\phi^\circ, \epsilon_z^\circ$ for t=2			$\sigma_1 = \frac{1}{3}(\sigma_{r_1}+\sigma_{\phi_1}+\sigma_{z_1})$ $\sigma_3 = \frac{1}{3}(\sigma_{r_3}+\sigma_{\phi_3}+\sigma_{z_3})$	$(\sigma_{r_1}-\sigma_1)=(\sigma_{r_3}-\sigma_3)$	$(\sigma_{\phi_1}-\sigma_1)=(\sigma_{\phi_3}-\sigma_3)$	$(\sigma_{z_1}-\sigma_1)=(\sigma_{z_3}-\sigma_3)$	$K^2=(\sigma_r-\sigma)^2+(\sigma_\phi-\sigma)^2+(\sigma_z-\sigma)^2$	Assumed Limiting Value of K^2 above which material yields		Stress Reduction Factor	Changes in Reduced Stress required in order that the relationship; $K^2 \leq \frac{2}{3}\sigma_{y.p.}^2$ will be satisfied.			Known Function of Temperature	Changes of $\epsilon_r^\circ, \epsilon_\phi^\circ, \epsilon_z^\circ$ which would produce the required changes of Reduced Stress if the size and shape of every element of the body remained constant; $\Delta\epsilon_r^\circ = \frac{-\Delta(\sigma_r-\sigma)}{2G}$, etc.			Values of the Residual Strains at the end of the previous time interval; t = 2 sec			Estimated Value of $\epsilon_r^\circ, \epsilon_\phi^\circ, \epsilon_z^\circ$ of t = 4 sec.		
																												$\epsilon_r^\circ = \Delta\epsilon_r^\circ + \epsilon_r^\circ\|_{t=2}$	$\epsilon_\phi^\circ = \Delta\epsilon_\phi^\circ + \epsilon_\phi^\circ\|_{t=2}$	$\epsilon_z^\circ = \Delta\epsilon_z^\circ + \epsilon_z^\circ\|_{t=2}$
													Ⓑ																	
													$\sqrt{\frac{3}{2}\frac{\sigma_{r_3}^2}{K^2}}$	1-Ⓑ	$\Delta(\sigma_r-\sigma)$	$\Delta(\sigma_\phi-\sigma)$	$\Delta(\sigma_z-\sigma)$	2G	$\Delta\epsilon_r^\circ$	$\Delta\epsilon_\phi^\circ$	$\Delta\epsilon_z^\circ$	$\epsilon_{r\ t=2}^\circ$	$\epsilon_{\phi\ t=2}^\circ$	$\epsilon_{z\ t=2}^\circ$	ϵ_r°	ϵ_ϕ°	ϵ_z°
		10^3 lb/in²	10^3 lb/in²	10^3 lb/in²	10^3 lb/in²	10^3 lb/in²	10^3 lb/in²	10^3 lb/in²	10^3 lb/in²	10^3 (lb/in²)²	10^3 (lb/in²)²	in/in	in/in	10^3 lb/in²	10^3 lb/in²	10^3 lb/in²	10^6 lb/in²	10^{-3} in/in	10^{-3} in/in	10^{-3} in/in	10^{-3} in/in	10^{-3} in/in	10^{-3} in/in	10^{-3} in/in	10^{-3} in/in	10^{-3} in/in
Sum of Lower Rows; Stresses due to Thermal Dilation and Residual Strain						$\sigma_r-\sigma$	$\sigma_\phi-\sigma$	$\sigma_z-\sigma$																					
	0					7.14	7.14	-14.28	3.05	1.35	.665	.335	-2.39	-2.39	4.78	13.75	.174	.174	-.348	0	0	0	.174	.174	-.348			
	0.2					5.24	7.84	-13.08	2.60	1.49	.757	.243	-1.23	-1.83	3.06	13.95	.088	.131	-.219	0	0	0	.088	.131	-.219			
	0.4					-5.16	12.95	-7.29	2.35	2.26	.980	.020	+0.10	-.25	+.15	14.94	-.007	.017	-.010	0	0	0	-.007	.017	-.010			
	0.6					-29.02	19.69	4.33	9.83	3.83	.624	.376	9.03	-7.40	-1.63	16.62	-.544	.446	.098	0	0	0	-.544	.446	.098			
	0.8					-30.64	17.70	12.94	14.19	5.59	.628	.372	11.40	-6.58	-4.82	18.26	-.624	.360	.264	-1.145	.658	.487	-1.769	1.018	.751			
	0.9					-30.04	15.58	14.46	13.54	6.05	.668	.332	9.97	-5.17	-4.80	18.87	-.528	.274	.254	-1.960	1.025	.935	-2.488	1.299	1.189			
	1.0					-26.85	12.97	13.88	10.82	6.28	.761	.238	6.39	-3.085	-3.305	19.27	-.332	.160	.172	-2.912	1.400	1.512	-3.244	1.560	1.684			

	A	σ_{r_3}	σ_{ϕ_3}	σ_{z_3}	$-\sigma_3$	$\sigma_{r_3}-\sigma_3$	$\sigma_{\phi_3}-\sigma_3$	$\sigma_{z_3}-\sigma_3$
Stresses due to Residual Strains, which were present at t=2 sec, at t = 4 sec	0	6.50	6.80	9.95	-7.65	-1.15	-1.15	2.30
	0.2	6.47	6.42	9.93	-7.61	-1.14	-1.19	2.32
	0.4	6.92	6.11	9.88	-7.47	-1.05	-1.36	2.41
	0.6	6.31	5.58	9.70	-7.20	-.89	-1.62	2.50
	0.8	4.98	-22.91	-14.66	10.87	15.82	-12.04	-3.79
	0.9	2.83	-42.10	-35.13	29.80	27.63	-17.30	-10.33
	1.0	0	-63.12	-58.97	40.70	40.70	-22.42	-18.27

	A	σ_{r_1}	σ_{ϕ_1}	σ_{z_1}	$-\sigma_1$	$\sigma_{r_1}-\sigma_1$	$\sigma_{\phi_1}-\sigma_1$	$\sigma_{z_1}-\sigma_1$
Stresses due to Thermal Dilation only, at t = 4 sec	0	-27.69	-27.69	-52.51	35.93	8.29	8.29	-16.58
	0.2	-26.96	-29.31	-48.75	33.34	6.38	9.03	-15.41
	0.4	-29.30	-6.37	-29.90	20.19	-4.11	13.82	-9.71
	0.6	-18.25	26.18	6.69	-9.87	-23.12	21.31	1.82
	0.8	-9.91	66.30	53.62	-36.67	-46.58	29.63	16.95
	0.9	-5.02	85.54	77.42	-52.65	-57.67	32.89	24.77
	1.0	0	102.93	99.66	-67.53	-67.53	35.40	32.13

In order to obtain greater flexibility in the use of linear combinations of solutions resulting from estimated values of $\epsilon_r^\circ, \epsilon_\phi^\circ$, and ϵ_z°, the above values of $\epsilon_r^\circ, \epsilon_\phi^\circ$, and ϵ_z° are divided into two sections (see table below), and in the previous portion of this Sample Calculation, the stresses due to these sections are computed.

A	Assumed Total Values of Residual Strain near center at t = 4			Assumed Total Values of Residual Strain near surface at t = 4		
	ϵ_r°	ϵ_ϕ°	ϵ_z°	ϵ_r°	ϵ_ϕ°	ϵ_z°
0	.174	.174	-.348	0	0	0
0.2	.088	.131	-.219	0	0	0
0.4	0	0	0	0	0	0
0.6	0	0	0	-.544	.466	.098
0.8	0	0	0	-1.769	1.018	.751
0.9	0	0	0	-2.488	1.299	1.189
1.0	0	0	0	-3.244	1.560	1.684

(Table VI)

(Table VII) contains the calculations necessary for (Section c) of the sample calculation: the selection of a suitable linear combination of the available independent solutions (for stresses due to assumed values of the residual strains) which, when added to the stresses due to the thermal dilation, achieves a satisfactory match between k^2 and $\frac{2}{3}\sigma^2_{y.p.}$ over the entire range in which yielding occurs. This table is largely self-explanatory. In (Table VII) it is indicated that the stresses due to the thermal dilation plus a linear combination of the stresses due to the assumed values of the residual strains near the surface and near the center will not form a satisfactory match between k^2 and $\frac{2}{3}\sigma^2_{y.p.}$ over the entire region. In general a second assumption of the required values of the residual strains would be necessary. In this particular case, however, it is indicated that the stresses at $t = 4$ seconds, due to the residual strains present at $t = 2$ seconds, may be used as a third independent solution. The remainder of (Table VII) constitutes one method of approximately solving the three simultaneous quadratic equations required to match k^2 and $\frac{2}{3}\sigma^2_{y.p.}$ exactly at three points. The final solution is then presented.

SAMPLE CALCULATION (continued) $t = 4$ sec

This table illustrates the use of linear combinations of known solutions to match K^2 and $\frac{2}{3}\sigma_{y.p.}^2$

	① Reduced Stresses Due to Thermal Dilation: ϵ^T			② Reduced Stresses Due to Assumed ϵ° values near surface			③ Reduced Stresses Due to Assumed ϵ° values near center			④ = ② + ③ Assumed Solution due to Residual Strains			⑤ = ① + ④ Total Solution due to ϵ^T and Assumed Residual Strains			$(\sigma_r-\sigma)^2+(\sigma_\phi-\sigma)^2+(\sigma_z-\sigma)^2$	10^6 (lb/in²)²	
A	$\sigma_{r_1}-\sigma_1$	$\sigma_{\phi_1}-\sigma_1$	$\sigma_{z_1}-\sigma_1$	$\sigma_{r_3}-\sigma_3$	$\sigma_{\phi_3}-\sigma_3$	$\sigma_{z_3}-\sigma_3$	$\sigma_{r_3}-\sigma_3$	$\sigma_{\phi_3}-\sigma_3$	$\sigma_{z_3}-\sigma_3$	$\sigma_{r_3}-\sigma_3$	$\sigma_{\phi_3}-\sigma_3$	$\sigma_{z_3}-\sigma_3$	$\sigma_r-\sigma$	$\sigma_\phi-\sigma$	$\sigma_z-\sigma$	K^2	$\frac{2}{3}\sigma_{y.p.}^2$	
0	8.29	8.29	-16.58	-2.02	-2.02	4.04	-1.997	-1.997	3.994	-4.02	-4.02	8.04	4.27	4.27	-8.54	109	135	
0.2	6.38	9.08	-15.41	-2.03	-2.05	4.08	-.881	-1.299	2.179	-2.91	-3.35	6.26	3.47	5.68	-9.15	128	149	
0.4	-4.11	13.82	-9.71	-1.69	-2.56	4.24	.330	.648	-.978	-1.36	-1.91	3.26	-5.47	11.91	-6.45	213	226	
0.6	-23.12	21.31	1.82	6.36	-9.85	3.50	.403	.652	-1.056	6.76	-9.20	2.44	-16.36	12.11	4.26	432	383	
0.8	-46.58	29.63	16.95	24.50	-19.18	-5.32	.495	.678	-1.174	25.00	-18.50	-6.49	-21.58	11.13	10.46	699	559	
0.9	-57.67	32.89	24.77	34.73	-23.34	-11.39	.502	.698	-1.201	35.23	-22.64	-12.59	-22.44	10.25	12.18	757	605	
1.0	-67.53	35.40	32.13	44.77	-26.68	-18.09	.505	.713	-1.218	45.28	-25.97	-19.31	-22.25	9.43	12.82	748	628	

It is apparent that a solution composed of ① + α② + β③ could be formed which would match K^2 and $\frac{2}{3}\sigma_{y.p.}^2$ at any two points, but in this case the remaining points would still not match satisfactorily. Ordinarily a new assumption of ϵ_r°, ϵ_ϕ° and ϵ_z° would be required, but in this case the strains at $t=2$ have nearly the proper relative values so that the solution at $t=4$ due to residual strains at $t=2$ may be used as a third independent solution. With three independent solutions it is possible to match K^2 and $\frac{2}{3}\sigma_{y.p.}^2$ at three points which in this case results in a satisfactory agreement for all values of A.

The required matching involves the solution of three simultaneous quadratic equations and the technique which follows is specific to this particular case.

	⑥ Reduced Stresses at $t=4.0$ due to $\epsilon_r^\circ, \epsilon_\phi^\circ, \epsilon_z^\circ$ from $t=2.0$			Solution for a value of γ such that ⑤ + γ⑥ satisfies $K^2=\frac{2}{3}\sigma_{y.p.}^2$ at A=1.0	Solution for a value of α such that ⑤ + α② satisfies $K^2=\frac{2}{3}\sigma_{y.p.}^2$ at A=1.0	Solution for a value of b such that $b(⑤+\gamma⑥)+(1-b)(⑤+\alpha②)$ satisfies $K^2=\frac{2}{3}\sigma_{y.p.}^2$ at A=0.8 and 1.0	⑦ Total Solution corresponding to: ⑤ + γb⑥ + α(1-b)②				Solution for a value of β such that ⑦ + β③ satisfies $K^2=\frac{2}{3}\sigma_{y.p.}^2$ at A=0	Solution for a value of α_1 such that ⑦ + β③ + $\alpha_1$② satisfies $K^2=\frac{2}{3}\sigma_{y.p.}^2$ at A=1.0
A	$\sigma_{r_3}-\sigma_3$	$\sigma_{\phi_3}-\sigma_3$	$\sigma_{z_3}-\sigma_3$	$(-22.25+40.70\gamma)^2$	$(-22.25+44.77\alpha)^2$	for $(⑤+\gamma⑥)$: $(\sigma_r-\sigma)\big\vert_{A=.8}=-20.89$	$\sigma_r-\sigma$	$\sigma_\phi-\sigma$	$\sigma_z-\sigma$	K^2	$2(4.053-1.977\beta)^2$	for ⑦ + β③: $(\sigma_r-\sigma)\big\vert_{A=1.0}=-20.48$
0	-1.15	-1.15	2.30	$+(9.43-22.42\gamma)^2$	$+(9.43-26.68\alpha)^2$	$(\sigma_\phi-\sigma)\big\vert_{A=.8}=10.57(\sigma_z-\sigma)\big\vert_{A=.8}=10.28$	4.053	4.053	-8.106	99	$+(8.106-3.994\beta)^2=135$	$(\sigma_\phi-\sigma)\big\vert_{A=1.0}=7.67$
0.2	-1.14	-1.19	2.32	$+(12.82-18.27\gamma)^2=6.28$	$+(12.82-18.09\alpha)^2=6.28$	$K^2\big\vert_{A=.8}=652$	3.24	5.46	-8.71	116	or $4.053-1.977\beta=\sqrt{\frac{135}{6}}$	$(\sigma_z-\sigma)\big\vert_{A=1.0}=12.81$
0.4	-1.05	-1.36	2.41	or	or	for ⑤ + α②: $(\sigma_r-\sigma)\big\vert_{A=.8}=-20.59$	-5.63	11.62	-5.99	203	$\therefore \beta=-0.349$	$(-20.48+94.77\alpha)^2+(7.67-26.68\alpha)^2$
0.6	-.89	-1.62	2.50	$2+938\gamma^2-2702.98\gamma+120.4=0$	$3043.4\alpha^2-2959.3\alpha+120.4=0$	$(\sigma_\phi-\sigma)\big\vert_{A=.8}=10.31$, $(\sigma_z-\sigma)\big\vert_{A=.8}=10.23$	-14.82	10.31	4.54	347	*The solution represented by ⑦ + β③ matches K^2 and $\frac{2}{3}\sigma_{y.p.}^2$ at A=0 and nearly matches them at A=0.8 & A=1.0*	$+(12.81-18.09\alpha_1)^2=628$
0.8	15.82	-12.04	-3.79			$K^2\big\vert_{A=.8}=6.33$	-19.30	9.28	10.03	559		or $3049.6\alpha_1^2-27.066\alpha_1+0.143=0$
0.9	27.63	-17.30	-10.33	or	or	$\therefore b\sqrt{652}+(1-b)\sqrt{633}=\sqrt{559}$	-20.18	8.50	11.68	616		$\alpha_1=0.00531$
1.0	40.70	-22.42	-18.27	$\gamma=0.04655$	$\alpha=0.04255$	$b=-4.0456$ $1-b=5.0456$	-20.30	7.92	12.38	628		
						$\gamma b=-0.1883$ $\alpha(1-b)=0.2147$						

	⑧ Solution for a value of β_1 such that ⑦ + (β+β_1)③ + $\alpha_1$② satisfies $K^2=\frac{2}{3}\sigma_{y.p.}^2$ at A=0	Summary of Multiplying Coefficients	Total Solution ① + 1.220② + 0.696③ + 0.1883⑥			$(\sigma_r-\sigma)^2+(\sigma_\phi-\sigma)^2+(\sigma_z-\sigma)^2$	10^6 (lb/in²)²	
A	for ⑦ + β③ + $\alpha_1$③: $(\sigma_r-\sigma)\big\vert_{A=0}=4.74$	Total Solution:	$\sigma_r-\sigma$	$\sigma_\phi-\sigma$	$\sigma_z-\sigma$	K^2	$\frac{2}{3}\sigma_{y.p.}^2$	
0	$(\sigma_\phi-\sigma)\big\vert_{A=0}=4.74$	① + [1 + α(1-b) + α_1]②	4.75	4.75	-9.50	135	135	
0.2	$(\sigma_z-\sigma)\big\vert_{A=0}=-9.98$	+ [1 + β + β_1]③ + [γb]⑥	3.54	5.91	-9.46	138	149	
0.4	$6(4.74-1.977\beta_1)^2=135$	Now:	-5.76	11.38	-5.62	194	226	
0.6	$\beta_1=-0.005$	$1+\alpha(1-b)+\alpha_1=1.220$	-14.93	10.03	4.93	348	383	
0.8		$1+\beta+\beta_1=0.646$	-19.35	8.94	10.42	563	559	
0.9		$\gamma b=0.1883$	-20.18	8.13	12.05	619	605	
1.0			-20.29	7.53	12.71	628	628	

This agreement between K^2 and $\frac{2}{3}\sigma_{y.p.}^2$ is considered adequate since the stress level due to ϵ^T is still rising and any mismatch will be corrected in the next time interval at a slight expense in the accuracy with which the law: $[d\epsilon_r^\circ/dt : d\epsilon_\phi^\circ/dt : d\epsilon_z^\circ/dt]$ is satisfied as $(\sigma_r-\sigma):(\sigma_\phi-\sigma):(\sigma_z-\sigma)$

Final Solution for $t=4$ sec. : 1.220 (value used in ②) + 0.696 (value used in ③) + 0.1883 (value in ⑥)

Total Residual Strains 10^3 in/in			Total Stress due to Residual Strains			Total Reduced Stress due to Residual Strains			Total Stress at t=4		
ϵ_r°	ϵ_ϕ°	ϵ_z°	σ_{r_3}	σ_{ϕ_3}	σ_{z_3}	$\sigma_{r_3}-\sigma_3$	$\sigma_{\phi_3}-\sigma_3$	$\sigma_{z_3}-\sigma_3$	σ_r	σ_ϕ	σ_z
0.112	0.112	-0.224	12.58	12.58	23.20	-3.54	-3.54	7.08	-15.07	-15.07	-29.31
0.057	0.085	-0.141	12.93	13.14	21.21	-3.84	-3.12	5.95	-14.53	-12.17	-27.59
0	0	0	11.56	11.67	18.19	-1.65	-2.44	4.09	-12.74	5.30	-11.71
-0.664	0.569	0.095	11.01	-8.46	5.94	8.19	-11.28	3.11	-7.24	17.72	12.63
-1.942	1.118	0.824	6.86	-41.07	-26.90	27.23	-20.69	-6.53	-3.05	25.23	26.72
-2.666	1.392	1.275	3.63	-58.62	-96.58	37.49	-29.76	-13.72	-1.39	26.92	30.84
-3.410	1.639	1.769	0	-75.15	-66.70	47.29	-27.87	-19.42	0	27.78	32.96

(Table VII)

(Fig. 23) shows the results of the sample calculation and of similar calculations. In this figure, the reduced stresses due to the residual strains present at $t = 1$, 2, 4, and 8 seconds are presented. Since this figure, together with (Fig. 17) and (Fig. 18), contains the essence of the results, plots of the stresses due to the residual strains and plots of the total stresses, although known, have been omitted. It was indicated, in Chapter VI, that $t = 8$ seconds was the last time at which appreciable yielding due to the stresses of thermal dilation occurred. Hence, no further yielding occurs until the stresses due to the thermal dilation become small enough so that yielding, in the opposite sense, caused by the stresses due to the residual strains commences.

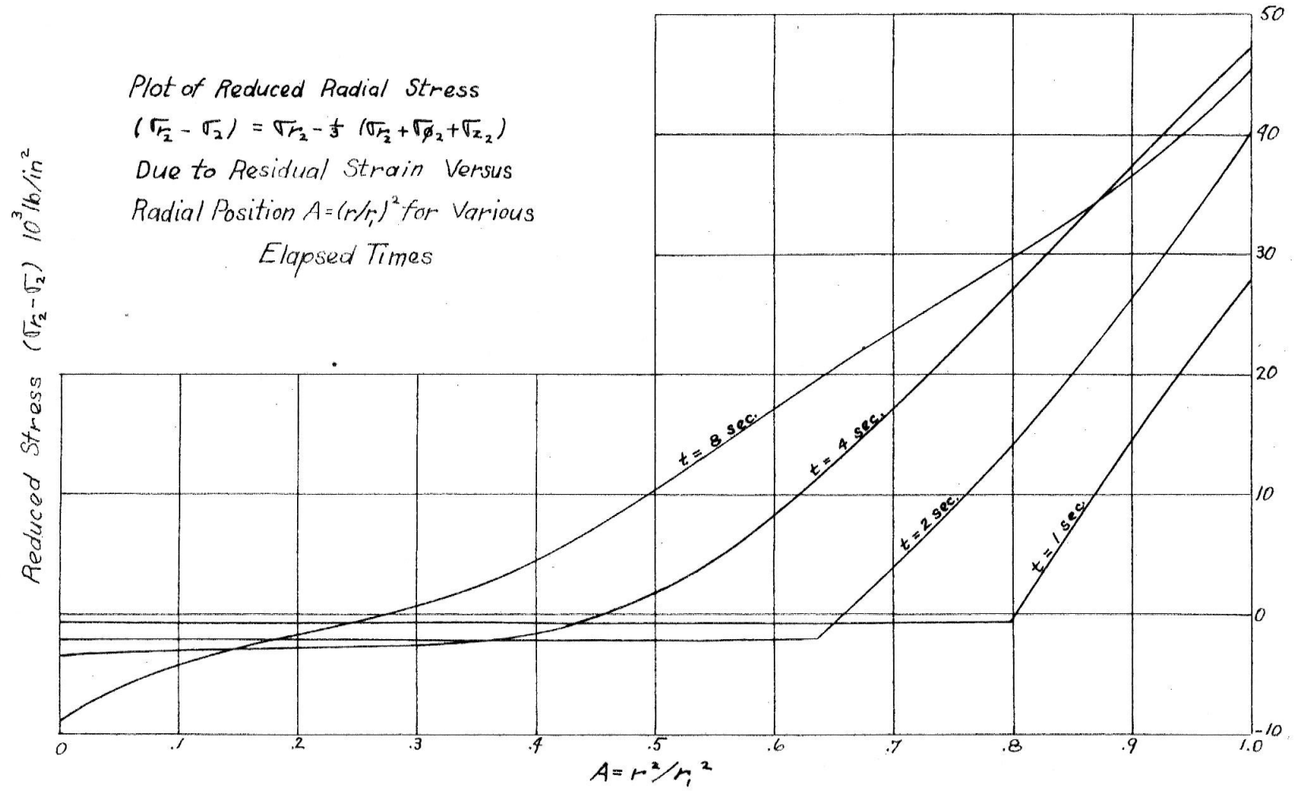
Plot of Reduced Radial Stress
$(\sigma_{r_2} - \sigma_2) = \sigma_{r_2} - \frac{1}{3}(\sigma_{r_2} + \sigma_{\phi_2} + \sigma_{z_2})$
Due to Residual Strain Versus
Radial Position $A = (r/r_1)^2$ for Various
Elapsed Times
Reduced Stress $(\sigma_{r_2} - \sigma_2)$ 10^3 lb/in^2
50
40
30
20
10
0
-10
t = 8 sec.
t = 4 sec.
t = 2 sec.
t = 1 sec.
0
.1
.2
.3
.4
.5
.6
.7
.8
.9
1.0
$A = r^2/r_1^2$

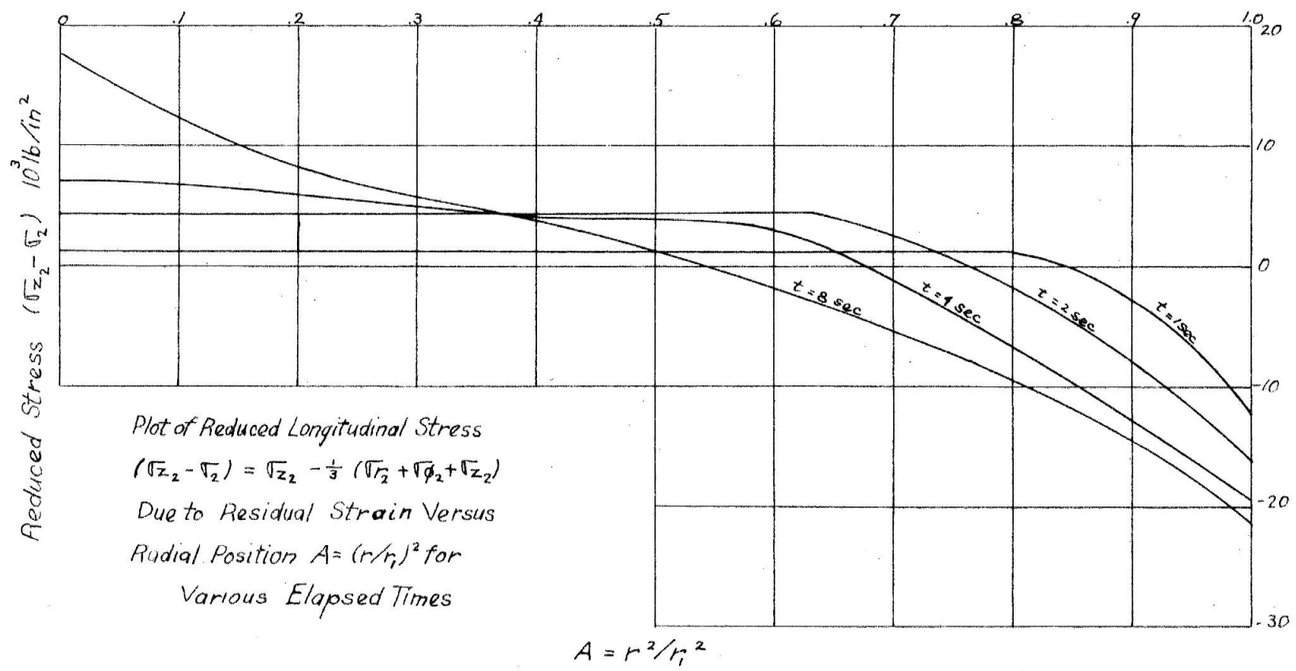
Reduced Stress $(\sigma_{z_2} - \sigma_2)$ 10^3 lb/in^2
20
10
0
-10
-20
-30
t = 8 sec.
t = 4 sec.
t = 2 sec.
t = 1 sec.
0
.1
.2
.3
.4
.5
.6
.7
.8
.9
1.0
Plot of Reduced Longitudinal Stress
$(\sigma_{z_2} - \sigma_2) = \sigma_{z_2} - \frac{1}{3}(\sigma_{r_2} + \sigma_{\phi_2} + \sigma_{z_2})$
Due to Residual Strain Versus
Radial Position $A = (r/r_1)^2$ for
Various Elapsed Times
$A = r^2/r_1^2$

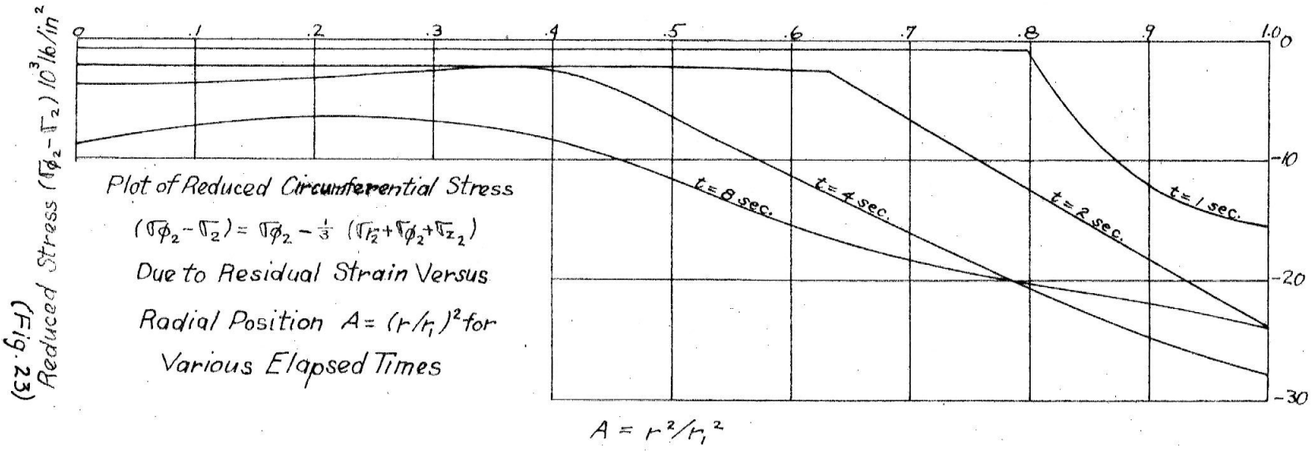
Reduced Stress $(\sigma_{\phi_2} - \sigma_2)$ 10^3 lb/in^2
0
-10
-20
-30
t = 8 sec.
t = 4 sec.
t = 2 sec.
t = 1 sec.
0
.1
.2
.3
.4
.5
.6
.7
.8
.9
1.0
Plot of Reduced Circumferential Stress
$(\sigma_{\phi_2} - \sigma_2) = \sigma_{\phi_2} - \frac{1}{3}(\sigma_{r_2} + \sigma_{\phi_2} + \sigma_{z_2})$
Due to Residual Strain Versus
Radial Position $A = (r/r_1)^2$ for
Various Elapsed Times
$A = r^2/r_1^2$

(Fig. 23)

It now remains to find the residual strains which are in the body when it reaches room temperature and to calculate the final residual stresses due to these strains.

In this particular case, since only a small amount of reversed yielding, caused by the stresses due to the residual strains, is expected as the cylinder further cools, it is presumed that the values of the residual strains present at $t = 8$ seconds remain constant until the cylinder reaches ambient temperature (20 °C). When the cylinder is uniformly at ambient temperature, the stresses due to the residual strains which were present at $t = 8$ seconds, are computed. It is found that k^2 exceeds $\frac{2}{3}\sigma_{y.p.}^2$ only from $A = 0.9$ to $A = 1.0$. The amount of (reversed) yielding required to match k^2 and $\frac{2}{3}\sigma_{y.p.}^2$ is then computed, in a manner similar to the sample calculation, and the final values of the residual stresses are determined. These calculations (when T = constant) are much simpler than the sample calculation, since $f_1(\sigma_r)$ and $f_2(\sigma_r)$ are zero, and since certain of the graphical integrations can be eliminnated.

The final values of the residual stresses are presented in (Fig. 24). These values will be compared with the experimental results of Bucholtz and Buhler in the next chapter.

Final Results of the Calculation of the Residual Stress for a 5cm. Diameter Mild Steel Cylinder quenched from 600°C. into Still Water at Ambient Temperature.

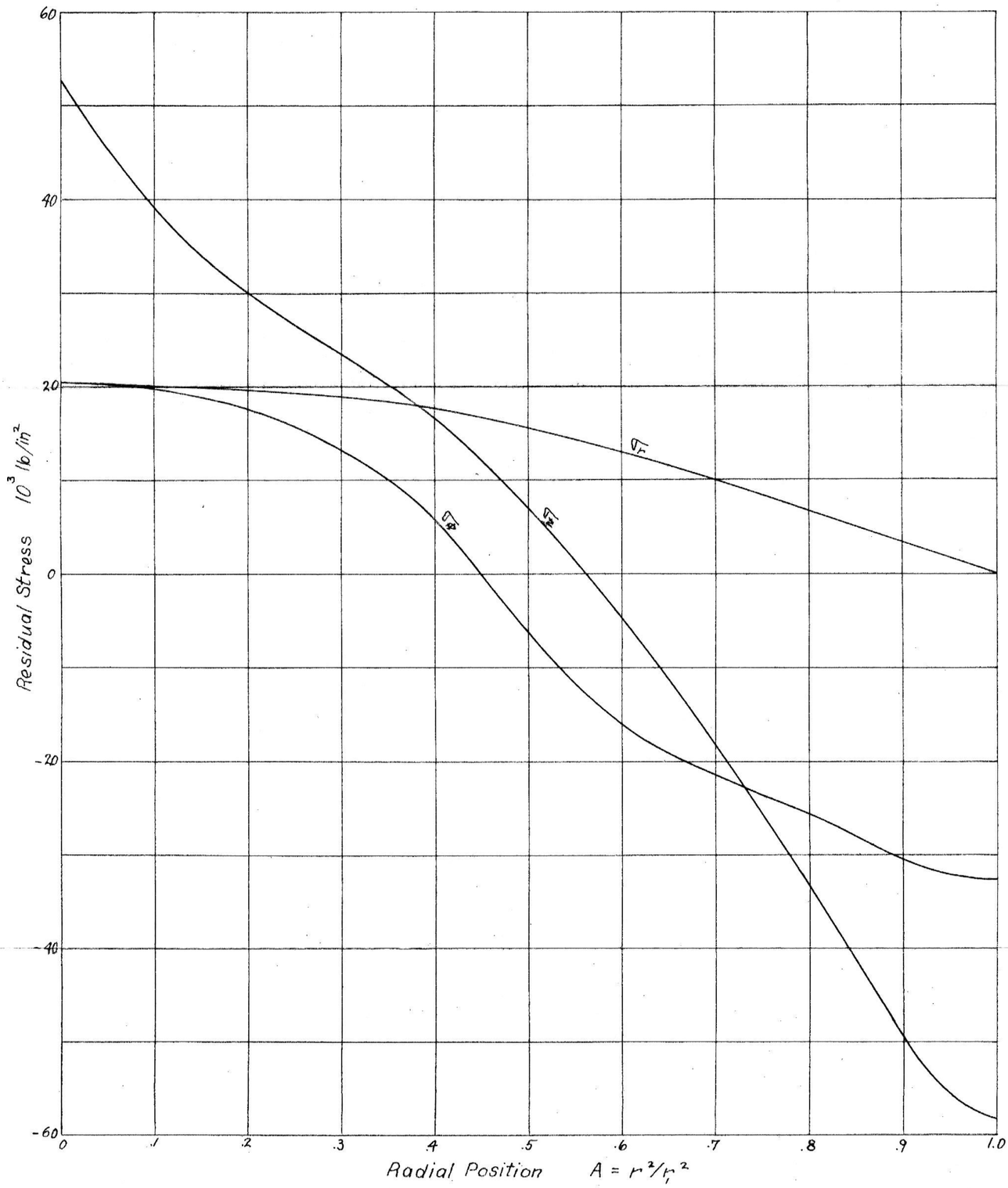

(Fig. 24)

In this chapter, a complete sample calculation of the residual strains present at $t = 4$ seconds, based upong the residual strains present at $t = 2$ seconds, and a calculation of the stresses due to these residual strains were presented. Graphical plots of the reduced stresses versus radial position, resulting from this and similar calculations, were presented for $t = 1, 2, 4,$ and 8 seconds. It was indicated how the residual strains present at $t = 8$ seconds (the last time at which yielding caused by the stresses due to the thermal dilation occurs) were used to determine the final residual stresses left in the cylinder when it reaches ambient temperature. The final residual stresses are plotted in (Fig. 24).

CHAPTER VIII

While the results of the calculation (Fig. 24) do not represent the exact solution to the calculated problem, it must be remembered that if the size of the time and distance intervals is decreased and the numerical accuracy is increased, the results of the calculation approach the exact solution to the calculated problem. By the calculated problem is meant the quench from 600 °C. in a fluid at 20 °C. of an infinitely long isotropic cylinder 5 cm. in diameter, where the boundary layer conductivity and the properties of the material, as a function of the temperature, are exactly as assumed. Thus, any difference between the results of the foregoing calculation and the exact solution to the calculated problem are attributable to the approximations resulting from the finite size of the steps and the finite accuracy of the numerical computations.

This chapter will be devoted to a critical comparison of the calculated values of the final residual stresses with the experimentally determined values of Bucholtz and Buhler (3), for the case of a 5 cm. diameter by 40 cm. mild steel cylinder quenched from 600 °C. in still water at ambient temperature. The calculated values of the final residual stresses are presented in (Fig. 24) and the experimental values are presented in (Fig. 25). While there is a general agreement of form and magnitude between these results, there are greater divergences between them than would be expected if the calculated problem corresponded exactly to the physical conditions of the experiment.

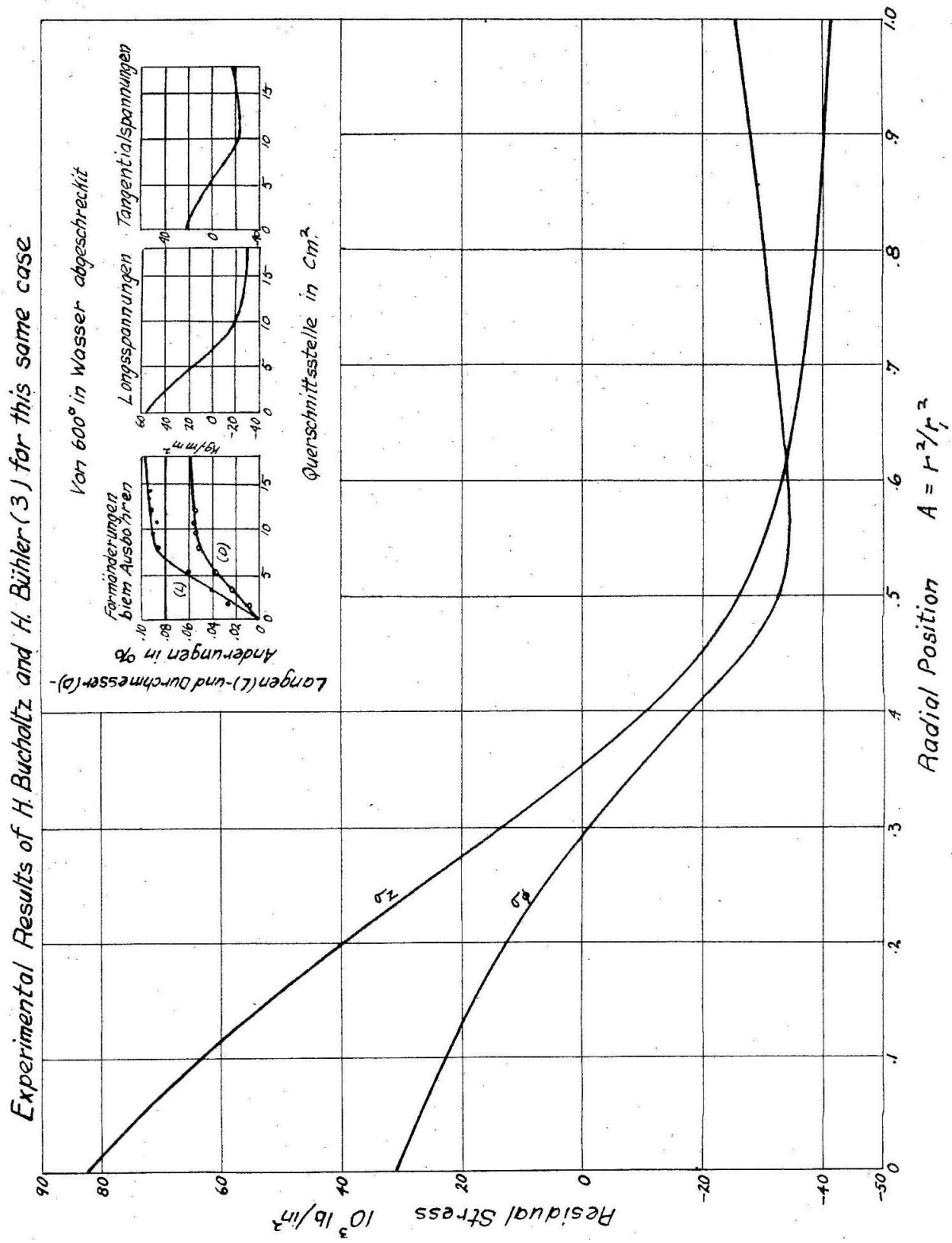
Experimental Results of H. Buchholtz and H. Bühler (3) for this same case
Von 600° in Wasser abgeschreckt
Querschnittsstelle in Cm²
Längen(L)-und Durchmesser(D)-Änderungen in %
Formänderungen beim Ausbohren
Longsspannungen
Tangential/spannungen
kg/mm²
Residual Stress 10³ lb/in²
Radial Position A = r²/r₁²
Sz
Sθ

(Fig. 25)

The major divergence lies in the fact that in the calculated results the largest stresses (corresponding to incipient yielding) appear at the surface of the cylinder, while in the experimental results, the largest stresses (corresponding to incipient yielding) appear in the center. In the calculated results, the stresses in the center are but 63% of the stresses required for yielding, while in the experimental results, the stresses at the surface are but 71% of the stresses required for yielding. A discussion of some of the factors which may be responsible for this divergence will now be made. This discussion will be divided into the following three parts.

1) A discussion of how nearly the calculated problem corresponds to the experimental conditions. The validity of certain assumptions, and the reliability of the assumed values of the parameters will be investigated.

2) A discussion of the errors involved in the calculation of the stated problem. The main emphasis will be on the errors involved in the finite difference approximations.

3) A discussion of the difficulties involved in the experimental determination of the residual stresses.

The first question which will be asked is how close does the assumed quenching rate correspond to the experimental quenching rate, remembering that all of the yielding due to thermal stresses occurs during the first eight seconds. The immersion of a cylinder 5 cm. in diameter by 40 cm. long takes a finite time. If rapidly done, it must result in high

variable fluid velocities, which certainly influences the boundary layer conductivity. If slowly done, the assumption that the partial derivative of all parameters with respect to z is zero is seriously compromised. In addition, while the cylinder is in the fluid, distinct variations of the boundary layer conductivity with z must be expected since there is initially rapid boiling, which must engender convection currents.

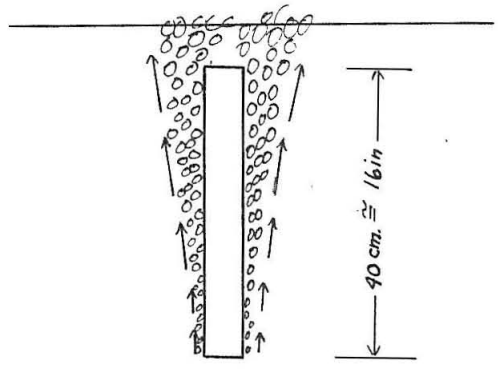

These currents may be expected to be more severe near the top of the cylinder, as illustrated. This means an additional varation of h with z. Further, the temperature and the time at which the transition in the mode of cooling occurs (from boiling with fluid contact to no boiling) may be expected to be seriously lowered and delayed near the top of the cylinder, due to the fact that the fluid passing the top has already absorbed large quantities of heat from the lower portions of the cylinder. Thus, the region (excepting for the difference in pressure) at which the boundary layer conductivity may be presumed to be closest to that which was assumed (based upon experiments with extremely small specimens) is near the bottom of the cylinder. At the center, where most interest is attached, the assumed boundary layer conductivity may be presumed to be altered by, at least, the following factors.

1) There are higher convection currents, which tend to increase h.

2) There is a greater thickness of the heated fluid and vapor layer, which tends to decrease h.

3) The surface temperature at which the transition in the mode of cooling occurs, is lowered, which tends to sustain the value of h (higher in the first mode of cooling) for a longer time.

It is the author's opinion that these factors may be expected to have somewhat the following overall effect near the longitudinal center of the cylinder.

1) The initial value of h is probably lower than assumed in the calculation.

2) The transition in h (due to the change in the mode of cooling) is probably smaller, much less well defined, and occurs at a lower temperature than assumed in the calculation.

3) Values of h after the transition are probably increased.

There is , however, no quantitative data available in the literature on these effects, hence they could not be included in the calculation.

The foregoing enumerated overall effects would tend to reduce the amount of yielding at the surface and tend to increase it at the radial center of the cylinder. A comparison of the calculated and experimental residual stresses, (Fig. 24) and (Fig. 25), indicates that these are precisely the effects which would be required to bring the calculated and experimental results into closer agreement, since they would reduce the residual stresses near the surface and increase them at the center.

In view of these factors, it may be concluded that the assumption of the value of the boundary layer conductivity is one of the critical points in the calculation. It may be further concluded that the deviations of the actual boundary layer conductivity, near the longitudinal center of the cylinder, from the assumed values of the boundary layer conductivity are an important cause of the deviations of the calculated and experimental results. A less important, though perhaps significant, factor is that the partial derivatives of all parameters with respect to z are not equal to zero in the experimental case.

Another critical point, although one extremely difficult to evaluate, lies in possible deviations between the actual and the assumed values of the elastic constants E, ν and G, as a function of temperature. This is particularly true since ν must be determined from $\nu = \frac{E}{2G} - 1$ and is hence an extremely critical function of the values of E and G. It is almost impossible to find reliable values of Poisson's Ratio; the reference used by the author being perhaps the best available. The selection of the value of G is also critical because the derivative of $1/G$ with respect to temperature is required.

The assumption of the value of the yield point is a critical assumption of comparable importance to the assumption of the boundary layer conductivity. This is true because at temperatures in the vicinity of 500 to 600 °C. there is an effect similar to creep appearing. This is evidenced by the fact that all of the experimenters who have attempted to determine the elastic constants in this temperature range were forced to use either unloading techniques or vibration techniques in order to obtain

consistent results. Unfortunately there is no quantitative data for "creep" available in the stress temperature levels involved in this type of problem. Available creep data is in terms of days, months and years, rather than seconds, and this data is at such low stress levels that the amount of creep per second is truly negligible. It must be remembered, however, that yielding due to "creep" is the easiest to compute in the type of problem under consideration, as was indicated in Chapter IV. In addition it would be mathematically simple to superimpose "creep" upon the type of calculation just completed.

It is interesting to note that the introduction of "creep" at high temperatures would tend to increase the residual strains present near the center in the problem just completed. This is apparent from an appraisal of the temperature distribution for various values of elapsed time, (Fig. 9). In this figure, it is seen that the surface drops below 500 °C. in 1 second while the center takes 16 seconds to achieve the same temperature drop. Furthermore, during the first 8 seconds, in which the calculation indicated that the yielding due to the stresses of thermal dilation ceased, the center temperature has only decreased about 10 °C. It follows, therefore, that virtually all of any "creep" which might have occurred would have occurred near the center. The increase in the residual strains near the center would result in increased final calculated residual stresses near the center. It would also decrease the residual strains present near the surface since yielding near the center during the quench would relieve the surface stresses. These factors are precisely the factors required to bring the calculated final residual

stresses and the experimental residual stresses, (Fig. 24) and (Fig. 25), into closer agreement.

The remaining parameters, k (conductivity), ρ (specific weight), c_p (specific heat), and ϵ^T (linear component of thermal dilation), are believed to be non-critical. A great deal of work has been done on the evaluation of these parameters as a function of the temperature for a variety of materials and their values are known to temperatures higher than 600 °C. for most common materials, consisting solely of a single phase.

The major remaining difference between the calculated problem and the actual physical experiment lies in the assumption, in the calculated problem and in the calculations involved in the experimental determination, that the cylinder is of infinite length. Since the cylinder's length was 8 times the diameter (at the time it was quenched) it may be expected that thermal end effects are completely negligible over a central region of 20 cm. of its 40 cm. length. Such a section was removed after the quench and the residual stresses determined in it by Sach's boring out technique. The removal of this central section changes the stress distribution near the ends of the removed section. These changes introduce small, but appreciable changes in the values of the residual stresses as determined by Sach's technique. The residual stresses are determined from the changes in length and diameter accompanying the boring out of the cylinder, and in this case the length of the total cylinder (including the disturbed ends) was measured.

The following list is a recapitulation of the deviations, between

the calculated problem and the experimental conditions, which have been discussed. The list is arranged in plausible order of decreasing importance.

1) Deviations between the actual and assumed boundary layer conductivities over the central (longitudinal) region of the cylinder.

2) Deviations between the actual and assumed yield points and the failure to include "creep" effects in the calculation.

3) Deviations between the assumed and actual values of the elastic constants E, ν and G.

4) Variation of the experimental boundary layer conductivity with z, and hence a variation of all temperature dependent parameters with z during the quench.

5) End effects caused by the finite length of the experimental cylinder.

6) Deviations between the assumed and actual values of $k/\rho c_p$, k, and ϵ^T.

No pretense is made that these are the only important possible deviations, but they are certainly the most obvious. In the opinion of the author, the correction of the above deviations would result in a close agreement between the calculated and experimental results.

The accuracy of the numerical portion of the computation is, in view of the foregoing deviations between the assumed and actual conditions, less important than the fact that it is capable of indefinite refinement. The accuracy of this calculation would have been slightly improved, for

the same amount of labor, if the residual strains had been computed at $t = 2, 4, 6$ and 8 seconds rather than at $t = 1, 2, 4$ and 8 seconds. The computation at $t = 6$ seconds might have caught slightly greater stresses in the intermediate region between the surface and the center of the cylinder. In addition, it is incumbent upon the author to point out that there is an implicit error in the calculation of the limit, as A approaches zero, of the following quantity at $t = 4$ and $t = 8$ seconds.

$$\lim_{A \to 0} \frac{\epsilon_\phi^\circ - \epsilon_r^\circ}{2A}$$

In order to avoid infinite derivatives in the stresses with respect to A, at the center of the cylinder, it is required that this limit be finite. In the numerical calculations for $t = 4$ and $t = 8$ seconds, it was, however, tacitly assumed that since $\epsilon_r^\circ\big|_{A=0} = \epsilon_\phi^\circ\big|_{A=0}$ the limit of the above quantity was zero. Referring to page 60 of this text, however, it is evident that this limit should have been estimated from the following equation.

$$\lim_{A \to 0} \frac{\Delta\epsilon_r^\circ - \Delta\epsilon_\phi^\circ}{2A} = \frac{1}{2G}\left(1 - \sqrt{\frac{\frac{2}{3}\sigma_{y.p.}^2}{K^2}}\right) \lim_{A \to 0} \frac{(\sigma_\phi - \sigma) - (\sigma_r - \sigma)}{2A}$$

Using the equation of equilibrium, (Eq. 5a), the above equation may be written in the following form.

$$\lim_{A \to 0} \frac{\Delta\epsilon_\phi^\circ - \Delta\epsilon_r^\circ}{2A} = \frac{1}{2G}\left(1 - \sqrt{\frac{\frac{2}{3}\sigma_{y.p.}^2}{K^2}}\right) \frac{d\sigma_r}{dA}\bigg|_{A=0}$$

Fortunately, the contribution of this error is negligible in this case due to the following factors. The term $d\sigma_r/dA\big|_{A=0}$ is small at $t = 4$ and $t = 8$ seconds and is identically zero at $t = 1$ and $t = 2$ seconds. This implicit error affects the term $\epsilon_\theta^o - \epsilon_r^o/2A$ only in the region $A < 0.2$. The term appears as $\int_0^A \frac{\epsilon_\theta^o - \epsilon_r^o}{2A} dA$ while the other terms have finite values at the center, hence the contribution of this term can never exceed approximately 1/10 the maximum error in the term, which in this case is already small. The fact that this error was allowed to creep in, however, indicates the care which must be exercised when limiting processes are involved.

It is believed by the author, although a substantiating discussion would be difficult, that the differences between the results of this calculation, (Fig. 24), and the exact results of the calculated problem would be everywhere less than 10,000 p.s.i. and that an average accuracy of better than 5000 p.s.i. might be expected.

The remaining factor which is involved in a comparison of the calculated and experimental values of the residual stresses is the question of how well the experimental results (Fig. 25) actually represent the residual stresses which existed in the cylinder. The experimental determination of these stresses also requires the assumptions that end effects are negligible and that the partial derivative of all parameters with respect to z is zero. The validity of these assumptions was previously discussed. In order to appreciate the difficulties (even if these assumptions were strictly true) in the experimental determination of the residual

stresses, it is necessary to investigate the mathematics of Sach's boring out technique (1).

Since one of the few references in English which even presents the required equations has serious typographical errors in its presentation, H. L. Wishart and R. K. Potter (5), it will be desirable to derive these equations.

Consider the following equations, which were derived in Chapter III for the stresses due to the boundary forces, when the elastic coefficients are constant.

$$\left.\begin{array}{ll} (17)_2 & \sigma_\phi + \sigma_r \\ (18)_2 & 2\frac{d}{dA}(A\sigma_r) \end{array}\right\} = \frac{2G}{1-\nu}(C + \nu\epsilon_z)$$

$$(21)_2 \qquad \sigma_z = \frac{2G}{1-\nu}(\epsilon_z + \nu C)$$

The first step is to show that the constant C may be identified with the circumferential strain at the surface. i.e. $C = \epsilon_\phi \Big|_{A=0}$. The integration of $(\text{Eq. } 18)_2$ gives:

$$2A\sigma_r = \frac{2G}{1-\nu}\left[(C + \nu\epsilon_z)A + D\right]$$

The application of the boundary condition $\sigma_r \Big|_{A=1} = 0$ gives:

$$(27) \qquad \sigma_r = -\frac{2G}{1-\nu}\,\frac{1-A}{2A}(C + \nu\epsilon_z)$$

Substituting (Eq. 27) in $(\text{Eq. 17})_2$ gives the following value for

$$(28) \qquad \sigma_\phi = \frac{2G}{1-\nu}\,\frac{1+A}{2A}\,(C+\nu\epsilon_z)$$

Evaluating (Eq. 9a) at the surface gives:

$$(9a) \qquad \epsilon_\phi\Big|_{A=1} = \frac{1+\nu}{E}\left[(1-\nu)\sigma_\phi\Big|_{A=1} - \nu\sigma_r\Big|_{A=1}\right] - \nu\epsilon_z$$

Substituting (Eq. 28) in (Eq. 9a), and noting that $\sigma_r\Big|_{A=1} = 0$ gives:

$$(29) \qquad \epsilon_\phi\Big|_{A=1} = \frac{1-\nu}{2G}\sigma_\phi\Big|_{A=1} - \nu\epsilon_z = (C+\nu\epsilon_z)\,\frac{1+A}{2A}\Big|_{A=1} - \nu\epsilon_z = C$$

This indicates that the constant C may be identified with the circumferential strain at the surface.

Sach's technique consists of boring out the center of the cylinder in successive increments and measuring the corresponding values of the resulting strains ϵ_z and $\epsilon_\phi\Big|_{A=1}$. (Eq. 27) indicates that in order to produce external strains ϵ_z and $\epsilon_\phi\Big|_{A=1}$ due to this boring out, the value of σ_r must change at the inner surface of the bore, $A = A_b$, by the following amount.

$$\Delta\sigma_r\Big|_{A=A_b} = -\frac{2G}{1-\nu}\,\frac{1-A_b}{2A_b}\,(\epsilon_\phi\Big|_{A=1} + \nu\epsilon_z)$$

The existing stress at $A = A_b$ in the original cylinder, $\sigma_{r_o}\Big|_{A=A_b}$, plus the change in this stress due to the boring out, $\Delta\sigma_r\Big|_{A=A_b}$, must equal the final stress after boring at the surface of the bore $\sigma_r\Big|_{A=A_b}$. i.e.:

$$\sigma_{r_o}\Big|_{A=A_b} + \Delta\sigma_r\Big|_{A=A_b} - \sigma_r\Big|_{A=A_b}$$

However, the radial stress at $A = A_b$ after boring must be zero, since this is the surface of the bore. Therefore, the following equation may be written.

$$\sigma_{r_o}\Big|_{A=A_b} = -\Delta\sigma_r\Big|_{A=A_b} = \frac{2G}{1-\nu}\,\frac{1-A_b}{2A_b}\left(\epsilon_\phi\Big|_{A=1} + \nu\epsilon_z\right)$$

This original stress must have satisfied the equation of equilibrium:

$$\sigma_\phi = 2\frac{d}{dA}(A\sigma_r) - \sigma_r \qquad (5b)$$

Therefore, the original circumferential stress in the cylinder before boring must be given by the following equation.

$$\sigma_{\phi_o}\Big|_{A=A_b} = \frac{2G}{1-\nu}\left\{2\frac{d}{dA_b}\left[(1-A_b)\left(\epsilon_\phi\Big|_{A=1} + \nu\epsilon_z\right)\right] - \frac{1-A_b}{2A_b}\left(\epsilon_\phi\Big|_{A=1} + \nu\epsilon_z\right)\right\}$$

$$= \frac{2G}{1-\nu}\left[(1-A_b)\frac{d}{dA_b}\left(\epsilon_\phi\Big|_{A=1} + \nu\epsilon_z\right) - \frac{1+A_b}{2A_b}\left(\epsilon_\phi\Big|_{A=1} + \nu\epsilon_z\right)\right]$$

Similarly, $(\text{Eq. } 21)_2$ indicates that in order to produce the external strains ϵ_z and $\epsilon_\phi\Big|_{A=1}$ due to this boring out, the value of σ_z at $A = A_b$ must change by the following amount.

$$\Delta\sigma_z\Big|_{A=A_b} = \frac{2G}{1-\nu}\left(\epsilon_z + \nu\epsilon_\phi\Big|_{A=1}\right)$$

The existing stress at $A = A_b$ in the original cylinder, $\sigma_{z_o}\Big|_{A=A_b}$, plus the change in the stress, $\Delta\sigma_z\Big|_{A=A_b}$, must equal the final stress after boring out, $\sigma_z\Big|_{A=A_b}$. i.e.:

$$\sigma_{z_o}\Big|_{A=A_b} + \Delta\sigma_z\Big|_{A=A_b} = \sigma_z\Big|_{A=A_b}$$

It is now necessary to determine the stress, $\sigma_z\Big|_{A=A_b}$, which exists at the surface of the bored out cylinder. Assume that an incremental amount dA_b is bored out from the cylinder. This reduces the axial force on the remainder of the cylinder by an amount $\sigma_z\Big|_{A=A_b} dA_b$, which must correspond to a uniform change of the axial stress over the remainder of the cylinder given by:

$$\sigma_z\Big|_{A=A_b} dA_b = \left[1-(A_b+dA_b)\right] d\sigma_z$$

Referring to $(\text{Eq. } 21)_2$, this may be written in the following form.

$$\sigma_z\Big|_{A=A_b} = \frac{2G}{1-\nu}\left[1-(A_b+dA_b)\right]\frac{d}{dA_b}\left(\epsilon_z + \nu\epsilon_\phi\Big|_{A=1}\right)$$

Neglecting second order terms, it follows that the original axial stress is given by the following equation.

$$\sigma_{z_o}\Big|_{A=A_b} = \frac{2G}{1-\nu}\left[(1-A_b)\frac{d}{dA_b}\left(\epsilon_z + \nu\epsilon_\phi\Big|_{A=1}\right) - \left(\epsilon_z + \nu\epsilon_\phi\Big|_{A=1}\right)\right]$$

For purposes of simplicity, the foregoing clumsy notation will be altered as indicated below.

Let: σ_r, σ_ϕ, σ_z be the original stresses before boring.

A be the dimensionless bored out area.

ϵ_z be the longitudinal strain caused by the boring out.

ϵ_ϕ be the circumferential strain at the surface caused by the boring out.

In terms of this notation, the equations by which the residual stresses are determined may be written in the following form.

$$(30) \qquad \sigma_r = \frac{2G}{1-\nu}\left[\frac{1-A}{2A}(\epsilon_\phi + \nu\epsilon_z)\right]$$

$$(31) \qquad \sigma_\phi = \frac{2G}{1-\nu}\left[(1-A)\frac{d}{dA}(\epsilon_\phi+\nu\epsilon_z) - \frac{1+A}{2A}(\epsilon_\phi+\nu\epsilon_z)\right]$$

$$(32) \qquad \sigma_z = \frac{2G}{1-\nu}\left[(1-A)\frac{d}{dA}(\epsilon_z+\nu\epsilon_\phi) - (\epsilon_z+\nu\epsilon_\phi)\right]$$

and $$\sigma_r+\sigma_\phi = \frac{2G}{1-\nu}\left[(1-A)\frac{d}{dA}(\epsilon_\phi+\nu\epsilon_z) - (\epsilon_\phi+\nu\epsilon_z)\right]$$

It is interesting to note that the stresses at the center are given by:

$$\sigma_z\Big|_{A=0} = \frac{2G}{1-\nu}\frac{d}{dA}(\epsilon_\phi+\nu\epsilon_z)$$

$$\sigma_\phi\Big|_{A=0} = \sigma_r\Big|_{A=0} = \frac{1}{2}\frac{2G}{1-\nu}\frac{d}{dA}(\epsilon_z+\nu\epsilon_\phi)$$

In order to appreciate the significance of the foregoing equations more easily, the following graphical construction may prove helpful. If the function $\frac{2G}{1-\nu}(\epsilon_z + \nu\epsilon_\phi)$ is plotted against A, the following construction gives the value of σ_z.

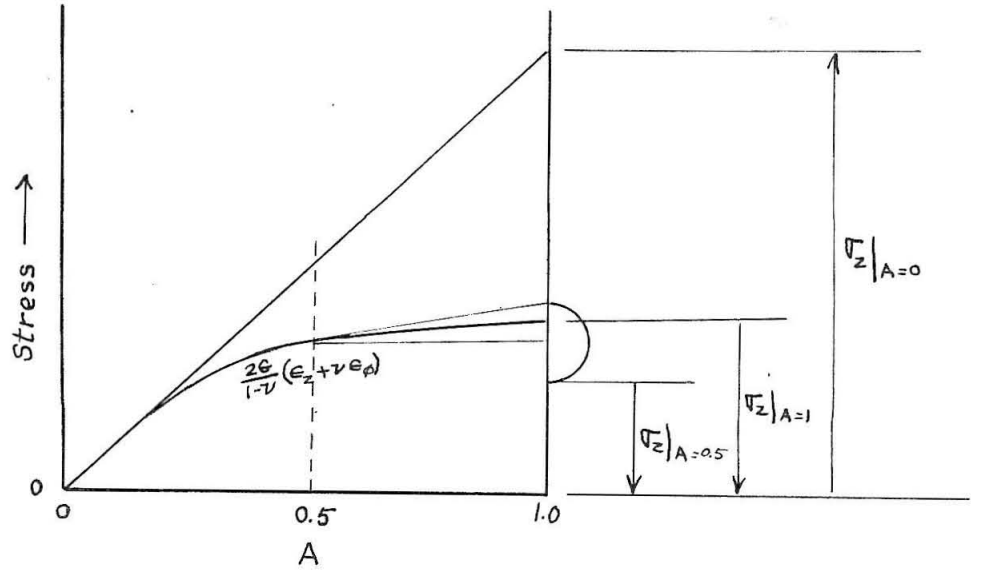

This graphical construction indicates quite clearly the importance not only of the value of the function $\frac{2G}{1-\nu}(\epsilon_z + \nu\epsilon_\phi)$, but also of the derivative of this function with respect to A. A similar graphical construction applies to the term $(\sigma_\phi + \sigma_r)$.

The magnitude of the measurements involved in the determination of the stresses by the above equations is indicated in the small figure shown in (Fig. 25). For example, the first point of the ϵ_ϕ curve corresponds to a change in the diameter of the cylinder of 2/10,000 of an inch, and this must be measured accurately enough to give a reliable slope. It must also be considered that these measurements were made by mechanical means rather than with strain gages. Referring to this figure, it is seen that if the first measured points of ϵ_z and ϵ_ϕ were used, rather than the smoothed curve, the initial values of σ_z and σ_ϕ would be changed by approximately 20%. Therefore, it may be concluded that the accuracy of the experimental residual stresses near the center is quite low. The accuracy, of course, improves as the size of the bore increases, but the measuring problem is still acute.

In view of these factors, and the unevenness of the original experimental mearements of ϵ_ϕ and ϵ_z, as indicated in the small figure shown in (Fig. 25), it is apparent that this experimental determination, particularly at the center, is subject to very large possible errors.

In this chapter, the calculated values of the final residual stresses have been compared with the experimental values determined by Bucholtz and Buhler. It was pointed out that, while the calculated results do not represent the exact solution to the assumed problem due to finite differ-

ence approximation errors, the use of a greater number of steps causes the calculated solution to converge on the exact solution. It was then indicated that the divergence between the calculated and experimental values of the final residual stresses was much greater than could be explained on the basis of the finite difference approximation errors. This divergence was attributed to errors in the assumed values of the parameters, variation of the experimental boundary layer conductivity with axial position, end effects and errors in the experimental determination of the residual stresses.

These divergences in no way detract from the method of calculation, which is capable of arbitrary accuracy. Rather, they indicate that much more reliable values of the parameters are required and that greater care must be taken in obtaining experimental results which do not appreciably violate the assumptions of infinite length and no variation with axial position.

PART III

The extension of Part I to cover the case of an infinitely long hollow cylinder.

The statement and brief discussion of other cases which can be simply handled.

The effects of introducing a phase change on the temperature and stress problem for all cases. A brief discussion of the additional information required.

CHAPTER IX

This chapter will be devoted to the extension of Part I to cover the case of a hollow cylinder. The problem, stated in its entirety, is the development of an analytical method for the prediction of the residual stresses induced in an infinitely long concentric hollow isotropic cylinder by a symmetrical quench in a large body of fluid, assuming that all of the pertinent parameters are known (graphical) functions of the temperature.

The first step in this problem is to indicate the modifications to Chapter I necessary to determine the temperature distribution. The notation used will be the same as that presented in Chapter I, page 2, except for the following additions.

Let: r_o be the inner radius of the cylinder.

x_o $= r_o/r_1$

h_o be the boundary layer conductivity on the inner surface.

h_1 be the boundary layer conductivity on the outer surface.

The required modifications consist of the introduction of a boundary layer at the inner surface as well as at the outer surface and a change in the division of the cylinder such that the distance r_1-r_o is divided up into n equal intervals Δr, or $(1-x_o)$ is divided up into n equal intervals Δx, the center of each interval being distinguished by the subscripts

$$\frac{x_o}{\Delta x} + \frac{1}{2}\ ,\ \frac{x_o}{\Delta x} + 1\tfrac{1}{2}\ ,\ \ldots\ldots\ \frac{x_o}{\Delta x} + n\ ,\ \ldots\ldots\ \frac{x_o}{\Delta x} + (n-\tfrac{1}{2})$$

These divisions are plotted in the same manner as indicated in (Fig.1), page 9, versus $\log_{10} x_r$ except that now there is a half interval (corresponding to $\frac{x_o}{\Delta x} - \frac{1}{2}$) inside the inner surface of the cylinder as well as a half interval (corresponding to $\frac{x_o}{\Delta x} + n + \frac{1}{2}$) beyond the outer surface of the cylinder. Referring to page 8, the boundary layer equation on the inner surface of the cylinder may be developed in a manner similar to the development of (Eq. 4). It is readily seen that this equation is:

$$\left.\frac{\partial T}{\partial x}\right|_{x=x_o} = \left.\frac{r_o h_o}{k \log_{10} e}(T - T_o)\right|_{x=x_o}$$

T_o has the significance of the bulk fluid temperature in the interior of the cylinder. This equation is satisfied in the same manner as the boundary layer equation was satisfied at the outer surface if a curve $k \log_{10} e / r_o h_o$ is plotted to the left of the inner surface. When this is done, the solution to the problem proceeds in exactly the same manner as outlined in Chapter I, except that everything said about the outer surface now applies to the inner surface as well.

The remaining step is to indicate the modifications to Chapter III required by a hollow cylinder. The notation used will be that used in Chapter III except for the following additions and changes.

Let: p_o be the internal pressure.

p_1 be the external pressure.

r_o be the internal radius.

$A_o = r_o^2 / r_1^2$

$f_1'(\sigma_r) = \frac{2G}{1-\nu} \int_{A_o}^{A} \sigma_r \frac{d}{dA}\left(\frac{1}{2G}\right) dA$

Let: $f_2'(\sigma_r) = \frac{2\nu G}{1-\nu}\int_{A_o}^{A} \sigma_r \frac{d}{dA}\left(\frac{1}{2G}\right) dA$

On page 33, the set of equations, (Eq. 17) through (Eq. 22), were given which defined the stresses in a solid cylinder. The only changes which occur in these equations when they are adapted to a hollow cylinder are a change in the limits of integration and a change in the boundary condition equations, (Eq. 19) and (Eq. 22). The equations for a hollow cylinder are presented below. The equations corresponding to those for a solid cylinder are distinguished from them by a prime.

$$\left.\begin{aligned} &(17)' \quad \sigma_\phi + \sigma_r \\ &(18)' \quad 2\frac{d}{dA}(A\sigma_r) \end{aligned}\right\} = \left[\frac{2G}{1-\nu}\int_{A_o}^{A} \sigma_r \frac{d}{dA}\left(\frac{1}{2G}\right) dA - \frac{2G}{1-\nu}\int_{A_o}^{A} \frac{\epsilon_\phi^\circ - \epsilon_r^\circ}{2A} dA - \frac{2G}{1-\nu}\left(\epsilon_\phi^\circ + \nu\epsilon_z^\circ\right) - \frac{E}{1-\nu}\epsilon^T + \frac{2\nu G}{1-\nu}\epsilon_z + \frac{2G}{1-\nu} C\right]$$

$$(19)' \quad 2A\sigma_r\Big|_{A=A_o} = -2A_o p_o \qquad (20)' \quad 2A\sigma_r\Big|_{A=1} = -2p_i$$

$$(21)' \quad \sigma_z = \left[\frac{2\nu G}{1-\nu}\int_{A_o}^{A} \sigma_r \frac{d}{dA}\left(\frac{1}{2G}\right) dA - \frac{2\nu G}{1-\nu}\int_{A_o}^{A} \frac{\epsilon_\phi^\circ - \epsilon_r^\circ}{2A} dA - \frac{2G}{1-\nu}\left(\nu\epsilon_\phi^\circ + \epsilon_z^\circ\right) - \frac{E}{1-\nu}\epsilon^T + \frac{2G}{1-\nu}\epsilon_z + \frac{2\nu G}{1-\nu} C\right]$$

$$(22)' \quad \int_{A_o}^{1} \sigma_z dA = (1-A_o)\,\sigma_{z\,avg.}$$

As before, this set of equations may be separated into three sets of equations which give the stresses due to the thermal dilation, the stresses due to the boundary forces, and the stresses due to the residual strains. Each of the separated sets of equations will be presented and the technique of solving them will be indicated. This technique is similar to that used in Chapter III.

For a hollow cylinder, the set of equations which gives the stresses due to the thermal dilation is given below. The corresponding set of equations for a solid cylinder was presented on page 39.

$$\left.\begin{array}{ll} (17a)_1' & \sigma_{\phi_1} + \sigma_{r_1} \\ (18a)_1' & 2\frac{d}{dA}(A\sigma_{r_1}) \end{array}\right\} = f_1'(\sigma_{r_1}) - \frac{E}{1-\nu}\epsilon^T + \frac{E}{1-\nu}\epsilon_z + \frac{2G}{1-\nu}C_1'$$

$$(19)_1' \quad 2A\sigma_{r_1}\Big|_{A=A_o} = 0 \qquad\qquad (20)_1' \quad 2A\sigma_{r_1}\Big|_{A=1} = 0$$

$$(21a)_1' \quad \sigma_{z_1} = f_2'(\sigma_{r_1}) - \frac{E}{1-\nu}\epsilon^T + \frac{E}{1-\nu}\epsilon_z + \frac{2\nu G}{1-\nu}C_1'$$

$$(22)_1' \quad \int_{A_o}^{1} \sigma_{z_1}\, dA = 0$$

The results of the integration of $(\text{Eq. } 18a)_1'$ and $(\text{Eq. } 21a)_1'$ are indicated below. Note that $(\text{Eq. } 19)_1'$ is satisfied due to the limits of integration.

$$(23)_1' \quad 2A\sigma_{r_1} = \int_{A_o}^{A} f_1'(\sigma_{r_1})\,dA - \int_{A_o}^{A}\frac{E}{1-\nu}\epsilon^T dA + \epsilon_z \int_{A_o}^{A}\frac{E}{1-\nu}dA + C_1'\int_{A_o}^{A}\frac{2G}{1-\nu}dA$$

$$(24)_1' \quad \int_{A_o}^{A}\sigma_{z_1}dA = \int_{A_o}^{A} f_2'(\sigma_{r_1})dA - \int_{A_o}^{A}\frac{E}{1-\nu}\epsilon^T dA + \epsilon_z\int_{A_o}^{A}\frac{E}{1-\nu}dA + C_1'\int_{A_o}^{A}\frac{2\nu G}{1-\nu}dA$$

The application of the boundary conditions, $(\text{Eq. } 20)_1'$ and $(\text{Eq. } 22)_1'$, results in a set of equations comparable to $(\text{Eq. } 25a)_1$ and (Eq. 26a), page 42, except that the approximations for $f_1'(\sigma_{r_1})$ and $f_2'(\sigma_{r_1})$ are not indicated.

$$(25b)_1' \qquad \epsilon_{z_1} = \frac{\int_{A_o}' \frac{E}{1-\nu}\epsilon^T dA}{\int_{A_o}' \frac{E}{1-\nu} dA} + \frac{\int_{A_o}' \frac{2\nu G}{1-\nu} dA \int_{A_o}' f_1'(\sigma_{r_1}) dA - \int_{A_o}' \frac{2G}{1-\nu} dA \int_{A_o}' f_2'(\sigma_{r_1}) dA}{\int_{A_o}' \frac{E}{1-\nu} dA \left[\int_{A_o}' \frac{2G}{1-\nu} dA - \int_{A_o}' \frac{2\nu G}{1-\nu} dA \right]}$$

$$(26b)_1' \qquad C_1' = \frac{-\int_{A_o}' f_1'(\sigma_{r_1}) dA + \int_{A_o}' f_2'(\sigma_{r_1}) dA}{\int_{A_o}' \frac{2G}{1-\nu} dA - \int_{A_o}' \frac{2\nu G}{1-\nu} dA}$$

The technique of solving these equations parallels that used in Chapter III. A first approximation to ϵ_{z_1} and C_1', denoted by $\bar{\epsilon}_{z_1}$ and $\bar{C}_1'$, is obtained from $(\text{Eq. } 25b)_1'$ and $(\text{Eq. } 26b)_1'$, assuming that $f_1'(\sigma_{r_1})$ and $f_2'(\sigma_{r_1})$ are zero. These values for the constants are used to obtain a first approximation to σ_{r_1}, denoted by $\bar{\sigma}_{r_1}$, from $(\text{Eq. } 23)_1'$, assuming that $f_1'(\sigma_{r_1})$ is zero. This value of $\bar{\sigma}_{r_1}$ is used to obtain a second approximation to the values of ϵ_{z_1} and C_1' by replacing $f_1'(\sigma_{r_1})$ and $f_2'(\sigma_{r_1})$ by $f_1'(\bar{\sigma}_{r_1})$ and $f_2'(\bar{\sigma}_{r_1})$ in $(\text{Eq. } 25b)_1'$ and $(\text{Eq. } 26b)_1'$. Using these second approximations for the values of the constants, a second approximation to σ_{r_1} is obtained from $(\text{Eq. } 23)_1'$, assuming that $f_1'(\sigma_{r_1})$ equals $f_1'(\bar{\sigma}_{r_1})$. This second approximation to σ_{r_1} is either used to replace $\bar{\sigma}_{r_1}$ in the foregoing argument and the process is repeated or this second approximation is considered close enough. When a satisfactory value of σ_{r_1} is obtained, σ_{ϕ_1} and σ_{z_1} are obtained from $(\text{Eq. } 17a)_1'$ and $(\text{Eq. } 21)_1'$.

Since the technique for solving the sets of equations which give the stresses due to the boundary forces and the stresses due to the residual strains is the same as described above, it will suffice to merely present the equations, and assume that the foregoing discussion is applied to them.

The set of equations which gives the stresses due to the boundary forces, for the case of a hollow cylinder, is given below.

$$\left.\begin{array}{ll}(17)_2' & \sigma_{\phi_2}+\sigma_{r_2} \\ (18)_2' & 2\frac{d}{dA}(A\sigma_{r_2})\end{array}\right\} = f_1'(\sigma_{r_2}) + \frac{2\nu G}{1-\nu}\epsilon_{z_2} + \frac{2G}{1-\nu}C_2$$

$$(19)_2' \quad 2A\sigma_{r_2}\Big|_{A=A_o} = -2A_oP_o \qquad (20)_2' \quad 2A\sigma_{r_2}\Big|_{A=1} = -2P_1$$

$$(21)_2' \qquad \sigma_{z_2} = f_2'(\sigma_{r_2}) + \frac{2G}{1-\nu}\epsilon_{z_2} + \frac{2\nu G}{1-\nu}C_2$$

$$(22)_2' \quad \int_{A_o}^{1}\sigma_{z_2}\,dA = (1-A_o)\sigma_{z_{avg.}}$$

$$(23)_2' \qquad 2A\sigma_{r_2} = \int_{A_o}^{A} f_1'(\sigma_{r_2})dA + \epsilon_{z_2}\int_{A_o}^{A}\frac{2\nu G}{1-\nu}dA + C_2\int_{A_o}^{A}\frac{2G}{1-\nu}dA - 2A_oP_o$$

$$(24)_2' \qquad \int_{A_o}^{A}\sigma_{z_2}\,dA = \int_{A_o}^{A} f_2'(\sigma_{r_2})dA + \epsilon_{z_2}\int_{A_o}^{A}\frac{2G}{1-\nu}dA + C_2\int_{A_o}^{A}\frac{2\nu G}{1-\nu}dA$$

$$(25b)_2' \qquad \epsilon_{z_2} = \frac{\int_{A_o}^{1}\frac{2G}{1-\nu}dA\left[(1-A_o)\sigma_{z_{avg.}} - \int_{A_o}^{1} f_2'(\sigma_{r_2})dA\right] - \int_{A_o}^{1}\frac{2\nu G}{1-\nu}dA\left[-2P_1 + 2A_oP_o - \int_{A_o}^{1} f_1'(\sigma_{r_2})dA\right]}{\left[\int_{A_o}^{1}\frac{2G}{1-\nu}dA\right]^2 - \left[\int_{A_o}^{1}\frac{2\nu G}{1-\nu}dA\right]^2}$$

$$(26b)_2' \qquad C_2 = \frac{\int_{A_o}^{1}\frac{2G}{1-\nu}dA\left[-2P_1 + 2A_oP_o - \int_{A_o}^{1} f_1'(\sigma_{r_2})dA\right] - \int_{A_o}^{1}\frac{2\nu G}{1-\nu}dA\left[(1-A_o)\sigma_{z_{avg.}} - \int_{A_o}^{1} f_2'(\sigma_{r_2})dA\right]}{\left[\int_{A_o}^{1}\frac{2G}{1-\nu}dA\right]^2 - \left[\int_{A_o}^{1}\frac{2\nu G}{1-\nu}dA\right]^2}$$

The foregoing equations are solved in an identical manner to the previous set, which gave the stresses due to the thermal dilation.

The set of equations which gives the stresses due to the residual strains, for the case of a hollow cylinder, is given below.

$$(17)'_3 \quad \sigma_{\phi_3} + \sigma_{r_3} \Big\} = f_1'(\sigma_{r_3}) - \frac{2G}{1-\nu}\int_{A_o}^{A} \frac{\epsilon_\phi^\circ - \epsilon_r^\circ}{2A}\,dA - \frac{2G}{1-\nu}(\epsilon_\phi^\circ + \nu\epsilon_z^\circ) + \frac{2\nu G}{1-\nu}\epsilon_{z_3} + \frac{2G}{1-\nu}C_3$$

$$(18)'_3 \quad \frac{2\sigma}{\partial A}(A\sigma_{r_3})$$

$$(19)'_3 \quad 2A\sigma_{r_3}\Big|_{A=A_o} = 0 \qquad (20)'_3 \quad 2A\sigma_{r_3}\Big|_{A=1} = 0$$

$$(21)'_3 \quad \sigma_{z_3} = f_2'(\sigma_{r_3}) - \frac{2\nu G}{1-\nu}\int_{A_o}^{A} \frac{\epsilon_\phi^\circ - \epsilon_r^\circ}{2A}\,dA - \frac{2G}{1-\nu}(\nu\epsilon_\phi^\circ + \epsilon_z^\circ) + \frac{2G}{1-\nu}\epsilon_{z_3} + \frac{2\nu G}{1-\nu}C_3$$

$$(22)'_3 \quad \int_{A_o}^{1} \sigma_{z_3}\,dA = 0$$

$$(23)'_3 \quad 2A\sigma_{r_3} = \int_{A_o}^{A} f_1'(\sigma_{r_3})\,dA - \int_{A_o}^{A}\left[\frac{2G}{1-\nu}\int_{A_o}^{A}\frac{\epsilon_\phi^\circ - \epsilon_r^\circ}{2A}\,dA\right]dA - \frac{2G}{1-\nu}\int_{A_o}^{A}(\epsilon_\phi^\circ + \nu\epsilon_z^\circ)\,dA + \epsilon_{z_3}\int_{A_o}^{A}\frac{2\nu G}{1-\nu}\,dA + C_3\int_{A_o}^{A}\frac{2G}{1-\nu}\,dA$$

$$(24)'_3 \quad \int_{A_o}^{A}\sigma_{z_3}\,dA = \int_{A_o}^{A} f_2'(\sigma_{r_3})\,dA - \int_{A_o}^{A}\left[\frac{2\nu G}{1-\nu}\int_{A_o}^{A}\frac{\epsilon_\phi^\circ - \epsilon_r^\circ}{2A}\,dA\right]dA - \frac{2G}{1-\nu}\int_{A_o}^{A}(\nu\epsilon_\phi^\circ + \epsilon_z^\circ)\,dA + \epsilon_{z_3}\int_{A_o}^{A}\frac{2G}{1-\nu}\,dA + C_3\int_{A_o}^{A}\frac{2\nu G}{1-\nu}\,dA$$

$$(25b)'_3 \epsilon_{z_3} = \frac{\int_{A_o}^{1}\frac{2G}{1-\nu}dA\int_{A_o}^{1}\left[\frac{2\nu G}{1-\nu}\int_{A_o}^{A}\frac{\epsilon_\phi^\circ - \epsilon_r^\circ}{2A}dA + \frac{2G}{1-\nu}(\nu\epsilon_\phi^\circ + \epsilon_z^\circ) - f_2'(\sigma_{r_3})\right]dA - \int_{A_o}^{1}\frac{2\nu G}{1-\nu}dA\int_{A_o}^{1}\left[\frac{2G}{1-\nu}\int_{A_o}^{A}\frac{\epsilon_\phi^\circ - \epsilon_r^\circ}{2A}dA + \frac{2G}{1-\nu}(\epsilon_\phi^\circ + \nu\epsilon_z^\circ) - f_1'(\sigma_{r_3})\right]dA}{\left[\int_{A_o}^{1}\frac{2G}{1-\nu}\,dA\right]^2 - \left[\int_{A_o}^{1}\frac{2\nu G}{1-\nu}\,dA\right]^2}$$

$$(26b)'_3 \quad C_3 = \frac{\int_{A_o}^{1}\frac{2G}{1-\nu}dA\int_{A_o}^{1}\left[\frac{2G}{1-\nu}\int_{A_o}^{A}\frac{\epsilon_\phi^\circ - \epsilon_r^\circ}{2A}dA + \frac{2G}{1-\nu}(\epsilon_\phi^\circ + \nu\epsilon_z^\circ) - f_1'(\sigma_{r_3})\right]dA - \int_{A_o}^{1}\frac{2\nu G}{1-\nu}dA\int_{A_o}^{1}\left[\frac{2\nu G}{1-\nu}\int_{A_o}^{A}\frac{\epsilon_\phi^\circ - \epsilon_r^\circ}{2A}dA + \frac{2G}{1-\nu}(\nu\epsilon_\phi^\circ + \epsilon_z^\circ) - f_2'(\sigma_{r_3})\right]dA}{\left[\int_{A_o}^{1}\frac{2G}{1-\nu}\,dA\right]^2 - \left[\int_{A_o}^{1}\frac{2\nu G}{1-\nu}\,dA\right]^2}$$

The foregoing equations are solved in an identical manner to the previous set, which gave the stresses due to the thermal dilation.

Outside of the foregoing modifications to the equations, the discussion of Part I applies in its entirety to the remainder of the computations required to determine the residual stresses in an infinitely long concentric hollow isotropic cylinder quenched in a large body of fluid.

In this chapter the modifications required to extend Part I to cover the case of a hollow cylinder have been indicated. This chapter is not intended to stand alone, but rather, is to be used in conjunction with the discussions of Part I.

CHAPTER X

This chapter will be devoted to the consideration of further extensions to Part I. It is apparent that only cases in which the variables may be considered to be functions of a single position parameter, at a given time, may be handled by similar techniques. This restriction effectively limits the extension of Part I, which may be made without drastic increases in the complexity of the method of solution, to the cases of the flat plate and the solid or hollow sphere. For other geometrical cases, the developments of Chapter II and Chapter IV still apply to the stress problem, but the application of these chapters to other geometrical shapes is beyond the scope of this thesis. The case of the flat plate will be considered in limited detail and the case of the sphere will be briefly mentioned. The modifications to Part I and the additional information required to handle cases in which a phase change is involved will be briefly considered.

The infinite flat plate is a limiting case of the hollow cylinder, in which (r_1-r_o) equals the plate thickness and r_1 is allowed to approach infinity. This is a simpler case than the cylinder because a plain scale (rather than a logarithmic) can be used in the graphical construction for the temperature problem and in the stress problem there are two constant strains rather than one. The case of the flat plate will now be briefly discussed.

Consider an infinite flat plate of thickness b, where x and y are coordinates parallel to the principle stresses in the xy plane.

Assume that T_1 and T_o respectively, are the fluid bulk temperature above and below the plate and that h_1 and h_o respectively, are the boundary layer conductivities above and below the plate.

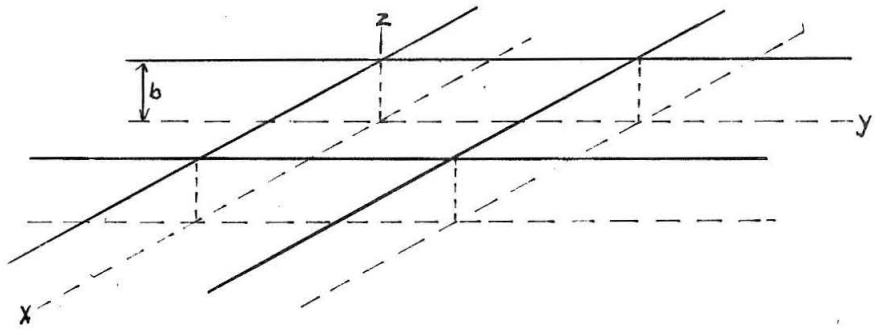

The equations corresponding to (Eq. 1), page 3, (Eq. 2), page 4, and (Eq. 3), page 6, are:

$$(1)' \qquad \frac{\partial T}{\partial t} = \alpha\left[\frac{\partial^2 T}{\partial z^2} + \frac{1}{K}\frac{\partial K}{\partial z}\frac{\partial T}{\partial z}\right]$$

$$(2)' \qquad \left.\frac{\partial T}{\partial z}\right|_{z=b} = -\frac{h_1}{K}\left.(T-T_1)\right|_{z=b} \qquad \text{and} \qquad \left.\frac{\partial T}{\partial z}\right|_{z=0} = +\frac{h_o}{K}\left.(T-T_o)\right|_{z=0}$$

$$(3)' \qquad T_{m,j+1} - T_{m,j} \cong \left(2\alpha_{m,j}\frac{\Delta t_{j+1}}{(\Delta z)^2}\right)\left\{\frac{1}{2}\left[T_{m+1,j} - 2T_{m,j} + T_{m-1,j}\right] + \frac{1}{8K_{m,j}}\left(K_{m+1,j} - K_{m-1,j}\right)\left(T_{m+1,j} - T_{m-1,j}\right)\right.$$

These equations may be solved by a graphical construction similar to (Fig. 1). The differences are that z need no longer be plotted to a log scale but may be plotted directly, and that there is now a boundary layer on each face of the plate. In (Fig. 1) the graphical construction for the boundary layer required a curve plotted at a distance $\frac{K \log_{10} e}{r_1 h}$ from the surface. For the case of the flat plate there are two curves required, at distance $\frac{K}{h_1}$ and $\frac{K}{h_o}$ respectively, from the upper and lower surface of the plate. Outside of these modifications,

the solution of the temperature problem proceeds in an identical manner to that presented in Chapter I.

For the case of an infinite flat plate where the parameters are independent of x and y, the required equations for the stresses are indicated below.

$$\epsilon_x = \text{constant}$$

$$\epsilon_y = \text{constant}$$

$$\epsilon_x = \frac{1}{E}\left[\sigma_x - \nu(\sigma_y + \sigma_z)\right] + \epsilon_x^\circ + \epsilon^T$$

$$\epsilon_y = \frac{1}{E}\left[\sigma_y - \nu(\sigma_z + \sigma_x)\right] + \epsilon_y^\circ + \epsilon^T$$

$$\sigma_z = -p$$ (p is the pressure on the upper and lower surfaces of the plate.)

$$\int_0^b \sigma_x dz = b\,\sigma_{x\,avg.}$$

$$\int_0^b \sigma_y dz = b\,\sigma_{y\,avg.}$$

($\sigma_{x\,avg.}$ and $\sigma_{y\,avg.}$ are average principal stresses in the xy plane due to boundary forces at the infinitely removed edges of the plate.)

These equations may be readily solved, and may be divided up, as in the case of the cylinder, into stresses due to the thermal dilation, stresses due to the residual strains and stresses due to the boundary forces. Unlike the case of the cylinder, explicit solutions are obtainable since no terms comparable to $f_1(\sigma_r)$ and $f_2(\sigma_r)$ appear. The general solution, particularly for the stresses due to the boundary forces, becomes fairly lengthy, hence for purposes of illustration it is desirable to use a less general case.

Consider the case of a flat plate in which the boundary forces are zero and the parameters are independent of the direction in the xy plane.

Letting ϵ_x represent both ϵ_x and ϵ_y, σ_x represent both σ_x and σ_y, and ϵ_x^o represent both ϵ_x^o and ϵ_y^o, the equations for the simplified case are:

$$\epsilon_x = \text{constant}$$

$$\epsilon_x = \frac{1-\nu}{E}\sigma_x + \epsilon_x^o + \epsilon^T$$

$$\int_o^b \sigma_x dz = 0$$

Separating this set of equations into two sets, giving respectively the stresses due to the thermal dilation and the stresses due to the residual strains, results in the following sets of equations.

$$\epsilon_{x_1} = \text{constant} \qquad \epsilon_{x_3} = \text{constant}$$

$$\epsilon_{x_1} = \frac{1-\nu}{E}\sigma_{x_1} + \epsilon^T \quad \text{and} \quad \epsilon_{x_3} = \frac{1-\nu}{E}\sigma_{x_3} + \epsilon_x^o$$

$$\int_o^b \sigma_x dz = 0 \qquad \int_o^b \sigma_x dz = 0$$

The solution to these sets of equations are respectively:

$$\sigma_{x_1} = \frac{E}{1-\nu}\left[\epsilon^T - \frac{\int_o^b \frac{E}{1-\nu}\epsilon^T dz}{\int_o^b \frac{E}{1-\nu} dz}\right] \quad \text{and} \quad \sigma_{x_3} = \frac{E}{1-\nu}\left[\epsilon_x^o - \frac{\int_o^b \frac{E}{1-\nu}\epsilon_x^o dz}{\int_o^b \frac{E}{1-\nu} dz}\right]$$

The techniques for determining the values of the residual strains are of course the same as in Part I.

Similar techniques for the solution of the temperature problem may be developed for the case of the sphere. In this case the graphical construction is similar to the case of the cylinder, except that the

reciprocal of the radius, rather than a log scale, must be used. The stress solution is simpler than for a cylinder since there are only two unknown stresses (assuming symmetry). The stress equations are readily developed in a manner similar to the developments of Chapter III, but will not be presented here.

The stress problem, as developed in Chapters II and IV, is quite general, but semi-graphical solutions for the temperature are only possible for the cases of the flat plate, the cylinder and the sphere. For other geometric shapes (where the temperature is a function of two or more position coordinates as well as time) it is necessary to develop new techniques for solving the temperature problem. A consideration of the extension of Part I to other geometric shapes is beyond the scope of this thesis.

The remaining question which will be considered is whether the developments of Part I can be extended to include a phase change during the quenching cycle. The answer to this question is yes, if the following additional conditions are satisfied.

1) The values of the pertinent parameters are known for each pure phase in the temperature range at which that phase is present and it is possible to determine the values of the parameters when two phases are simultaneously present.

2) It is possible to determine the phase change rate at any time in terms of the past history of the point under consideration.

Assuming that these conditions are satisfied, the first change in

Part I is in the interpretation of the terms. In addition to being functions of the temperature, all of the parameters are now functions of the amount of phase change completed. For example, let α be the first phase and β be the second phase and λ be the fraction of α which has transformed to β. Let ϵ_α^T be the thermal expansion of α and ϵ_β^T be the thermal expansion of β. Then if there are two phases present,

$$\epsilon^T = (1-\lambda)\epsilon_\alpha^T + \lambda\epsilon_\beta^T$$

Although all of the properties, when two phases are present, may not be determined as simply as this, the parameters used in Part I may still be considered to be a function of the amount of phase change completed. When this is understood, there are no modifications to the stress problem outlined in Part I.

In the temperature problem, however, there is an additional term. Let H be the amount of heat evolved per unit weight in the complete transformation of α to β. Referring to page 3, there is now an additional term appearing. This term is:

$$\text{The rate of heat generation} = 2\pi r\,dr\,\rho\,H\frac{\partial\lambda}{\partial t}$$

The equation for heat flow in cylindrical coordinates is then obtained by equating the rate of heat entering the ring from the inner radius r plus the rate of heat generation in the ring to the rate of heat storage in the ring plus the rate of heat leaving across the outer radius $r-dr$. With this additional term, (Eq. 1), page 3, becomes:

$$\frac{\partial T}{\partial t} = \alpha\left[\frac{1}{r}\frac{\partial}{\partial r}\left(r\frac{\partial T}{\partial r}\right) + \frac{1}{K}\frac{\partial K}{\partial r}\frac{\partial T}{\partial r}\right] + \underbrace{\frac{H}{C_p}\frac{\partial\lambda}{\partial t}}_{\text{new term}}$$

This means that to the right hand side of (Eq. 3), page 6, the following term must be added.

$$\frac{H_{m,j}}{Cp_{m,j}}\left(\lambda_{m,j+1} - \lambda_{m,j}\right)$$

A discussion of methods of satisfying conditions 1) and 2), page 150, is beyond the scope of this thesis. A simplified approach to condition 2) is given by Russell (*10*) for steel of eutectoid composition.

In this chapter it has been indicated that similar techniques to those used in Part I can be applied to the cases of the flat plate and the sphere. The extension of the problem to include phase change has been indicated, and the character of the additional information required to solve the problem when phase change is present has been pointed out.

CONCLUSION

This thesis presents, for the first time, a method whereby the variation with temperature of the thermal conductivity and of the thermal diffusivity may be included in the calculation of the temperature versus position and time for the particular cases considered. In certain portions of the numerical calculation presented in Chapter V, the time derivatives of the temperature at the surface were 30% greater and at the center were 30% less than would have been obtained if average values, rather than variable values, of the thermal conductivity and thermal diffusivity were used.

In the temperature calculation it was indicated that size and position effects on the boundary layer conductivity are very important, and that at present they are not known. It was also pointed out that the boundary layer conductivity in the case of a large cylinder (similarly for a flat plate) could be computed, if a temperature near the surface were known versus time. For example, if a long solid cylinder is quenched in a vertical position, the variation with height of the boundary layer conductivity may be computed. If this is done with cylinders of various diameters and lengths, size and shape effects may be investigated. (In these cases, of course, suitable precautions must be maintained to insure that the axial flow of heat is negligible.)

The basic contribution of this thesis to the stress problem is the development and use of the concept of the separability of the total stresses into the stresses due to the thermal dilation, the stresses due

to the boundary forces and the stresses due to the residual strains. It is this concept which allows the development of the finite difference techniques whereby the stresses may be investigated at the end of a succeeding time interval in the knowledge of a theory of strength, thereby allowing residual strain increments in that time interval to be predicted. This concept, and the additional developments of Chapters II and IV, open an approach whereby actual numerical values may be obtained to a whole host of problems involving yielding. This concept of separability is based upon the assumption that the values of the elastic coefficients are the same in each of the set of equations which gives the total stresses. The author, by assuming that the values of the elastic coefficients are unique functions of the temperature and that they represent the values obtained by unloading an infinitesimal element, has merely chosen the simplest way of satisfying the required assumption.

In the specific cases of the cylinder and the plate, the contribution of this thesis lies largely in the developments whereby the effects of the variations of the elastic coefficients with temperature may be exactly included. In this regard, the equations and the semi-graphical techniques for their solution presented in Chapter III are original contributions.

Perhaps the most important contribution of this thesis, however, lies in the knowledge it affords that, assuming the values of the parameters are known and end effects are negligible, arbitrarily exact calculations of the residual stresses due to symmetrically quenching a solid or hollow cylinder (or infinite flat plate) may actually be carried out. In this

connection it must be pointed out, however, that the results of the calculation presented in Part II indicate that a large amount of further work is necessary before the values of the pertinent parameters are adequately known. In particular, better values of the boundary layer conductivity and of the "creep" properties of materials at high temperatures and stress levels are required.

The most important direct extension of this thesis, briefly mentioned in Chapter X, is the consideration of the case where phase change is involved (i.e. steel quenched from the austenite region). This can be accomplished if the factors tabulated on page 150 are known.

REFERENCES

(1) G. Sachs, Z. Metallkunde, (1927), V 19, p 352.

(2) H. Buhler, H. Bucholtz & E. Schulz, Arch. Eisenhuttenesen, (1932) V 5, p 413.

(3) H. Buhler & H. Bucholtz, Arch. Eisenhuttenwesen, (1932), V 6, p 247.

(4) H. Huhler & E. Scheil, Arch. Eisenhuttenwesen, (1932), V 6, p 283.

(5) H. B. Wishart & R. K. Potter, Trans. Am. Soc. for Metals, (1949), V 41, p 692.

(6) O. J. Horger, H. R. Neifert & R. R. Regen, Soc. for Exp. Stress Analysis, (1943), V 1, No. 1, p 10.

(7) C. S. Barrett, Soc. for Exp. Stress Analysis, (1944), V 2, No. 1, p 147.

(8) G. Sachs & G. Espey, The Iron Age, (1941), V 148, p 63.

(9) F. Laszlo, J. Iron & Steel Inst., (1943), V 147, p 173; (1943), V 148, p 137; (1944), V 150, p 183; (1945), V 152, p 207.

(10) J. E. Russell, Institute of Metals Monograph and Report Series, No. 5, (1948), p 95. "Symposium on Internal Stresses".

(11) H. Treppschuh, Arch. Eisenhuttenwesen, (1940), V 13, p 429.

(12) E. Schmidt, Forschg. Ing. Wes., (1942), V 13, p 177.

(13) M. A. Grossman & M. Asimov, Trans. Am. Soc. for Metals, (1940), V 28, p 949.

(14) A. Rose, Arch. Eisenhuttenwesen, (1940), V 13, p 345.

(15) N. B. Pilling & T. D. Lynch, Trans. Am. Inst. Min. & Metallurg. Engrs., (1918/1919), V 62, p 665.

(16) F. Everett & J. Miklowitz, J. App. Ph., (1944), V 15, p 592.

(17) G. Verse, Trans. Am. Soc. Test. Matl., (1935), V 57, p 1.